January 2012

# Smart Packaging: A Novel Technique For Localized Drug Delivery For Ovarian Cancer

Eva Christabel Williams
*University of South Florida*, eves.cw@gmail.com

# Smart Packaging: A Novel Technique For Localized Drug Delivery For Ovarian Cancer

by

Eva Christabel Williams

A dissertation submitted in partial fulfillment
of the requirements for the degree of
Doctor of Philosophy
Department of Chemical and Biomedical Engineering
College of Engineering
University of South Florida

Major Professor: Norma Alcantar, Ph.D.
Ryan Toomey, Ph.D.
Julie Harmon, Ph.D.
Mark Jaroszeski, Ph.D.
Johnathan Lancaster, M.D., Ph.D.

Date of Approval:
June 13, 2012

Keywords: niosome, chitosan, thermo-responsive hydrogel, cell culture, confocal microscopy, xenogen

## DEDICATION

This dissertation is dedicated to:

My dad and mom who have shown me what perseverance, love and faith can accomplish.

My brother Allen, for being my role model and the one I can always rely on.

My husband Julian, for being the best part of my life and for showing me that love has no boundaries.

Without all your love and support I would cease to exist.

## ACKNOWLEDGMENTS

I would like to thank my advisor Dr. Norma Alcantar without whose help and guidance this dissertation would not have been completed. I am forever indebted to her. Sincere gratitude is extended to Dr. Ryan Toomey for his insightful knowledge and advice in the data presentation. I would also like to thank my committee members Dr. Julie Harmon, Dr. Mark Jaroszeski and Dr. Jonathan Lancaster for all the help and suggestions that made this dissertation better. A special thanks to Dr. Marzenna Wiranowska for training me in cell culture experiments and for her valuable insights. Thanks to all my fellow graduate students and friends Ajay Vidyasagar, Audrey Buttice, Dawn Fox, Marlyn Colon, and Daniella Stebbins for making this Ph.D. experience fun. I would also like to thank the NIH grant Ruth L. Kirschstein National Research Service Award for Individual Predoctoral Fellowship (F31CA145736) from the National Cancer Institute, the Florida Center of Excellence for Biomolecular Identification and Targeted Therapeutics (FCoE-BITT), and the Seed Grant and Signature Program in Neuroscience, College of Medicine, for the funding provided for this research. I also thank Dr. Vinay Gupta for the use of the DLS apparatus under the NER award (CTS-0508309) from the National Science Foundation and also Betty Lorramm, Ed Haller and the Integrative Biology Microscopy Core Laboratory at USF for assistance and discussion regarding the TEM.

## TABLE OF CONTENTS

## LIST OF TABLES

## LIST OF FIGURES

## ABSTRACT

Localized drug delivery is emerging as an effective technique due to its ability to administer therapeutic concentrations and controlled release of drugs to cancer sites in the body. It also prevents the contact of harsh chemotherapy drugs to healthy regions in the body that otherwise would become exposed to current treatments.

This study reports on a model chemotherapy drug delivery system comprising non-ionic surfactant vesicles (niosomes) packaged within a temperature-sensitive chitosan network. This smart packaging, or package-within-a package system, provides two distinct advantages. First, the gel prevents circulation of the niosomes and maintains delivery in the vicinity of a tumor. Secondly, the chitosan network protects the niosomes against fluctuations in tonicity, which affects delivery rates. Tonicity is the sum of the concentrations of the solutes which have the capacity to exert an osmotic force across the membrane. Release rates were monitored from both bare niosomes alone and niosome-embedded, chitosan networks. It was observed that chitosan networks prolonged delivery from 100 hours to 55 days in low ionic strength environment and pH conditions similar to a tumor site. The primary effect of chitosan is to add control on release time and dosage, and stabilize the niosomes through a high ionic strength surrounding that prevents uncontrolled bursting of the niosomes. Secondary factors include cross-link density of the

chitosan network, molecular weight of the individual chitosan polymers, dye concentration within the niosomes, and the number density of niosomes packaged within the chitosan network. Each of these factors can be altered to fine-tune release rates. Release rate experiments were conducted with 5,6-carboxyfluorescein, a fluorescent dye and chemotherapeutics paclitaxel and carboplatin. *In vitro* studies showed a preferential affinity of the smart packaged system to ovarian carcinoma cell line OV2008 as compared to normal epithelial cell lines of Ilow and MCC3. Further, feasibility of the drug delivery system was evaluated *in vivo.* Toxicity studies revealed that the system was non-toxic and feasible *in vivo.* The final outcome of this study includes tuning of the variables mentioned above that will contribute to the development of low cost and improved methods for drug delivery with application to intracavitary ovarian cancer treatment and other types of cancer.

# CHAPTER 1 BACKGROUND AND MOTIVATION

## 1.1 Cancer Facts and Figures

Cancer is the second leading cause of death in the United States next to cardiovascular disease [1]. There are more than 100 different types of cancers that exist with some being more invasive and fast growing than others. In the year 2007 alone, 10 percent of the 58 million deaths worldwide occurred due to this disease [2]. Cancer occurs due to uncontrolled growth and spread of cells leading to malignant tumors. However not all tumors are cancerous. Benign tumors do not invade or metastasize to other parts of the body, are less dangerous and can be removed [2]. On the other hand, malignant tumors are cancerous and if not contained in full will invade adjacent tissues or metastasize [2].

Cancer can affect people at all ages, including fetuses. It is not site or region specific and can develop in nearly any organ or tissue. However, certain parts of the world are seen to have greater occurrences for some types of cancers. Japan, for instance, exhibits a higher risk for gastric cancer due to their high dietary salt intake [3]. This type of cancer rarely occurs in the United States [3]. In the same manner, colorectal cancer, whose risk factors are associated with intake of diets rich in fat, alcohol or red meat is

more common in the United States and other developed countries [4, 5] and are rarely found in developing countries, giving it the name ‘a rich man’s cancer’[4, 5].

Although the exact cause of cancer still remains unknown, several characteristics are now being considered as risk factors that increase the probability of cancer. Diet and obesity contribute to nearly 25-30% of cancer cases [6, 7]. Tobacco [6-8], infections [9, 10], radiation [11, 12], stress, lack of physical activity [13, 14], environmental pollutants [15] are still other factors believed to increase the risk of cancer.

Over the years diseases such as heart diseases, cerebrovascular diseases, influenza & pneumonia and cancer have showed a decrease in the death rate.[2] However if the percentage decrease in death is taken into consideration, then an alarming trend can be seen: communicable diseases like influenza and pneumonia showed a drastic percentage decrease in death rate to the order of 95.55% [2]. Fatality due to heart diseases also showed quite a dramatic decrease, 56.34%, closely followed by cerebrovascular diseases [2]. However, the percentage decrease in death in cancer is extremely low, only 19.04% [2]. This can be attributed to a number of factors such as insufficient research investigations in the area and current treatment techniques not efficient enough to bring down their numbers. Further, most of the cancer deaths are reported in developing countries [2] due to high cost of treatment, lack of efficient drug delivery systems and limited health care facilities.

Of the three factors listed above, the most appalling is the fact that nearly 70 percent of all cancer deaths occur in developing and emerging economic countries. Several reasons may be attributed to this growing problem, the most obvious being the lack of financial resources and facilities [16, 17]. Since limited resources are available to governments in such countries, they are left with the immense dilemma to determine the spending priorities. It is not surprising that health expenditure takes a back seat when dealt with much pressing problems like providing food and clean drinking water to the population. All the more, the modest amounts that are spent on health care are for transmissible diseases [17]. Most developing countries are well equipped to deal with communicable diseases that require immediate attention. This leaves less room for specialized diseases such as cancer and the like, hence the alarmingly high death rates in these countries.

### 1.2 Ovarian Cancer: Facts and Current Treatment Techniques

There are nearly 100 different types of cancers that occur in the human body. It can occur in almost all parts of the body with some being easier to detect than others but all being equally dangerous if not treated immediately.

Ovarian Cancer is the fourth leading cause of death due to cancer in women [18, 19], the leading cause of death from gynecologic malignancies and the second most commonly diagnosed gynecologic malignancy [20, 21]. There are nearly 30 types of ovarian malignancies broadly classified into 3 categories depending on the type of cells in which they originate [22]. It is the most commonly diagnosed and the leading cause of death in

American women [22, 23]. An estimated 15,280 deaths occurred in 2007 in the United States alone [18, 19]. It occurs in female population of all ages, including infancy, childhood and even in fetus [24]. But most of the cases have been reported in the age group of 60-74 [21-24].

Of the various cancers, ovarian cancer is the hardest one to detect in its earlier stages. This is because most of the women show absolutely no or just mild symptoms until it is in an advanced stage and difficult to treat [19-21]. Hence the relative survival rate is very low, only 46% [18, 19, 25] and it has not increased during the past 30 years. Surgery is the first step in the treatment and is also frequently necessary for diagnosis [19, 20, 26]. Chemotherapy is used after surgery to treat any residual tumors [25, 27-30]. The traditional clinical treatment technique, intravenous (IV) chemotherapy, involves infusing the drugs directly into the blood stream [31-35]. This technique has been used over the past years. It has been successful in containing the spread of tumors and hence treating many a cancer type [33-35]. However, since it is not localized, it exposes the whole body to chemotherapeutics [33-38]. Hence, apart from destroying tumor cells, they also attack normal healthy cells [32-35] resulting in extensive temporary side effects such as nausea, loss of appetite, hair-loss, rashes on the limbs, mouth sores, bleeding, fatigue and infection or severe side effects like kidney or nerve damage [33-38].

Another technique which is in use in recent years is the intraperitoneal chemotherapy [33, 39-44]. This is more localized than the above mentioned technique since the drugs are delivered directly into the intraperitoneal cavity [33, 39] using a catheter- a tube through

which drugs can be administered on a regular basis [40-44]. But this technique has challenges of its own. It involves exposing tumors present in the abdominal cavity to higher concentrations of the drug for longer periods of time resulting in increased hematologic, metabolic and neurologic toxicity [32, 33, 39-45]. The catheters may become plugged over time [45, 46] leading to infections and other complications [40-44, 46]. Moreover, this technique is available only to select patients with minimal residual tumors [1, 46].

To overcome the tribulations associated with ovarian cancer treatment and to provide a localized low cost drug delivery system, we have designed an ingenious 'Smart Packaged Drug Delivery System' consisting of drug encapsulated non-ionic surfactant vesicle/ niosome embedded in a cross-linked temperature sensitive hydrogel (chitosan) network. The term 'Smart Packaged' is used due to the fact that it is responsive to external stimulus, in this case, to temperature. Our system is a clear liquid at 25$^{o}$C (room temperature), however, as the temperature is raised to 37$^{o}$C (body temperature), it turns into an opaque non-flowing gel. After surgery the tumor resection sites are inhomogeneous [32, 46] which makes it difficult for the drugs to reach each and every part of the tumor cavity [27, 39, 46]. Our system will be particularly useful here since in the liquid state (at room temperature) it can be injected into the tumor cavity and as it starts to gel (at body temperature) it can take up the shape of the cavity thus ensuring uniform exposure of drugs to every part of the residual tumor.

## 1.3 Significance of this Research

The past decade has seen an enormous advance in the designing and development of new and improved techniques for drug delivery. Localized and regulated release of drugs have been achieved through their encapsulation in a variety of vehicles such as microspheres [47-52], nano-particles [53-57], micelles [58-61], liposomes [62-67], niosomes [68, 69] and biodegradable polymers [70-75]. Encapsulation of drugs not only facilitates a protective environment for drugs that are labile, but is also effective in reducing the toxicity to healthy cells by restricting the release of drugs to the required extent. A key issue, nonetheless, concerns sustained release over extended periods of time with precise control of drug dosage [76, 77]. In this study we present the validation of protecting the drugs and providing controlled release by packaging them simultaneously in two vehicles, a bilayer non-ionic surfactant vesicle- niosome and a thermo-sensitive cross-linked hydrogel- chitosan. This double packaging or 'package-within-a-package' system can be fine-tuned to achieve precise control over the release amount and release time.

Liposomes have been used for controlled delivery over the years. They are lipid bilayer vesicles which can be used as delivery vehicles for intravenous administration [63, 65, 67, 78]. Their versatile nature allows for their application in diverse fields. They can be used to encapsulate wide variety of drugs with different polarity, size and charge [63, 65, 67, 78]. Although liposomes have shown promise over the years, they have certain inherent disadvantages. They are prone to degradation due to oxidation of the phospholipids [63, 65, 67, 78, 79], hence making storage and handling difficult. In

addition, the synthesis of phospholipids is expensive as is the case with naturally occurring phospholipids [63, 65, 67, 68, 78]. Another mode of drug delivery is a microsphere which comprises of a hollow spherical shell [47-52]. They are made of biodegradable polymers and are encapsulated with therapeutics. The sizes of these particles are usually in the micrometer range [47-52]. The encapsulated therapeutic is released at the targeted site by the degradation of the outer polymer shell [47-52]. Although microspheres provide localized delivery, their disadvantages far outgrow their advantages. They are difficult to manufacture and each distinct application requires a customized fabrication process [49-52, 80]. This puts a large burden on its cost efficiency. All the more, nearly 25-50% of drugs can be lost during the encapsulation process [49-52, 80] which adds to the cost of its manufacture, making it an inefficient mode of drug delivery. The components used in this drug delivery design strategy were chosen in view of their inherent advantages over other components. The first component is a non-ionic surfactant vesicle, also known as a niosome. Niosomes, which are closed bilayer structures [79] with a hydrophilic core and a hydrophobic bilayer [68, 79, 81-84], have been proven to be more chemically and physically stable in solution [81-85], less expensive [79, 81-84] and easier to manufacture and store [68, 81-84] as compared to other categories of bilayer vesicles such as liposomes and other drug delivery carriers such as microspheres. The utmost advantage of niosomes is that since they are uncharged, there is no charge-charge interaction between the encapsulated drug and the niosome [81-84].

Hydrogels, which consist of a network of polymer chains, are insoluble in water although they can absorb large quantities of water [53, 86-94]. Hydrogels possess many desirable physicochemical characteristics and hence they find widespread applications in drug delivery [73, 87, 89, 91, 92, 95]. Their manufacturing process is relatively simple and thus cost effective [53, 86-94]. Hydrogels, such as poly-NIPAAm, though thermo-responsive and biocompatible [96-99] tend to impart toxicity over extended periods of time due to their lack of biodegradability [86, 100]. This characteristic of poly-NIPAAm makes it an ineffective alternative for drug delivery over extended periods. Polyethylene-glycol (PEG) is highly biocompatible [101-105]. However it is not biodegradable [101-104], and hence it is difficult for the body to dispose it. Another thermo-responsive system: PEG and poly(lactic acid) block copolymers [106-110], which gels when cooled to 37$^{o}$C from its solution state at 45$^{o}$C, poses the risk of damaging the drug due to the need to heat the system for drug incorporation [111]. This attribute makes the system less realistic [111]. To accommodate for these shortcomings, we chose the second component of our delivery system to consist of a biodegradable, cross-linked, thermo-responsive polymer hydrogel chitosan, a biopolymer obtained from crustacean shells [112-117]. It has innumerable advantages relating to its biodegradability, biocompatibility [100, 113-117], non-toxicity [113-118], ease of availability and cost effectiveness [100, 113-117]. Nanoparticles and vesicles made from polymeric chitosan have been used to encapsulate cancer drugs. However, when such systems are used, drug clearance occurs at high rates and low control over release time is shown [119]. On the other hand, by enclosing the drug first in the niosomes and then embedding them in the polymeric chitosan network, complete control of the release amount and time can be achieved. Cross-linked chitosan,

can be made to respond to external stimuli such as temperature, pH and ionic strength [95, 113-117]. In this study we concentrated on the former type rendered temperature sensitive by the addition of a cross-linker, ß-glycerophosphate [100, 112, 120].

The dual packaging concept in the novelty of this drug delivery mechanism is attributed to the amalgamation of two packaging systems (niosome and chitosan), which ensures the ability to control the release by fine tuning either the niosome/chitosan or both lending a double control over the release. Control over the mesh size in the chitosan network is important since niosomes would pack loosely or densely depending on this parameter. Mesh size can be controlled by modifying the ratio of the cross-linker ß-glycerophosphate to chitosan. This drug delivery system provides stability to the niosomes and an additional control over the release rate. Since the mesh size of the cross-linked chitosan can be controlled by the amount of ß-glycerophosphate added, this system can be applied directly to the tumor site, thus enabling the stabilization of the drug and preventing systemic exposure to healthy cells. Other important characteristics that make the niosome/chitosan system attractive is the ability of sustained drug delivery over extended periods, which eliminates the need for frequent administration, and that the drug efficacy remains intact since therapeutics are encapsulated in non-ionic systems (niosomes), which guarantee drug stability. The components used in the system are biocompatible and biodegradable and is readily available and cost effective. All these characteristics make the chitosan-niosome an ideal drug delivery system. Potential applications include intra-cavitary drug delivery in ovarian cancer, brain tumors, and in the administration of labile drugs.

## 1.4 Components in the Drug Delivery System

A number of components have been employed in this drug delivery system. These are described in detail in the following sections.

### 1.4.1 Non-Ionic Surfactant Vesicles/ Niosomes

The first component in our drug delivery system is a non-ionic surfactant vesicle also known as a niosome. It is a bilayer vesicle formed by the self-assembly of non-ionic amphiphiles [68, 69, 81, 83, 84] (Figure 1.1). This process occurs in an aqueous medium and the bilayer formation transpires through the application of either physical agitation or heat as it is not a spontaneous process [68, 69, 81, 83, 84]. Hydration leads to vesicle formation where the hydrophilic head group is in contact with the aqueous solvent and the hydrophobic tail group is shielded from the same [68, 69, 84, 121]. The resulting vesicle has a hydrophilic core and a hydrophobic bilayer [68, 69, 84]. Therapeutics can be encapsulated either in their core or the bilayer depending on their polarity. Additionally, the surfaces of the niosomes can be functionalized for targeted delivery. Niosomes are non-toxic [68, 69, 84] and increases the therapeutic efficiency of the drug by restricting its action to the target cells, thus preventing exposure of normal cells to the therapeutics [68, 69, 84]. It also provides a protective shield to the encapsulated therapeutics and maintains its efficacy and stability [68, 69, 84]. Since the therapeutics is encapsulated within the niosomes, they aid in the controlled delivery as well. The surfactants used in niosome formulation are biocompatible, biodegradable as well as non-immunogenic making niosomes an ideal candidate for drug delivery [68, 69, 84]. Above

all, the storage and handling of niosome does not require any unique condition, making it cost effective as well. Niosomes are also osmotically active and swell or shrink depending on the tonicity of [44] their environment. Osmotic swelling, in particular, can drastically enhance the permeability of niosomes [45] and alter release rates. Release from niosomes, however, can be modulated [46] independent of environment by embedding the niosomes in chitosan.

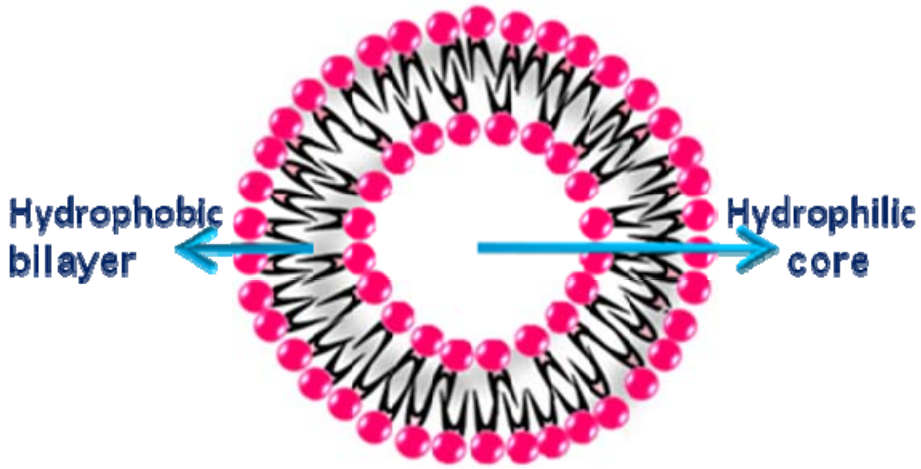


**Figure 1.1** Illustration of a non-ionic surfactant vesicle/niosome

The niosomes used for this study were prepared by thin film hydration of the surfactant sorbitan monostearate, Span-60 (figure 1.2), cholesterol (figure 1.3) and dicetyl phosphate (figure 1.4) in chloroform. Vesicle stability is provided by cholesterol which decreases their permeability and enhances solute retention [68, 122, 123]. Encapsulation efficiency would be lowered if the membrane were more permeable (cholesterol free) since such a membrane would entrap lower amounts of the drug [68, 69, 123]. The third constituent in niosome formulation, dicetyl phosphate is used to prevent aggregation of

the vesicles by providing electrostatic stabilization [69, 85, 123]. Surfactants form vesicles depending on the following two conditions: i) the hydrophobic lipophilic balance (HLB) and ii) the critical packing parameter (CPP) [68, 69, 84]. The surfactant used in this study, Span-60 or sorbitan monostearate has been found to form a vesicle when the HLB falls between 4 and 8 [69, 124, 125]. CPP, which is a dimensionless number, is a measure of the aggregation ability of the amphiphiles [68, 69]. It is measured using the formula CPP = $\upsilon / l_c a_0$; where $\upsilon$ = hydrocarbon chain volume, $l_c$= critical hydrophobic chain length (the length above which the chain fluidity of the hydrocarbon may no longer exist), and $a_0$= area of hydrophilic head [123-125]. A CPP value of 0.5 – 1.0 was indicated as the range where the amphiphiles would form a vesicle [121, 123-125].


**Figure 1.2** Structure of Span-60 (sorbitan monostearate)

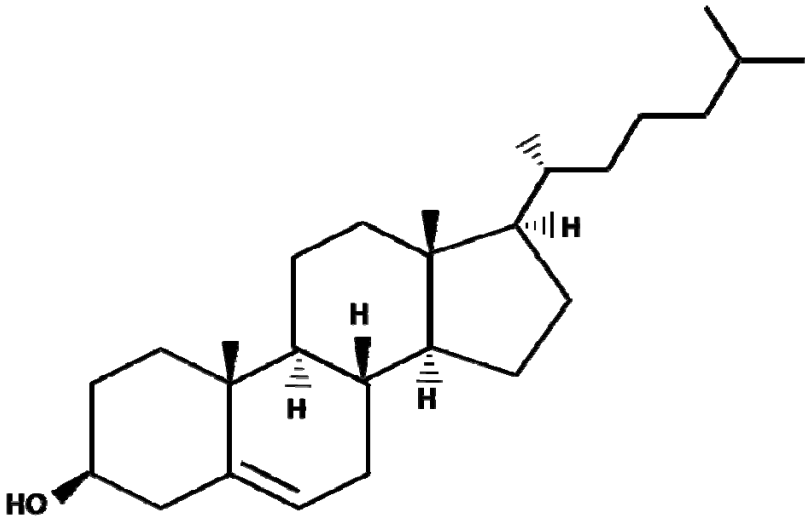


**Figure 1.3** Structure of cholesterol

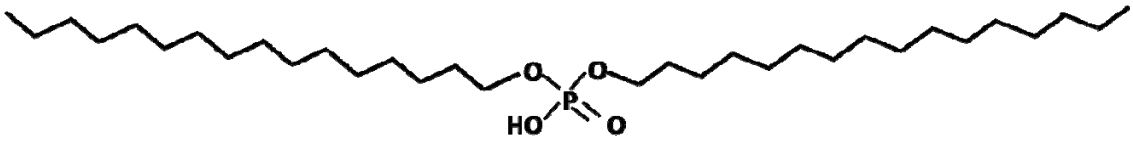


**Figure 1.4** Structure of dicetyl phosphate (DCP)

Another factor to be considered in vesicle formation is the temperature of hydration. This temperature must be above the gel to liquid transition temperature of the surfactant [124, 125]. The niosomes used in this work was found to have a hydration temperature of 60$^{o}$C which is the transition temperature of the surfactant Span-60 [121]. The type and physical

nature of the molecule encapsulated within the niosome influences their stability [68, 69, 85]. Niosome dispersion is considered to be stable when their sizes do not change with time and the quantity of the encapsulated molecule remains constant without any leakage [68, 69, 85]. Additionally, the membrane constituents should not produce any precipitation with time. The storage temperature of niosome is another factor that determines whether they would remain stable for a longer period of time [68, 69, 85]. Changes in storage temperature would lead to changes in the properties of the individual constituents or the system as a whole and hence results in an unstable system [68, 69, 85]. Further, incorrect storage temperature would also result in an increase in the release of the encapsulated molecules. Hence, in the formulation of niosomes certain factors are essential such as the hydration type and temperature, the nature of the encapsulated molecule, storage temperature [68, 69, 85] etc.

### 1.4.2 Temperature Sensitive Cross-Linked Chitosan Hydrogel

Chitosan (figure1.5) is an amino-polysaccaride obtained by alkaline deacetylation of chitin (figure 1.6), which is a natural component of shrimp or crab shells [112, 113, 120, 126, 127]. It is a copolymer of glucosamine and N-acetyl glucosamine [120, 126]. Chitin is a naturally occurring polysaccharide. However, its application in biomedical field is limited because of its chemical inertness. Deacetylation of chitin with concentrated alkaline solution converts the acetamide groups to amino groups [120, 126]. The resulting product is known as chitosan- a biocompatible and biodegradable pH dependent cationic polymer [112, 113, 126, 127]. It does not produce any inflammation or allergic reactions

in the human body and is not toxic [118]. It is known to act as an antimicrobial agent and has the ability to absorb harmful metals like lead (Pb), cadmium (Cd) and mercury (Hg) [112]. It is digestible by lysozyme depending on the amount of N-acetyl groups and their distribution in the backbone [100]. Over a period of time, chitosan breaks down to amino sugars [112, 113, 127] which are harmless to the human body, and hence, it is readily absorbed.

Chitosan is mucoadhesive and is a cationic polymer which means it has a positive charge [112, 118, 120]. Its structure is similar to cellulose. It is a long chain polymer and its average molecular weight ranges between 3,800 and 500,000 Da [112, 120]. Commercially, chitosan is available in two molecular weight ranges: i) low molecular weight chitosan which has an average molecular weight from 50,000-190,000 Da; ii) and medium molecular weight chitosan with average molecular weights from 190,000-310,000 Da [112, 113, 127]. Chitosan is insoluble in water due to the presence of free amino groups [126, 128]. Hence, it has to be dissolved in an acidic medium [126, 128]. For this study, 0.1M HCl was used as the dissolving medium for chitosan. The free amino groups provide sites that are readily available for cross-linking. Since chitosan is cationic, it permits ionic cross-linking [112, 113, 127]. Hence multivalent anions are suitable candidates as cross-linkers.

Chitosan has been formulated in a variety of particles for drug delivery. These include capsules, microspheres/ microparticles, nanoparticles, beads, films and gels [53, 112, 113, 126-129]. Formulation of these particles has shown to be advantageous over

conventional methods since they can improve the efficacy of the encapsulated therapeutics and reduce their toxicity [112, 113, 127]. Further, it also increases patient compliance. However, encapsulating therapeutics directly into these particles has certain disadvantages. Since the pores of these particles are relatively large, they provide channels for drug passage [53, 126, 128]. Thus a greater clearance for therapeutics is observed as compared to particles formulated from surfactants and the like [126, 128, 129]. This study provides a solution to this problem by encapsulating therapeutics initially into nanoparticles niosomes and further embedding these particles into the chitosan gel which prevents premature clearance of therapeutics from chitosan.

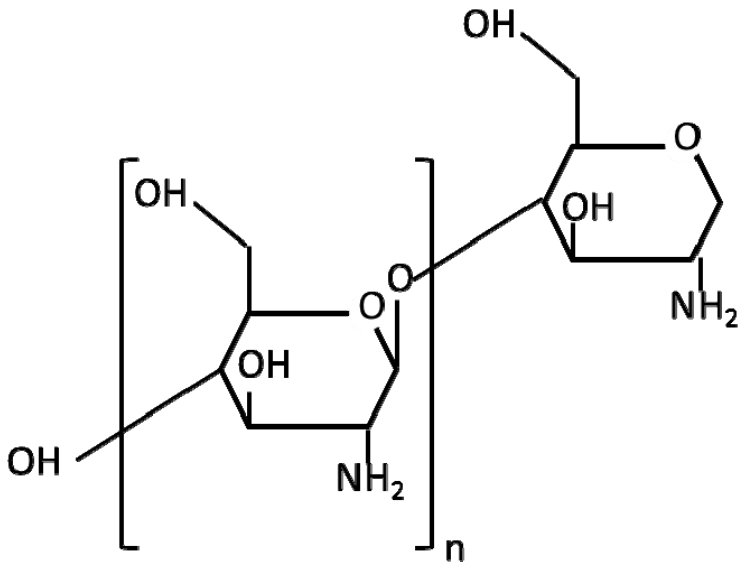


**Figure 1.5** Structure of chitosan

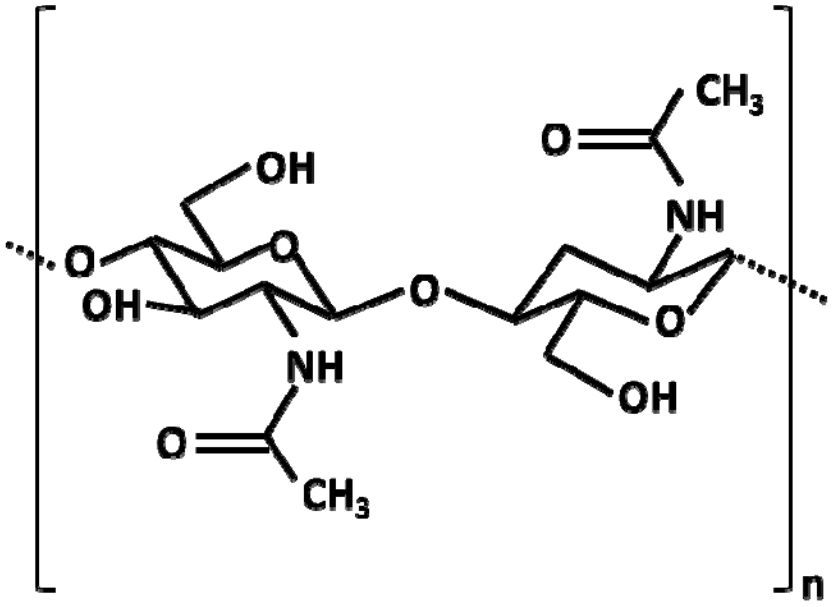


**Figure 1.6** Structure of chitin

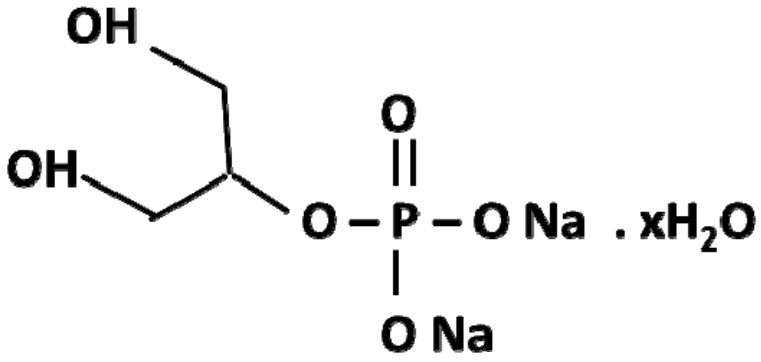


**Figure 1.7** Structure of the cross-linker ß-glycerophosphate

Chitosan can be made to respond to external stimuli such as temperature, pH and ionic strength [95, 112, 113, 127]. In this study we worked on chitosan, rendered temperature sensitive by the addition of a polyol ß-glycerophosphate (figure 1.7). Chitosan is typically not soluble in water, but its solutions can be obtained in acidic aqueous medium which protonate chitosan amino groups, rendering the polymer positively charged and thereby overcoming associative forces between chains [112, 113, 120, 127]. ß-glycerophosphate plays three essential roles: i) to increase the pH to the physiological range of 7.0-7.4; ii) to prevent immediate precipitation or gelation and iii) to allow for controlled hydrogel formation when an increase in the temperature is imposed [100, 120, 126]. The resulting chitosan- ß-glycerophosphate system is a liquid at room temperature (25$^{o}$C) and gels as the temperature is increased to 37ºC , the body temperature [100, 112, 113, 120, 127] (figure 1.8). Three types of interactions are involved in the gelation process: i) electrostatic attraction between the ammonium group of the chitosan and the phosphate group of the glycerophosphate; ii) hydrogen bonding between the chitosan chains as a consequence of reduced electrostatic repulsion after neutralization of the chitosan solution with GP and iii) chitosan- chitosan hydrophobic interactions [95, 112, 113, 127].

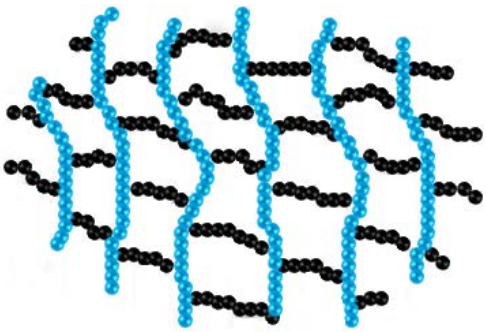

**Figure 1.8** Schematic of cross-linked chitosan

### 1.4.3 Molecules Encapsulated

In this research various molecules were encapsulated into the delivery system as described below:

#### 1.4.3.1 Fluorescent Molecule 5,6-carboxyfluorescein

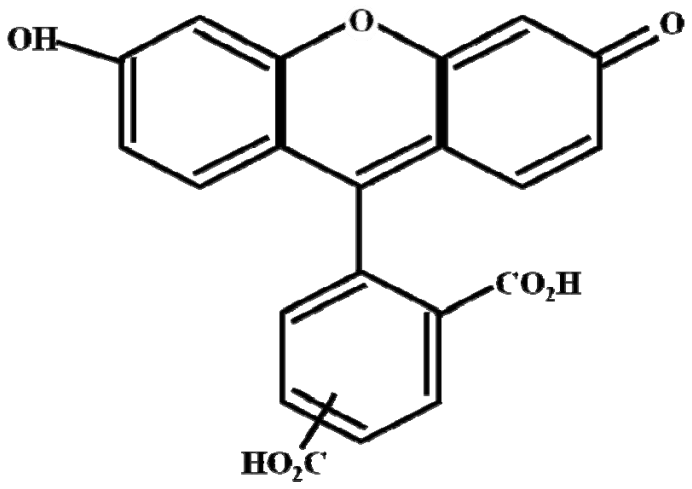


**Figure 1.9** Molecular structure of 5,6-carboxyfluorescein

5,6-carboxyfluorescein is a fluorescent synthetic yellow orange organic compound available in solid form (figure 2.3) [130]. Its chemical formula is $C_{21}H_{12}O_7$ and molecular weight is 376g/mol [130]. It is soluble in DMF/DMSO or in water having a pH greater than 7.0 [130]. The molecular structure of 5,6-carboxyfluorescein[130] is shown in figure 1.9. It has an absorbance at 494nm and emission at 519 nm.

Increase in the pH (above 7.0) of this molecule results in deprotonation of the hydroxyl group making it a trivalent anion [130]. The carboxyl group can be attacked at either the 5 or 6 carbon in the structure [130]. It is a membrane impermeant and can be loaded into cells by microinjection [131]. Since it is a fluorescent molecule it should be stored at a temperature of 4$^{o}$C and should be protected from direct light [130].

#### 1.4.3.2 Paclitaxel

Paclitaxel is a white to off-white powder with molecular formula $C_{47}H_{51}NO_{14}$ and molecular weight 853 Da [39, 132]. Its melting point is 217$^{o}$C (Figure 1.10) [132]. It is a diterpenoid pseudoalkaloid- a mitotic inhibitor, which was first isolated from the bark of the pacific yew tree in 1967 [132]. Its anti-tumor activity stems from the fact that it is very effective in stabilizing the microtubules to depolymerization, thus interfering with the process of cell division [39, 132].

Microtubules are involved in cellular activities such as mitosis and transport of organelles within the cell and paclitaxel interferes with their normal breakdown thus restricting the abnormal growth of cells [39, 45, 132]. It is used as an anti-tumor agent against a wide variety of tumors like ovarian cancer, breast cancer, head and neck cancers, lung cancer and prostate cancer [39, 45].

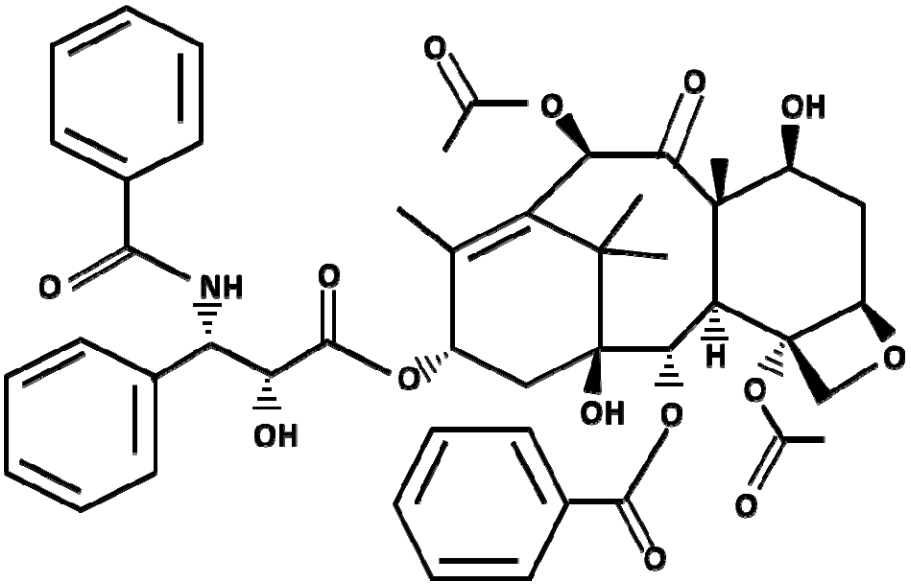


**Figure 1.10** Molecular structure of paclitaxel

Although paclitaxel has an immense anti-tumor activity, it has few shortcomings as well. It is highly hydrophobic and hence poorly soluble in aqueous medium although it can be dissolved in organic solvents [39, 45]. Also, pH manipulation does not enhance its solubility since paclitaxel lacks ionizable functional groups in a pharmaceutically useful range [39, 132]. Other forms of increasing the solubility such as production of alternate salts are also not feasible for paclitaxel [39, 132]. Owing to its highly hydrophobic nature it has to be administered in combination with other formulation vehicles [39, 132]. One such formulation which is commonly used is Cremophor EL, which is a polyoxyethylated castor oil [39, 132]. Cremophor EL is associated with a number of side effects like peripheral neuropathy, nephrotoxicity, aggregation of erythrocytes, hyperlipidemia and hypersensitivity [39, 132]. Improvements in the formulation vehicle would not only enhance the efficacy of the drug but also help reduce toxicity associated with traditional

formulation vehicles. This is where our drug delivery system holds a plethora of benefits. Encapsulating paclitaxel in niosome followed by their embedment in the cross-linked chitosan can entirely eliminate the need for Cremophor EL. Additionally, the ability to fine tune the drug delivery system promises control over the release rates as well.

Paclitaxel conjugated with BODIPY 564⁄570 [133] has also been used in this study. BODIPY 564⁄570 (figure 1.12) is a red-orange fluorescent dye with an excitation of 564 nm and emission of 570 nm [133]. This fluorescent dye is attached to the N-benzoyl substituent of the 3-phenylisoserine part of paclitaxel [133]. In this study, conjugated paclitaxel [133] was used for *in vitro* studies using confocal microscope.

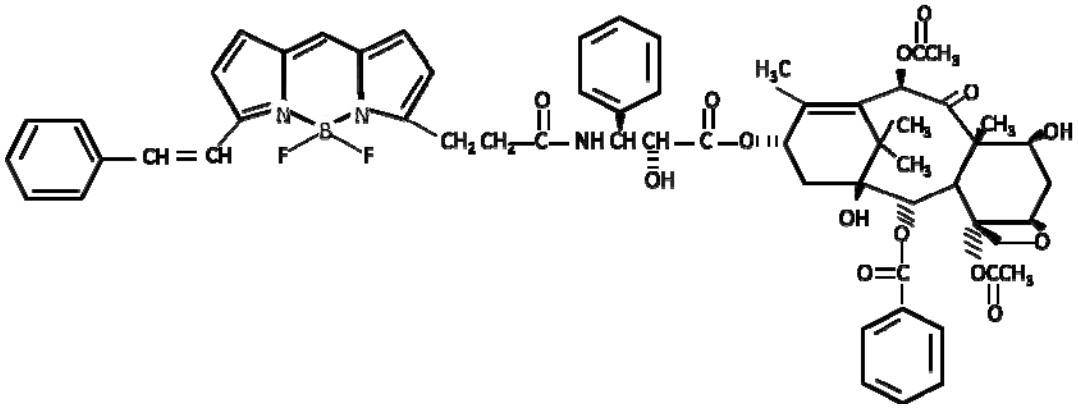

**Figure 1.11** Molecular structure of BODIPY 564⁄570

### 1.4.3.3 Carboplatin

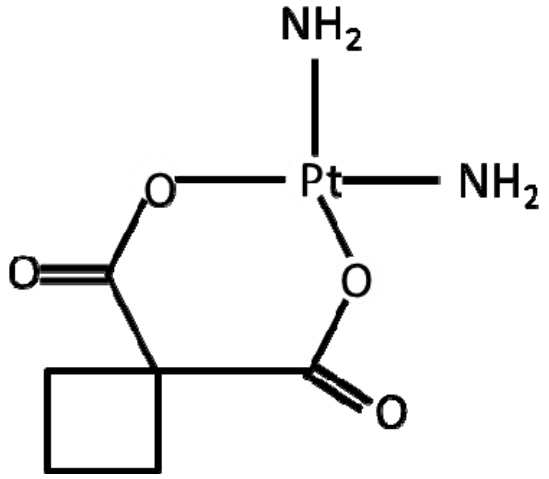


**Figure 1.12** Molecular structure of carboplatin

Carboplatin is a white crystalline solid with molecular formula $C_6H_{12}N_2O_4Pt$ and molecular weight 371.249 g/mol [134]. It is soluble in water and almost insoluble in ethanol, acetone and dimethylacetamide [134]. Carboplatin is an anticancer drug used in the treatment of several cancers especially ovarian cancer [135-138]. It is an alkylating agent and a second generation platinum drug, the first generation being its analogue drug cisplatin [139] (Figure 1.12). Carboplatin is an improvement over the platinum drug cisplatin with similar chemical mechanisms [140] but with better biochemical characteristics [136, 140] and hence lower toxicity. Carboplatin has a bidentate dicarboxylate ligand [135, 140] which differentiates it from its analogue cisplatin consisting of labile chloride ligands [137].

Carboplatin is usually administered as part of a combination drug therapy regimen consisting or two or more drugs [39]. It is used for a wide variety of tumors such as ovarian cancer, lung cancer, head and neck cancers and stomach cancer [39]. Cancer cells are destroyed by carboplatin when the drug attaches to DNA [135, 139, 140] and interfere with the repair mechanism of the cell. This leads to cell growth inhibition and cell death.

Carboplatin is less potent than cisplatin [136] even though the clinical dosage of carboplatin is four times that of cisplatin [135, 136]. However, the effectiveness of carboplatin can be increased by incubating it in NaCl solution before administration [135, 136, 140]. In this study, carboplatin was used to study the release rate when encapsulated in the hydrophilic core of the niosome. Its effect was also studied in the 'cocktail niosomal formulation' when the hydrophobic drug was encapsulated in the hydrophobic bilayer with carboplatin encapsulated in the hydrophilic core.

The main disadvantage of carboplatin is that it is a myelosuppressant [139], which causes the platelet and blood cell output from bone marrow to decrease drastically [137, 139]. This can lead to further complications like increased chances of infections [137], which can become fatal if not remedied immediately.

In summary, figure 1.13 shows a schematic illustration of the drug delivery system that was employed for this study. This drug delivery strategy was designed to fulfill the following tasks: i) to provide controlled and targeted delivery to tumor cells while sparing normal cells; ii) to reduce the toxicity resulting from chemotherapeutics; iii) to

provide a delivery system that would be easy to manufacture and most importantly be cost effective.

This system, also called the 'Smart Packaged Drug Delivery System' consists of non-ionic surfactant vesicle/ niosome which is encapsulated with therapeutic molecules. The term 'Smart Packaged' is used due to the fact that it is responsive to external stimuli, in this case, to temperature. The molecules used for encapsulation are either 5,6-carboxyfluorescein/ paclitaxel/ conjugated paclitaxel/ carboplatin. These encapsulated niosome dispersions are embedded into a cross-linked temperature sensitive hydrogel (chitosan) network The 'Smart Packaged Drug Delivery System' is a liquid at room temperature ($25^{o}C$) and forms a non-flowing gel at body temperature ($37^{o}C$). The system has been designed such that each cross-link mesh size commensurate the size of niosomes. With time, chitosan, being a biocompatible and biodegradable polymer, breaks down into simple compounds such as amino sugars. This exposes niosomes to body fluids which eventually lead to their breakage and release of the encapsulated molecules. Desired release kinetics can be obtained by fine-tuning the properties of niosomes and chitosan such as the concentration of encapsulated molecules, size of the niosome, chitosan cross-link mesh dimensions and packaging density of the niosomes. Detailed studies of each of these parameters are discussed in the following chapters. Localized drug delivery systems might be the missing link for effective, low cost treatments that could have a significant impact in developing countries too.

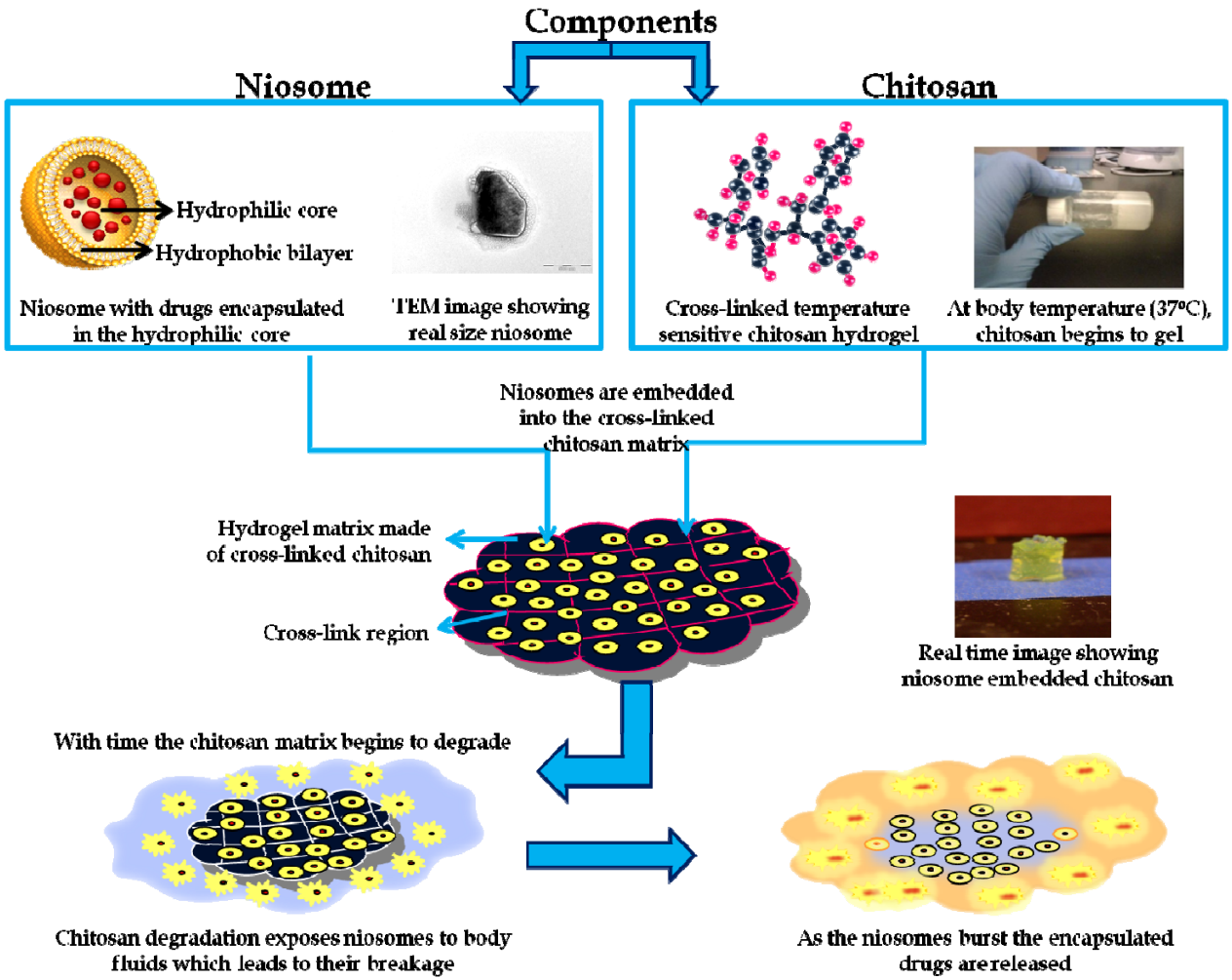


**Figure 1.13** Schematic of the smart packaged drug delivery system

# CHAPTER 2 EXPERIMENTAL PROCEDURES

## 2.1 Materials

The following materials were purchased from Sigma Aldrich : Sorbitan monostearate (Span-60) (catalog# S7010-250G), Cholesterol (catalog# C8503), Dicetyl phosphate (catalog#D2631) , Chitosan (medium molecular weight -catalog# 448877), low molecular weight- catalog# 448869 and practical grade- catalog# 419419), Beta-glycerophosphate (catalog# G9891), PBS (Phosphate Buffer Saline- catalog#P5368 and Slide-A-Lyzer Mini Dialysis Units (10K MWCO- catalog# 69570). 5,6-carboxyfluorescein (catalog# 51013) was purchased from Biotium Inc. Paclitaxel (catalog# AC32842), carboplatin (catalog# ICN19887325), round bottom flask 50ml (catalog# 10-068-1A) and glass vials (catalog#14-955-319) were purchased from Fisher Scientific. Ultracentrifuge tubes (catalog# 41121703) and caps (catalog# 338906) were purchased from Beckman Coulter. Materials for the extrusion process- mini extruder (catalog#610000), filter support (catalog#610014), 1mL syringe (catalog#610017), heating block (catalog#610024), Teflon seals (catalog#610029), plunger assembly (catalog#610032), polycarbonate (PC) membrane(catalog# 610004) were purchased from Avanti polar lipids. (Paclitaxel-BODIPY® 564⁄570 (catalog# P7500) was purchased from Invitrogen. Glass bottom dishes (catalog# P35G-1.5-20-C.S) for confocal imaging were purchased from Mattek Inc. All other chemicals were reagent grade.

## 2.2 Methods

### 2.2.1 Preparation of Niosomes

#### 2.2.1.1 Niosomes with 5(6)-Carboxyfluorescein

5(6)-carboxyfluorescein was dissolved in 0.01M PBS and concentrations of 2mM, 5mM, 10mM, 15mM and 20mM were prepared. Niosomes were prepared by the thin film hydration method [68, 79, 85]. Surfactant Span 60, cholesterol and dicetyl phosphate were taken in a 1:1:0.1 molar ratio respectively and dissolved in 3 ml of chloroform. This solution was transferred to a 50mL round bottom flask attached to a Buchi rotary evaporator. Chloroform was allowed to evaporate leaving behind a thin film. The film was left to dry overnight. Hydration of the film was performed in the following way: 3mL of 5(6)-carboxyfluorescein solution was added to the flask containing the thin film and placed in rotary evaporator maintained at 60$^{o}$C. After the film dissolved, the flask was taken out. This process takes an hour. The next step is the size reduction process which was done using a mini extruder. Mini extruder consists of a heating block over which the extruder and two syringes were placed as shown in figure 2.1(A). Syringes were inserted into the extruder. Niosome solution was taken in one syringe and passed through the extruder into the other syringe. This process was repeated 12 times. The extrusion process was carried out at 60$^{o}$C by placing the heating block over a hot plate.

Two different protocols were followed for niosome synthesis: i) the first one involved making thin films, hydrating them with a fluorescent dye 5,6-carboxyfluorescein,

constricting their size by extrusion (Figure 2.1) and removal of the free dye by ultracentrifugation (60000 rpm for 40 minutes); ii) in the second method all the steps till the hydration were the same after which they were sonicated for 15min. The free dye was removed using gel exclusion chromatography. Niosomes were prepared with various concentrations of the dye and were stored at 4$^{o}$C prior to embedding into the chitosan network.

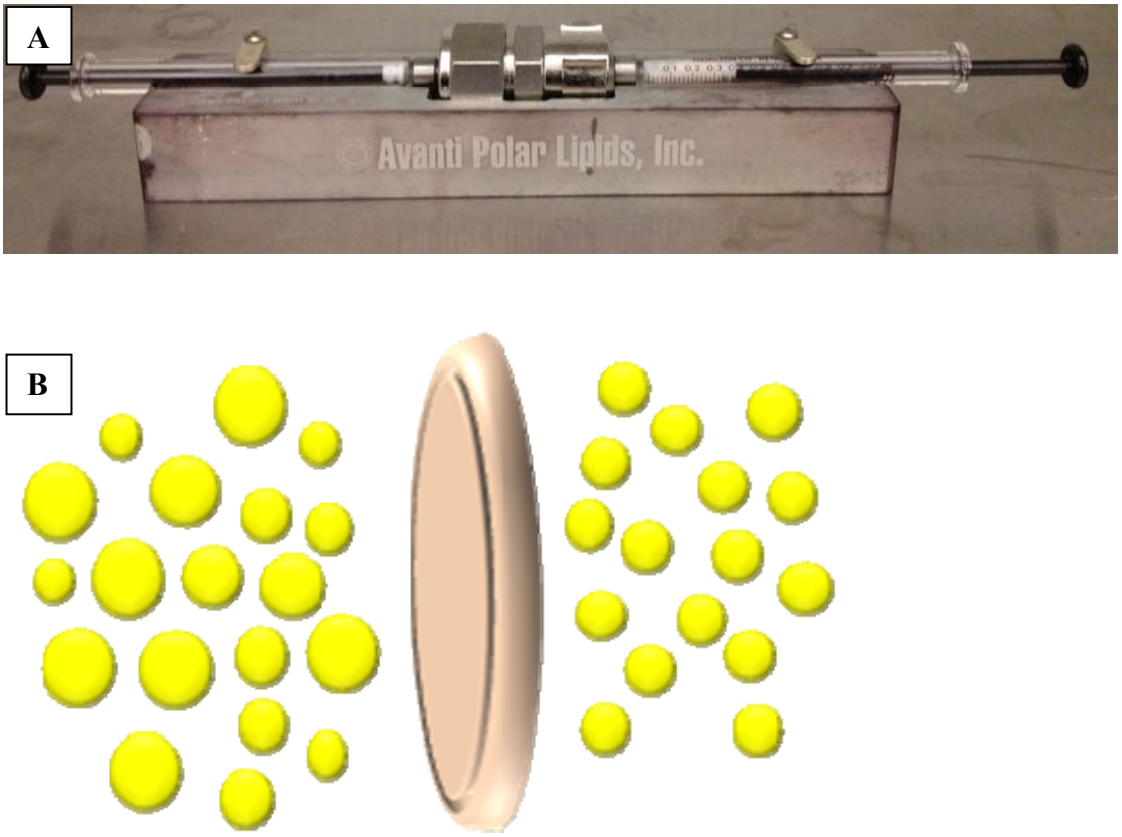


**Figure 2.1** Experimental set up for mini extruder. The mini extruder consists of a heating block, two 1ml syringes inserted into the extruder containing polycarbonate membranes (A); Extrusion process consists of passing niosomes through the mini extruder 12 times at 60$^{o}$C which gives niosomes with narrow size distribution (B)

#### 2.2.1.2 Niosomes with Paclitaxel

Surfactant Span-60, cholesterol and dicetyl phosphate in 1:1:0.1 molar ratio respectively were dissolved in chloroform. Paclitaxel was added to this solution and thin films were made using round bottom flask and Buchi evaporator as described in section 2.2.1.1. Hydration was done using 3ml of 0.01M PBS at 60$^{o}$C. As with the previous methodology the size was constricted by extrusion. Free dye was removed by ultracentrifugation. Concentrations of paclitaxel used were 2mM, 5mM, 10mM, 15mM and 20mM.

#### 2.2.1.3 Niosomes with Carboplatin

The same methodology as with 5(6)-carboxyfluorescein encapsulation (section 2.2.1.1) was followed here also. Thin films were made with the surfactant Span-60, cholesterol and dicetyl phosphate in 1:1:0.1 molar ratio respectively. Hydration was done using 3ml of carboplatin solution. Size constriction was done by extrusion and free drug removal by ultracentrifugation. Concentrations of carboplatin used were 2mM, 5mM, 10mM, 15mM and 20mM.

#### 2.2.1.4 Cocktail Niosomal Formulation

This formulation was designed in our lab. Using this niosomal formulation it is possible to encapsulate multiple drugs of varied polarity into the same niosome vesicle. The integrity of each drug is maintained since they are encapsulated at different sites in the same niosome and are not in contact at any time until they are at the site of delivery.

Procedure for 'cocktail niosome' formulation is as follows: surfactant Span-60, cholesterol and dicetyl phosphate in 1:1:0.1 molar ratio respectively were dissolved in chloroform. Paclitaxel was added to this solution and thin films were made. Hydration was done using carboplatin, size constricted by extrusion and free dye removed by ultracentrifugation. Paclitaxel and carboplatin concentrations used were 2mM, 5mM, 10mM, 15mM and 20mM.

### 2.2.2 Preparation of Thermo-Sensitive Cross-Linked Chitosan Solution

The second packaging system was prepared as reported in literature with slight modifications: 3ml of 65% (w/v) β-glycerophosphate solution (in water) was added to 9ml of 2.78% (w/v) chitosan solution (in 0.1M HCl) drop-wise, stirring continuously over an ice-bath. The final solution was stirred for an additional 10 minutes to ensure complete mixing. This solution contained a molar ratio of 4:1 of β-glycerophosphate: chitosan (Figure 2.2). A range of cross-link molar ratios were used in this study ranging from 3.0:1 to 5.0:1.

### 2.2.3 Preparation of Niosome Embedded Chitosan Solutions

This procedure which was designed in our lab is as follows: niosomes, stored at 4$^{o}$C was allowed to equilibrate to room temperature. They were then embedded into the chitosan network by adding them into the prepared chitosan- β-glycerophosphate solution. It was then mixed thoroughly at 25$^{o}$C (room temperature). It was then heated to 37$^{o}$C (body

temperature) to facilitate cross-linking. Niosome to chitosan-β-glycerophosphate molar ratios of 0.15:1 to 0.45:1 were used for this study.

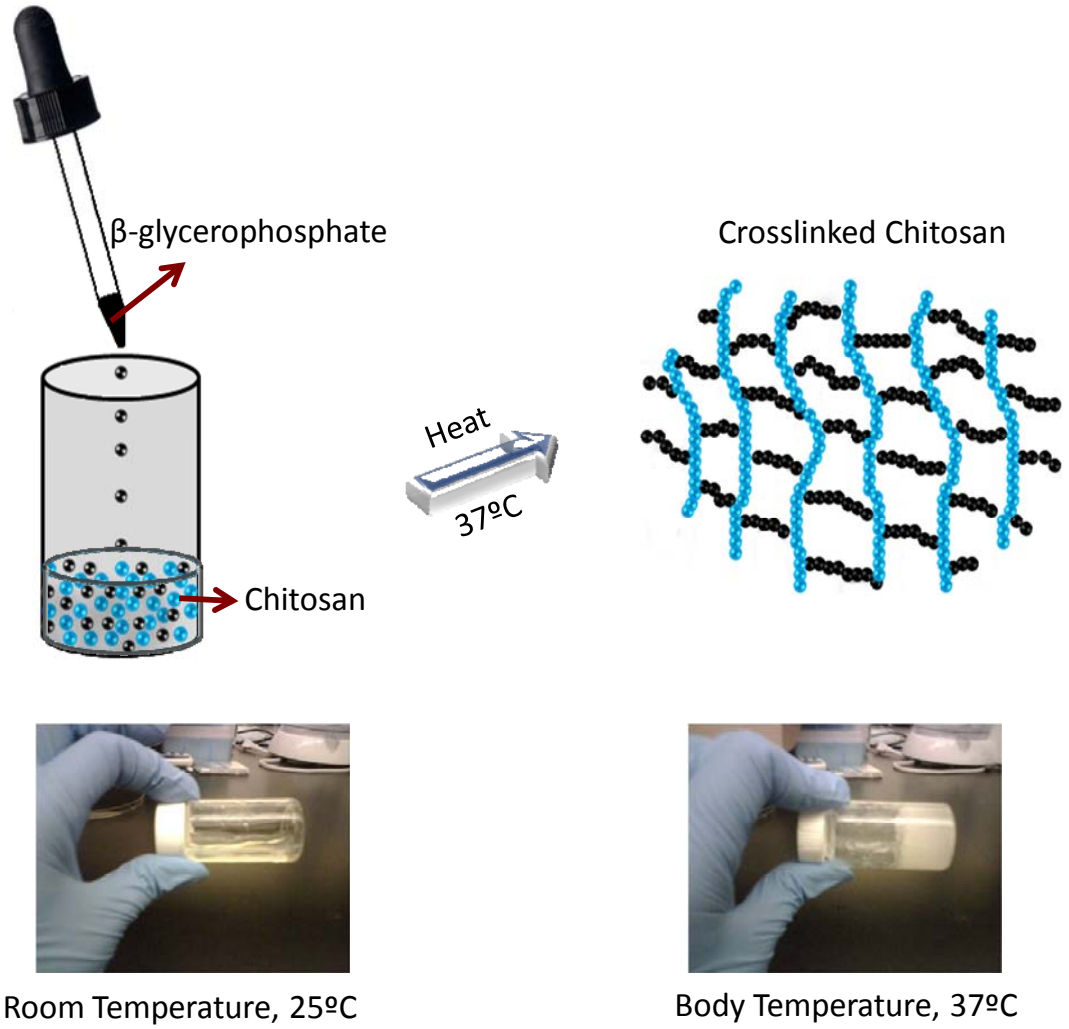


**Figure 2.2** Preparation of cross-linked chitosan solution using the cross-linker β-glycerophosphate. The resulting solution shows thermo-responsive behavior.

Parameters of importance in a drug delivery system are related to the quality of the packaging system and its composition. The parameters evaluated in this study are the effects of chitosan molecular weight, its cross-link density and the packaging density. For the cell-free studies different composition of the niosome-chitosan solution were prepared:

a) for studies on the effect of the molecular weight on the release rate three different chitosan grades were used: i) medium molecular weight (190,000-310,000 Da); ii) low molecular weight (50,000-190,000 Da) and iii) practical grade (190,000-375,000 Da). The molar ratio of β-glycerophosphate to chitosan used was 4:1 and the niosome to chitosan-β-glycerophosphate molar ratio used was 0.35:1.

b) For studies on the effect of the cross-link density, medium molecular weight chitosan and niosome to chitosan-β-glycerophosphate molar ratio 0.35:1 were chosen. Molar ratios of β-glycerophosphate to chitosan used ranged from 3.0:1 to 5.0:1.

c) For studies on the effect of the packaging density, medium molecular weight chitosan and a molar ratio of β-glycerophosphate to chitosan of 4:1 were chosen. Niosome to chitosan-β-glycerophosphate molar ratios of 0.15:1 to 0.45:1 were used.

### 2.2.4 Viscosity Measurements

The change in the viscosity of chitosan- β glycerophosphate solution with increasing temperature was measured using a falling sphere viscometer [141]. Chitosan- β glycerophosphate solution was taken in a vertical glass tube placed over a water bath. A steel sphere of known size and density was allowed to descend through this solution and

the time taken for the sphere to fall through the solution was measured from which the terminal velocity ($V_s$) of the sphere was calculated. Knowing this velocity, the size and density of the sphere, and the density of the liquid, the equation for terminal velocity from Stokes' law $V_s = \frac{2}{9}\frac{r^2\, g(\rho_p - \rho_f)}{\mu}$ was used to calculate the dynamic viscosity ($\mu$) of the fluid [58], in this case chitosan- β glycerophosphate solution. In this equation, g represents gravitational acceleration, $\rho_p$ the density of the particle and $\rho_f$, the density of chitosan- β glycerophosphate, r the radius of the particle. Viscosity of Chitosan-β glycerophosphate solution at temperatures ranging from 25°C to 37°C was measured.

### 2.2.5 Conductivity Measurements

Ionic strength of the experimental solutions were extrapolated by measuring the conductivity of niosome, chitosan solution and the media used- PBS buffer (pH 7.4) and salt free water (pH 6.0), using a multimeter [142]. The electrodes of the multimeter were kept at a finite distance (1cm) and the resistance was measured. This value of resistance is also the resistivity since the distance between the electrodes is unity (1 cm). The inverse of resistivity is the conductivity of the test sample.

### 2.2.6 Size Analysis of Niosomes

Size is an important parameter in the delivery of the encapsulated molecules. The analysis of size of the niosomes was obtained by two independent methods: Dynamic Light Scattering (DLS) and Transmission Electron Microscopy (TEM).

### 2.2.6.1 Dynamic Light Scattering (DLS)

A one-tenth (1/10) dilution of niosome dispersion was made with 0.01M phosphate buffer saline (PBS). The size distribution was measured using dynamic light scattering (DLS) (Zetasizer Nano ZS) manufactured by Malvern Instruments in the following way: 1ml of the niosome solution was taken in a cuvette and placed in the DLS. The temperature was set at 25$^{o}$C and the cuvette was equilibrated for 10 minutes. The measurements were then taken.

DLS is a size profile determination technique which makes use of the Brownian motion of small particles in a solution/dispersion [143, 144]. When monochromatic light is shone over small particles undergoing Brownian motion it produces a shift in the wavelength also known as the Doppler Shift which is caused when light hits the particles in motion [143, 144]. This shift is correlated to the size of the particle [143, 144]. The size distribution of the particles could then be computed by measuring the diffusion coefficient and using Einstein- Stokes equation [143, 144].

### 2.2.6.2 Transmission Electron Microscopy (TEM)

Transmission electron microscopy (TEM) is a useful technique in directly visualizing biological systems with high spatial resolution [145, 146]. In this technique, a high energy electron beam is transmitted through a thin film of the sample to image the structure of the sample with atomic scale resolution [145, 146].

Imaging of niosomes was done as follows. One drop of the niosome solution was deposited on a carbon-coated copper grid (Formvar/Carbon 150 mesh copper grids from Electron Microscopy Sciences) and left to adhere for one minute. The excess solution was absorbed using the tip of a filter paper and left to dry for 5min (Figure 2.3) before loading it into the vacuum chamber. The sample was then observed under TEM (Morgagni 268D TEM) at an accelerating voltage of 80kV.

TEM was also used to characterize the cross-linked chitosan with embedded niosomes in the following manner. One drop of the niosome-chitosan-β-glycerophosphate solution was stratified into a copper grid, left to adhere for one minute and placed on a spin coater for one minute at 4000 rpm. The grid was then placed on a petridish over a $37^0$C bath for 15 minutes in order to facilitate cross-linking. It was then left to dry for 5 minutes and observed under the TEM at an accelerating voltage of 80kV.

Optical analysis of the images was accomplished using Kontron Elektronik KS Lite digital analysis program v2.0. Using this program we were able to measure the area of each cross-link mesh in the image.

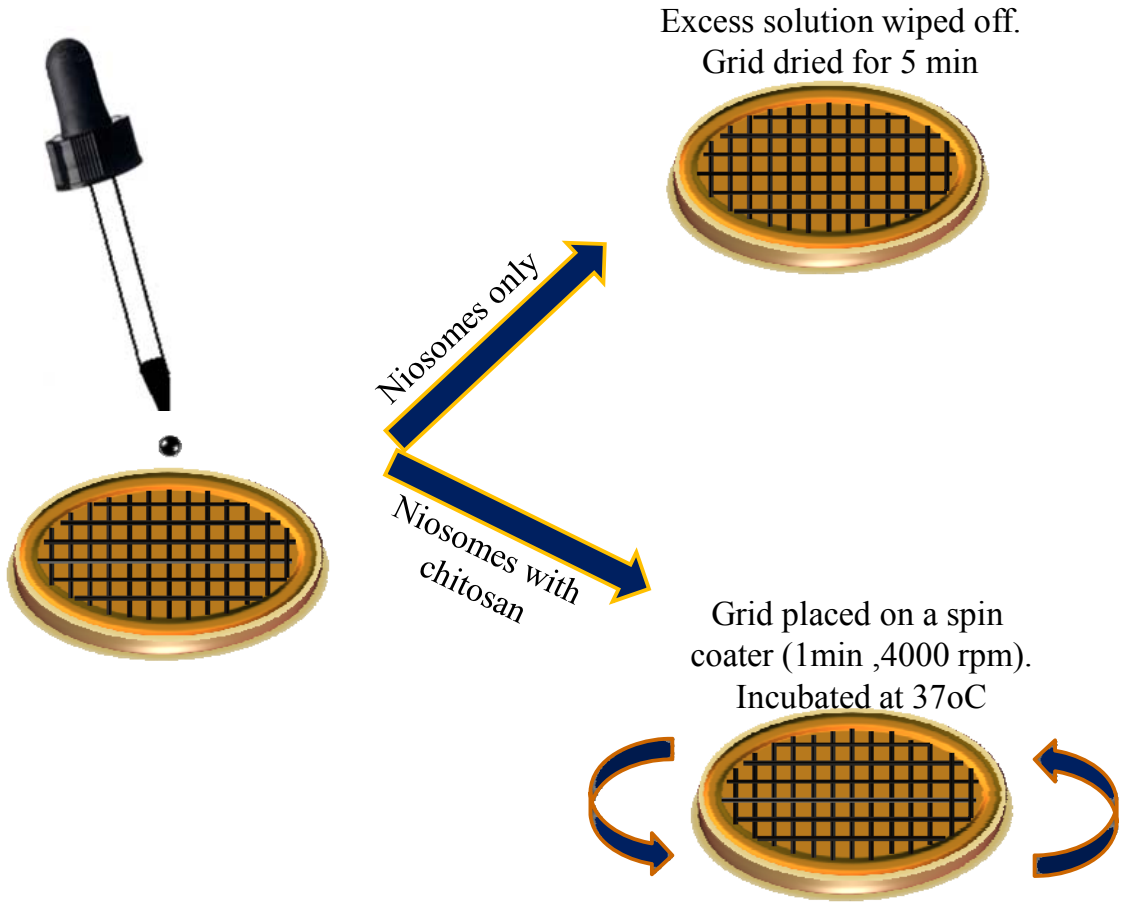


**Figure 2.3** TEM sample preparation method

### 2.2.7 Dye Release Studies

Figure 2.4 shows the experimental setup for the release rate studies. Three models were developed for the release rate studies. The first two models were set up to characterize the behavior of the niosomes alone without the chitosan network and the third model with the chitosan network.

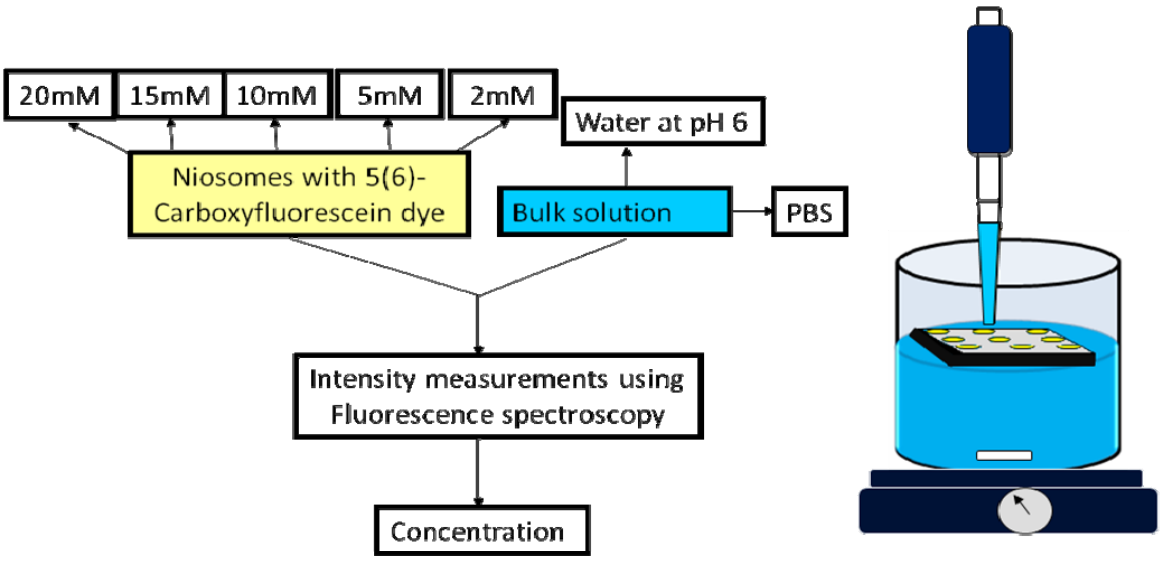


**Figure 2.4** Experimental set-up for release rate studies

The first model was designed to mimic the behavior of niosomes alone when exposed to tumor-like conditions. For this, 200 µL of niosomes (dispersed in 0.01M PBS) were placed in mini dialysis units containing cellulose membrane (MWCO 10,000). Since tumor sites have a slightly acidic pH [147] around 6.0, this condition was mimicked for our model using water at pH 6.0 as the solution medium.

The second model mimicked the behavior of the niosomes when exposed to normal physiological conditions. Phosphate buffer saline (0.01M PBS) with a pH of 7.4 was used as the medium in this case. Mini dialysis units containing niosomes were placed on dialysis floats and submerged in 100ml of their respective media maintained at $37^0$C and 200 rpm. Samples (600 µL) were collected at specified time intervals and its

concentration was measured by evaluating its fluorescence (Figure 2.4) using a fluorescence spectroscopy.

In our third model, the release rate was studied with niosomes embedded into the cross-linked chitosan network. Chitosan with different characteristics such as molecular weights, cross-link densities ranging from molar ratios 3.0:1 to 5.0:1 and niosome to chitosan ratios ranging from 0.15:1 to 0.45:1 were used for this study. In each case, the niosome mixed chitosan-β-glycerophosphate solution at 25$^{o}$C was transferred to a 30ml beaker and placed in a 37$^{o}$C bath. The solid gel thus formed was then placed in a beaker containing 100 ml of water solution of pH 6.2 maintained at 37$^{o}$C and 200 rpm. Samples of 600 μL each were collected at specified time intervals and were tested for their fluorescence. Since niosomes can also be prepared in a cocktail mixture, release studies for niosomes packed with paclitaxel, carboplatin or both the drugs were done following the above protocol. The drug concentration of the niosomes embedded in chitosan released into water (pH 6.0) were analyzed and quantified using a high performance liquid chromatography (HPLC) system. Details of the equipment are mentioned in the following section.

### 2.2.8 Equipment and HPLC Conditions

A Shimadzu HPLC system was used for quantitative studies for paclitaxel and carboplatin in the drug delivery system. The HPLC system consists of a system controller (SCL-10AVP), a pump (LC-10ATVP), a degasser (DGU- 14A), a uv-vis detector (SPD-

10AVP) and an autoinjector (SIL-10AD). The separation column used was a 5µm, 25cm x 4.6mm Inertsil ODS-3V column from GI Sciences. The mobile phase consisted of 0.2µm filtered acetonitrile and water. The sample (20µL) was injected into the system and the flow rate was maintained at 1mL/min. The detection was carried out at a wavelength of 227nm.

### 2.2.9 Studies with Cells

#### 2.2.9.1 Cell Culture and Plating

Ovarian carcinoma cell line OV2008 and normal epithelial ovarian cell lines Ilow and MCC3 were grown in culture medium (M199 + 10% FBS + L-glutamin + pennicillin + streptomycin) at 37$^{o}$C with 5% $CO_2$. Tissue culture flasks containing the cells were trypsinized with 1ml trypsin three times and placed back into the incubator for 5 minutes. 5mL of medium was then added and thoroughly mixed to separate out the cells. Next, glass bottom culture dishes (Mattek corporation P35G-1.5 20-C.S) with 1.5mL of culture medium were incubated at 37$^{o}$C for 30 minutes. The medium was then taken out and $10x10^3$ cells were plated in the center of each mattek plate and left to adhere for 2 hours after which 2mL of the culture medium was added and placed in the incubator overnight (figure 2.5).

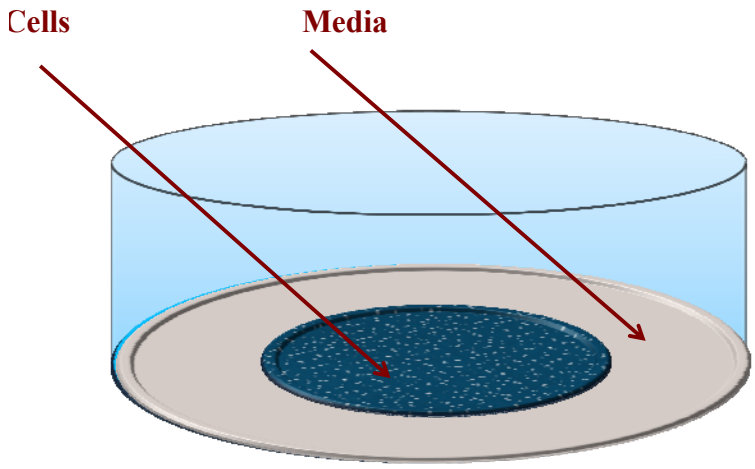


**Figure 2.5** Experimental set up for cell plating. $10x10^3$ cells were plated in the center of the glass bottom dish and 2ml of the medium was added to the outer edges till the cells were fully covered.

### 2.2.9.2 Confocal Imaging and Quantitative Analysis

The glass bottom dishes plated with the cells were taken out of the incubator right before the imaging. The media from the outer edge of the dish was pipetted out and 300µL of chitosan-niosome system encapsulated with fluorescent tagged paclitaxel (red-orange fluorescent BODIPY 564/570 paclitaxel (P7501) from Invitrogen) added to the outer edges of the dish. The dish was then placed in the incubator for 3 minutes to facilitate cross-linking of chitosan. After this 400µL of media was added to the dish and imaging of each sample were obtained with a Leica TCS SP5 laser scanning confocal microscope through a 63 ×/1.4NA or 100 ×/1.4 NA (Leica Microsystems, Germany) (figure 2.6).

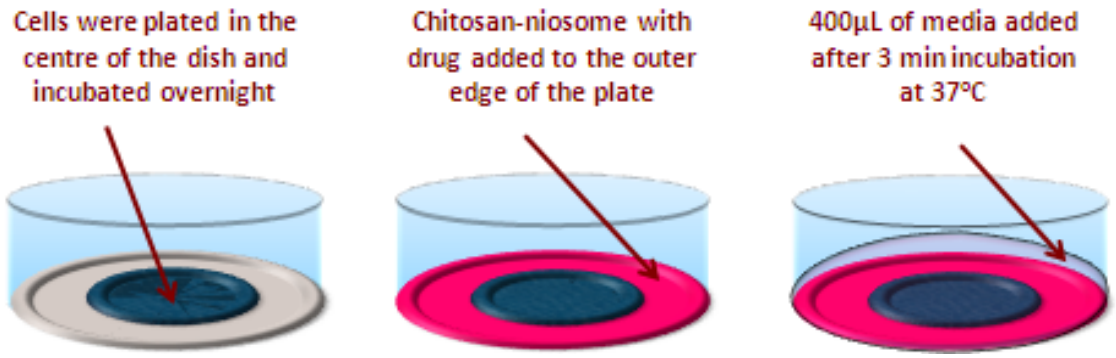


**Figure 2.6** Experimental set up for confocal imaging. $10x10^3$ cells were plated in the center of the dish and incubated overnight. The next day media from the outer edge of the dish was pipetted out and 300uL of chitosan-niosome system encapsulated with fluorescent tagged paclitaxel (red-orange fluorescent BODIPY 564/570 paclitaxel added to the outer edges of the dish. After 3 minute incubation at 37°C, 400uL of media was added. The samples were images using confocal microscopy

### 2.2.9.3 Attenuated Total Reflectance- Fourier Transform Infra-Red (ATR-FTIR) of Cell Lines- Interactions between Cell Lines and the 'Smart Packaged System'

For these experiments a flow cell containing ZnSe crystal attached to a temperature controller was used. Cells were grown in tissue culture flasks, trypsinized, counted and placed in culture tubes. The cell lines OV2008 and Ilow were incubated at 37°C and the spectra were collected for 240 min to study changes in the spectra with time. The flow cell was maintained at 37°C using the temperature controller. The reference medium used was the culture medium (minimum essential medium (MEM) + 10% FBS + L-glutamin + pennicillin + streptomycin). Chitosan was added after 240 min (4 hours) and spectra were collected for 24hours. The background used was ZnSe with 'media'. Media refers to the solution in which the cells were incubated.

### 2.2.10 *In Vivo* Studies

*In vivo* studies were performed on 8 week old female mice, Strain: FVB/NJ. Whole body imaging of the mice was done using Xenogen Bioluminescence Imaging System (Xenogen IVIS Spectrum from Caliper Life Sciences). Xenogen is a high-sensitivity, low noise, non-invasive light imaging technique that is capable of imaging bioluminescence and fluorescence in living animals. It consists of a light imaging chamber coupled to a highly sensitive CCD camera system cooled to -95$^{o}$C which can quantify single-photon signals emanating within the tissue of the living animal. It is useful in the visualization and tracking of cellular and genetic activity within a living organism. Xenogen is connected to an integrated isoflurane gas manifold that provides temporary anesthesia to the mice during the imaging process. It has the capability of imaging five mice simultaneously.

For this study, mice were anesthetized in isoflurane chamber and transferred to a thermoregulated, dark chamber of the i*n Vivo* Imaging System. 500µL of chitosan-niosome-dye system was injected subcutaneously into the left flank of the mice. Imaging was done every 3hours on the first day. Subsequent images were taken every morning for 2 weeks. After each imaging session the mice were awakened by placing them in the isoflurane chamber and switching off the isoflurane flow and thus allowing only oxygen to flow into the chamber. The complete Xenogen workstation contains the isoflurane anesthesia system (with induction chamber and oxygen scavenging), light and temperature controlled (37$^{o}$C) chamber with anesthesia nose cone manifold, CCD

camera, cryogenic unit (for cooling the camera), and computer to control and analyze biofluororescent imaging.

# CHAPTER 3 CONTROLLED RELEASE NIOSOME EMBEDDED CHITOSAN SYSTEM: EFFECT OF CROSS-LINK MESH DIMENSION ON DRUG RELEASE[1]

## 3.1 Introduction

A sustained drug release for extended periods of time with precise control over drug dosage is an important issue to be addressed for drug delivery systems [80]. A dual packaging system affords a feasible solution for this continual release over time. Liposome packaged in a polymer network has been shown to deliver small molecular-weight hydrophilic compounds for weeks together [63, 95, 100]. In this chapter, the author explores a more effective analogous system, a niosome embedded chitosan gel matrix, in an effort to assess the relationship between the embedded niosomes, gel structure and release characteristics.

Niosomes are non-ionic closed bilayer structures with a hydrophilic core and a hydrophobic bilayer [68, 69, 81, 84, 85]. They are osmotically active and swell or shrink depending on the tonicity of their environment [69]. Their osmotic swelling in particular,

[1]The figures and tables in this chapter are part of a previously published article (Williams et al., 2012) [161] and are utilized with permission of the publisher.

can drastically increase the permeability of niosomes and alter the release rates [68,69]. This chapter shows that, by embedding the niosomes in chitosan, the release from niosomes can be regulated independent of external environment. The author here uses a thermo-gelling chitosan network. The structure of this network is controlled by the addition of ß-glycerophosphate. The amino moieties present in the chitosan network provides localized counterions and increase the tonicity around the embedded niosomes [127]. This protects the niosomes from fluctuations in external environment. The relationship between the gel structure and the release of the drug molecules encapsulated in the embedded niosomes is not yet clearly understood. It is postulated that long-term release profiles will be sensitive to the niosome packing density, the cross-link density, and local structure of the chitosan gel around the niosome. No systematic investigations have yet been carried out to find out these relationships. If the niosomes fail to completely fit into the spaces between cross-links, the gel would burst out the niosomes. A more open structure might also fail to protect the niosomes properly. An optimum in the characteristics of gel structure is desired for a long-term sustained drug release. The author in this chapter carries out detailed investigations of the size of the mesh, the niosome size characteristics, and how controlled drug release could be achieved by changing either or both of these parameters. The results obtained demonstrate that the slowest release rates are achieved when the embedded niosome is of the order of the mesh size of the network. This is an important finding in design criterion and must be adhered to for obtaining the longest release rate as desired by the administrator. This would have significant positive implications for the use of these systems in intra-cavitary drug delivery in ovarian cancer, brain tumors, and in the administration of labile drugs.

### 3.2 Results and Discussion

The factors that affect the release of an encapsulated cargo from the niosomes are the niosome size and permeability which can be expressed by the equation:

$$\frac{C}{C_o} = \exp\left(-\frac{P}{R}t\right) \tag{1}$$

where, $C_o$ is the initial concentration of the cargo, R is the radius of the niosome with a permeability P, $(C/C_o)$ is the fraction of cargo remaining after time t.

Two methods for dye encapsulation-extrusion and sonication were employed for these studies. Analysis of the two methods revealed that extrusion led to a higher encapsulation efficiency (Table 3.1). Hence it was selected as the preferred method to encapsulate 5,6-carboxyfluorescein in Span-60 niosomes. The residual dye after encapsulation was removed through the process of ultracentrifugation.

Release of 5,6-carboxyfluorescein dye from Span-60 niosomes into PBS buffer is shown in Figure 3.1. Concentrations of 5,6-carboxyfluorescein ranging between 2–20 mM in PBS buffer were used for encapsulation in niosomes. The initial release is adequately described by equation (1) for all 5,6-carboxyfluorescein concentrations till a value of $C/C_o > 0.6$. Beyond the value of 0.6 there is a deviation in the release rates from the prediction in equation (1) with a slowing down of the release. It was found that the initial dye concentration in the niosomes has an influence on the release rate. This was most likely due to the osmotic effect of the encapsulated dye.

Since the exterior and interior of the niosomes contain PBS of identical ionic strength, the dye concentrations must be adequate to enhance osmotic swelling of the niosome. It is this osmotic swelling that augments the permeability of the niosomes.

**Table 3.1** Encapsulation efficiency of niosomes containing various dye concentrations.

| Concentration of encapsulated dye in niosomes [mM] | Encapsulation efficiency (%) |
|---|---|
| 2 | 60.27 |
| 5 | 62.89 |
| 10 | 64.41 |
| 15 | 66.99 |
| 20 | 68.05 |

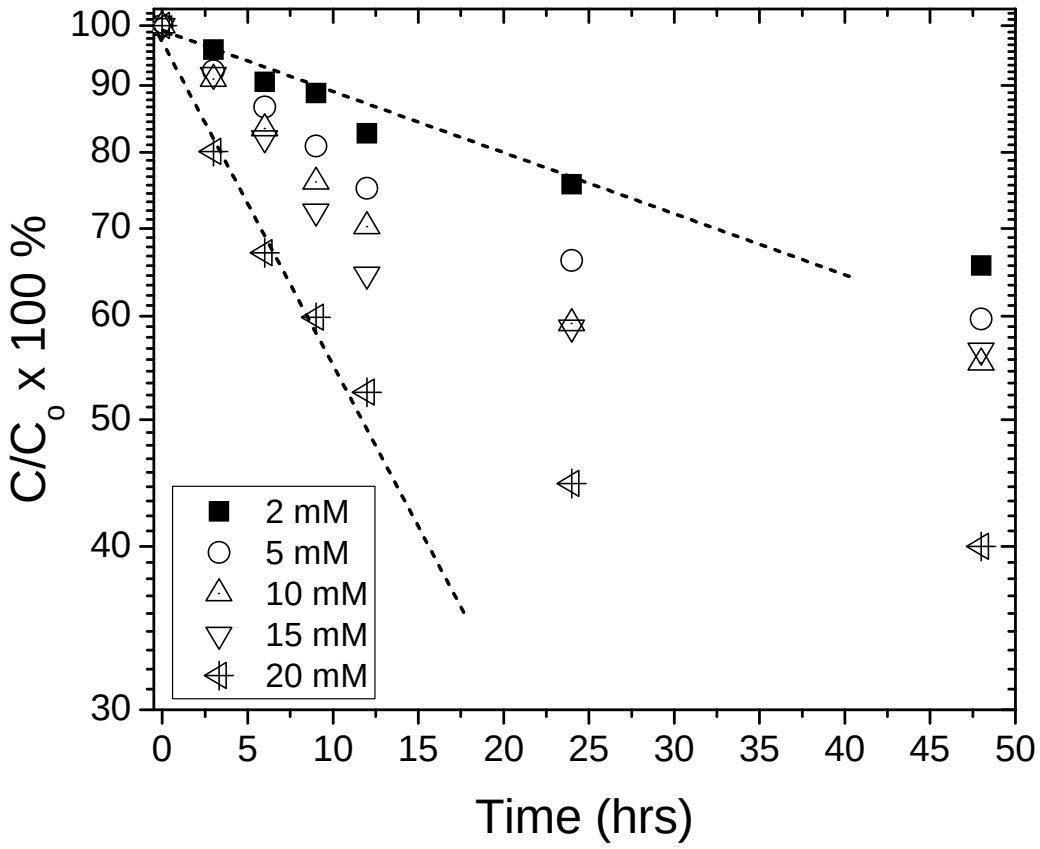


**Figure 3.1** Fraction ($C/C_o$) of 5,6-carboxyfluorescein dye retained in Span-60 niosomes upon exposure to PBS as a function of the initial dye concentration. The broken lines represent fits to Equation 1, n=3

The release rate of the encapsulated cargo is also dependent on the niosome size as predicted by equation (1). The dynamic light scattering method was used to determine the niosome size distribution. Shearing of niosomes in the extrusion process determines the final niosome size which is largely controlled by pore size. Table 3.2 shows that under identical extrusion conditions, the niosome increases in size as the concentration of the dye is increased (from 0.799 μm at 2 mM to 1.220 μm at 20 mM). We hypothesize that hydrogen bonding between the carbonyl group of the dye and the alcohol head group of Span-60 alters the rigidity of the niosome and enhances resistance to shear. Hence as the dye concentration is increased, the size of the niosome also increases accordingly. To verify that the niosome size is a function of the encapsulated reagents type, niosomes were prepared without the dye, which only encapsulated either PBS or water. In both these cases, it was observed that the size distribution obtained were similar and much smaller than niosomes with dye (0.248 μm for niosomes containing PBS and 0.235 μm for niosomes containing water). This implies that the dye molecules have an influence over the size of the niosomes. According to the prediction in equation (1), the increase in radius of the niosome with increasing dye concentration should lead to slower release rates. This is opposite the trend as seen in figure 3.1. Consequently, this indicates that the osmotic difference across the niosomal wall, and not the niosome size, is the root cause of concentration dependent release rates. Further, an increase in the hypo-tonicity of the external medium would augment the release rates. To investigate the dependence of external tonicity on the release of the encapsulated cargo, the niosomes were exposed to an extremely hypotonic medium consisting of salt free water at pH=6.0. The corresponding release rates are shown in figure 3.2. In this case also the release rate could

be predicted with equation (1), where the equation remains true till a value of $C/C_o$ greater than 0.4. Beyond this value the release deviates from the prediction and begins to slow down. Figure 3.3 shows the half-times, $t_{1/2}$, for complete release for niosomes exposed to either PBS buffer or salt-free water at pH=6.0. Half-time is the time taken for 50% of dye release. The half-time for niosomes exposed to PBS buffer is between 20-100 hours, whereas in salt-free pH=6.0 water, the half-time is between 4-10 hours which is an order of magnitude greater than in PBS buffer. The half-time decreases with concentration in both the cases, confirming dependence of release on osmotic swelling of the niosomes. Hence, these results validate that the release of the encapsulated cargo from the niosomes is sensitive to the tonicity of the external and internal environment of the niosomes.

**Table 3.2** Physical parameters of niosomes with encapsulated dye

| Encapsulated dye concentration(mM) | Size(μm) | Surface area/Volume($\mu m^{-1}$) |
|---|---|---|
| 2 | 0.799 | 7.509 |
| 5 | 0.872 | 6.881 |
| 8 | 0.920 | 6.522 |
| 10 | 0.992 | 6.048 |
| 13 | 1.035 | 5.797 |
| 15 | 1.110 | 5.405 |
| 20 | 1.220 | 4.918 |

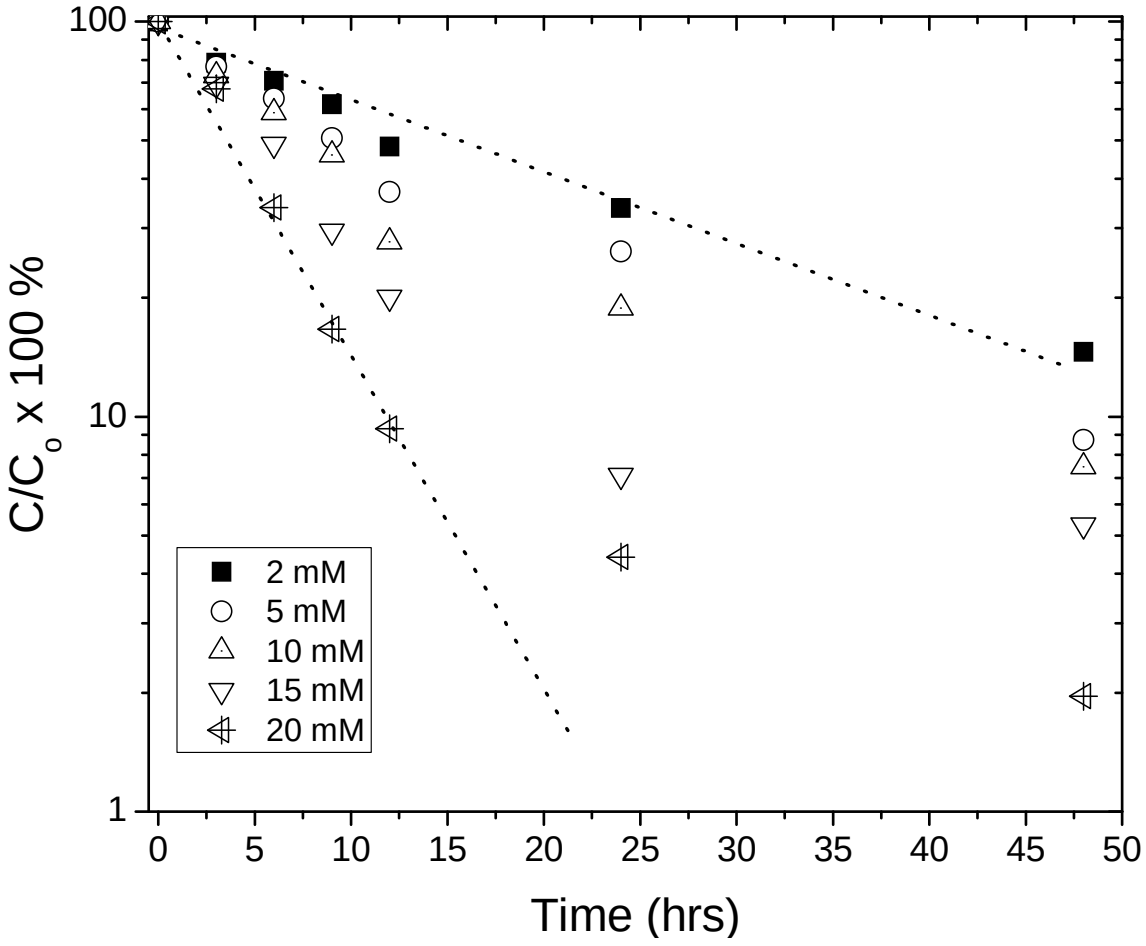


**Figure 3.2**. Fraction ($C/C_o$) of 5,6-carboxyfluorescein dye retained in Span-60 niosomes upon exposure to salt-free pH=6.0 water as a function of the initial dye concentration. The broken lines represent fits to equation (1), n=3

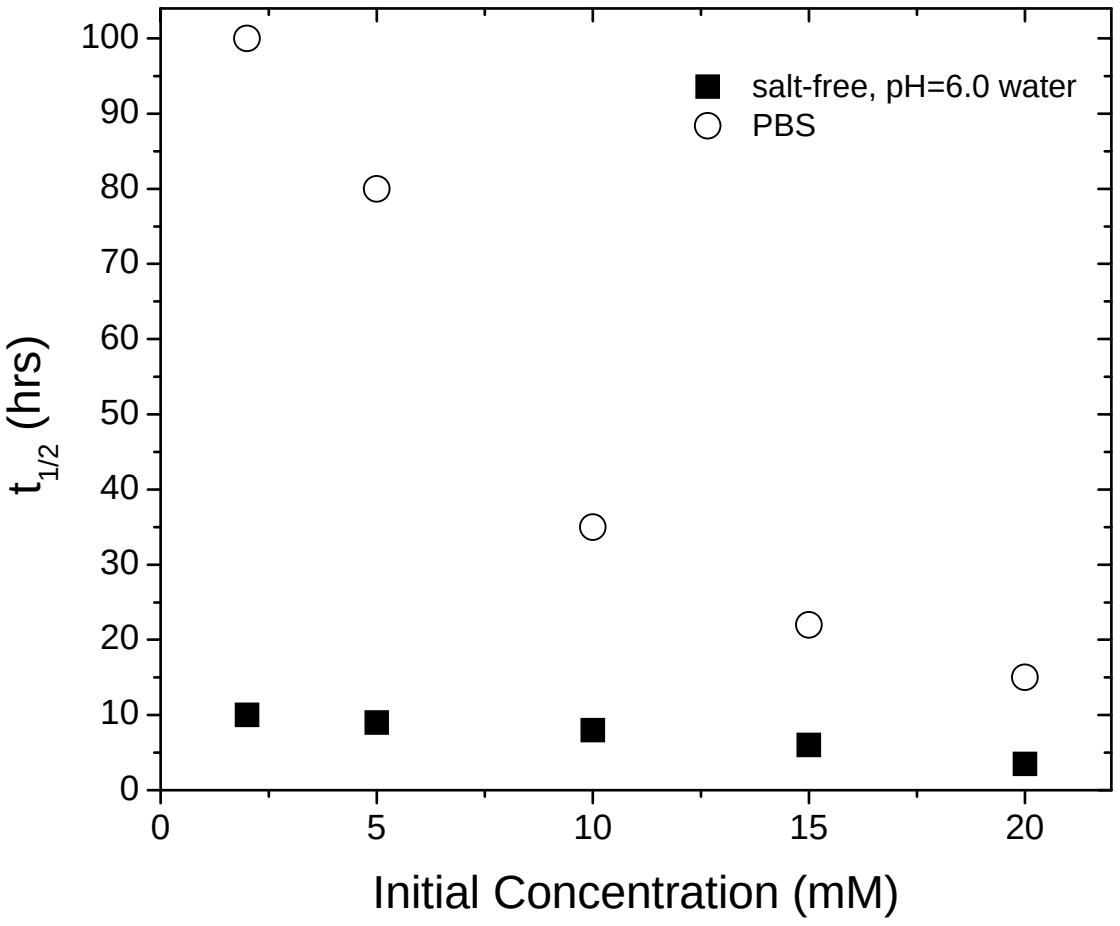


**Figure 3.3**. Half-time of 5,6-carboxyfluorescein release from bare Span-60 niosomes as a function of the initial dye concentration, n=3

Since encapsulated cargo release is sensitive to external pressure gradients, the niosomes were embedded in a temperature-responsive cross-linked chitosan gel which provides stability to the niosomes. The cross-linker used is β-glycerophosphate. Gelling of chitosan occurs at 37$^{o}$C as shown in figure 3.4. Figure 3.5 shows the release rate comparison plots for niosome embedded chitosan gel exposed to salt-free pH=6.0 water versus bare niosomes in PBS buffer or salt-free pH=6.0 water. The initial concentration ($C_o$) of encapsulated cargo, 5,6-carboxyfluorescein in all the cases is 5mM. As mentioned earlier, the initial release corresponds to $C/C_o > 0.4$ for the bare niosomes in salt free pH=6.0 water and $C/C_o > 0.6$ for the bare niosomes in PBS. As with bare niosomes, the embedded niosome release could also be predicted with equation (1). However, in this case the equation holds true only for values of $C/C_o > 0.9$. Hence, for all the three cases the initial fast release could be predicted through equation (1), beyond which there is a deviation from the predicted values followed by a subsequent slowing of the release. For embedded niosomes, the slow regime occurred continually for 55 days (1320 hours) with corresponding half-times in excess of 25 days (600 hours), despite the fact that the niosome-chitosan composite was exposed to salt-free pH=6.0 water. In contrast, bare niosomes in salt-free pH=6.0 water has a half-time of only 8 hours and bare niosomes in PBS buffer has a half-time of 80 hours (more than 3 days). The large difference in $t_{1/2}$ for embedded niosomes as compared to bare niosomes is due to the presence of counterions associated with the amino moieties of chitosan, which are charged at acidic to neutral pH. The counterions provide local hypertonicity that limits swelling of the niosomes even when placed in a hypotonic environment.

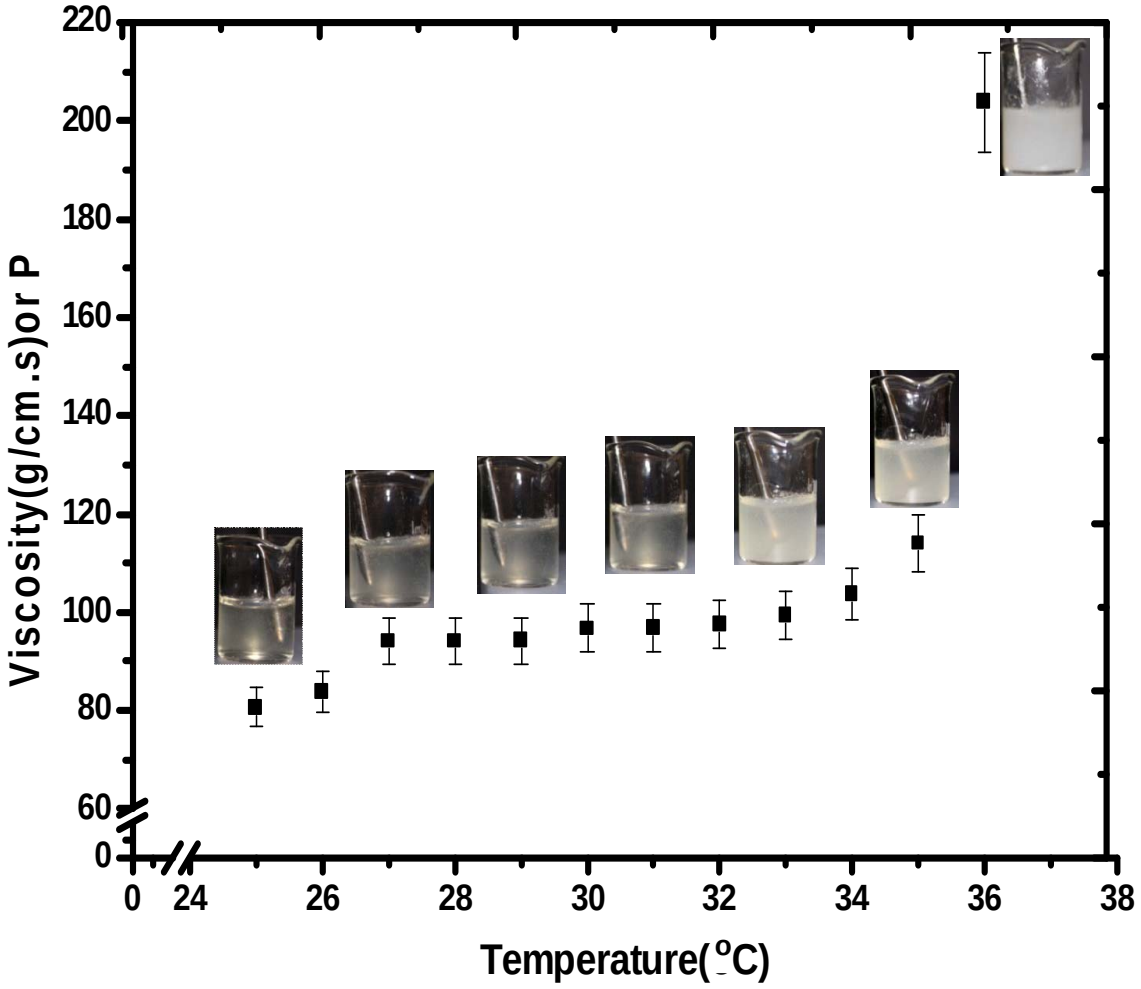


**Figure 3.4** Viscosity of chitosan-β glycerophosphate solution as a function of temperature. Viscosity increased gradually up to 35°C. At 36°C, a steep increase was noticed and at 37°C, the solution completely transformed into a non-flowing solid gel. Hence viscosity measurement was not possible. Images depicting the transformation with temperature is also shown where chitosan-β glycerophosphate, which exist in liquid state at 25°C transforms into a non-flowing opaque sold gel at 37°C, the body temperature

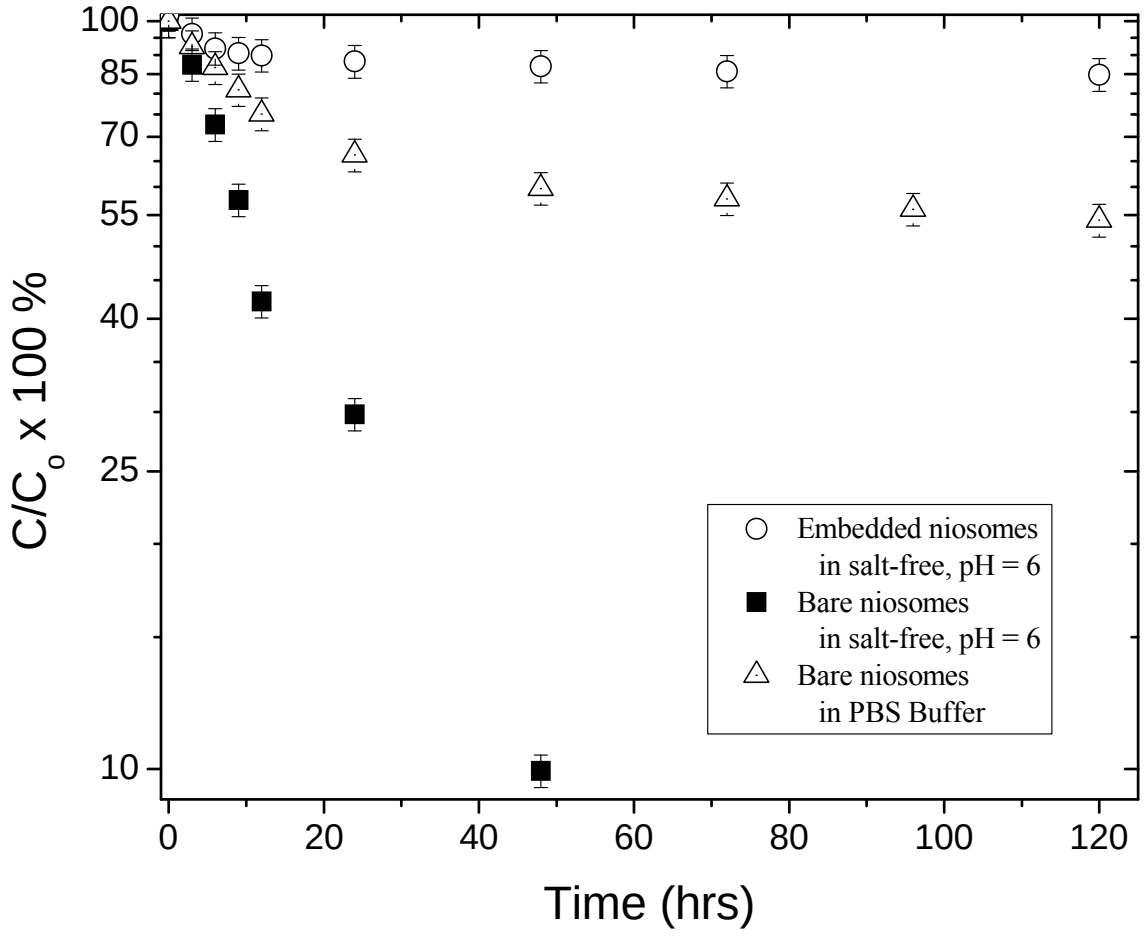


**Figure 3.5** Comparison of 5,6-carboxyfluorescein release from chitosan-embedded niosomes and bare niosomes. The initial concentration of dye for all samples was 5 mM.

Apart from local tonicity of the medium, the structure of chitosan also affects release of encapsulated cargo from niosomes. In the next few paragraphs and figures, the author discusses the influence of chitosan structure on the release of the cargo, which can be altered by changing any of the following three parameters- the niosome packing ratio, the cross-link density of the chitosan gel, and the molecular weight of chitosan. The concentration of niosomes loaded into the chitosan network, also known as the packing ratio, remarkably influenced the rate of dye release for extended time periods. Niosome to chitosan molar ratios ranging from 0.15:1 to 0.45:1 were investigated for these studies. The corresponding release rate plots are shown in figure 3.6 for three molar ratios 0.15:1, 0.35:1, and 0.45:1. The release rates for all the ratios are characterized by two regimes, an initial fast release period till roughly 20 hours, followed subsequently by a slower regime with a slow continual release for 55 days (1320 hours). During the initial fast release period, all the ratios have approximately similar release rates. Beyond this region, the release diverges with the slowest release obtained with the 0.35:1 packing ratio. This behavior can be explained by structural differences of chitosan gel at various molar ratios. Figure 3.7 compares the percentage of dye released at the end of 55 days. The TEM images in insets in figure 3.7 show the structural differences for various packing ratios. Remarkably, at the slowest release ratio of 0.35:1, the niosomes fit into the natural mesh of the chitosan network. At the lowest packing ratio of 0.15:1, since the niosomes were not evenly distributed in the chitosan gel, they were subject to local variations in the structure of the gel. Finally, at the highest packing ratio of 0.45:1, the density of niosomes is too large to completely commensurate with the chitosan mesh. Hence, this result demonstrates the sensitivity of the release to the local structure of chitosan gel.

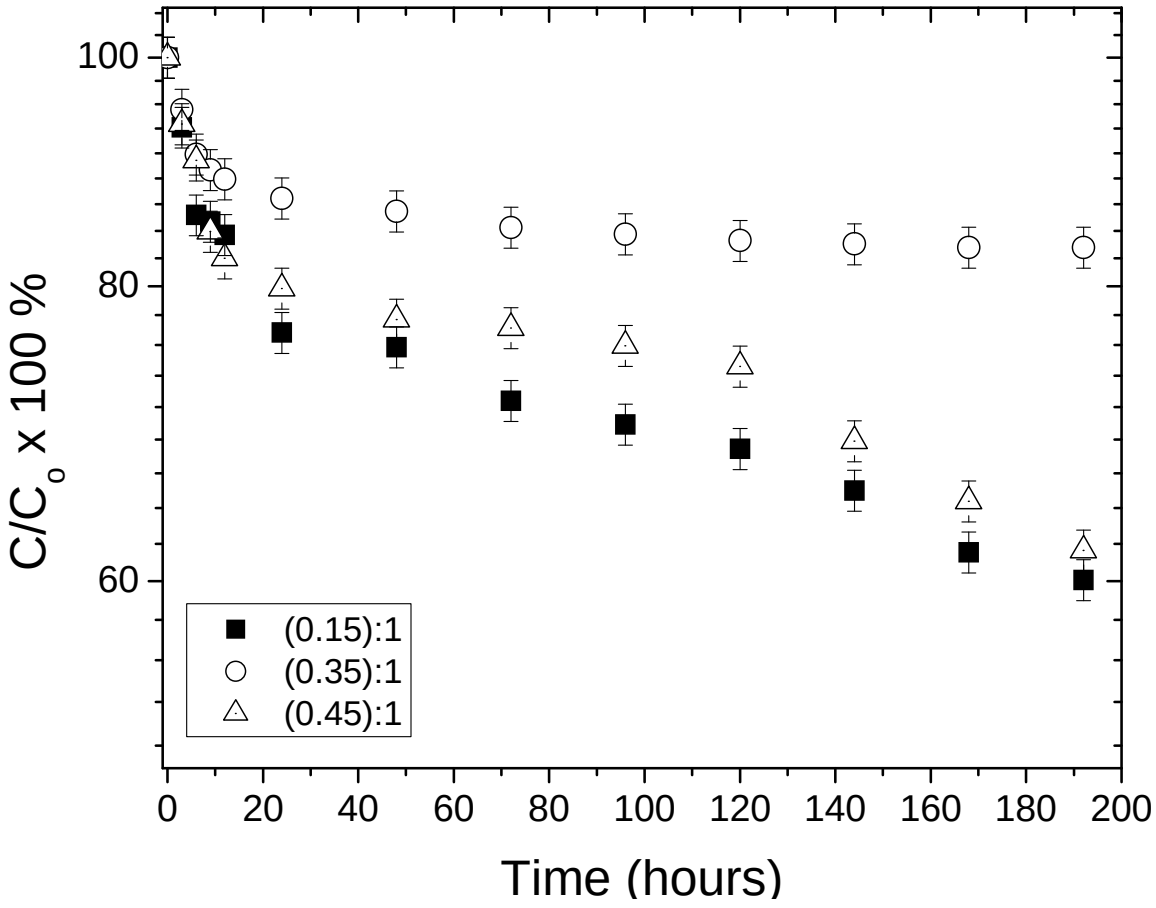


**Figure 3.6** Fraction ($C/C_o$) of 5,6-carboxyfluorescein dye retained in embedded Span-60 niosomes as a function of the mass packing ratio. The initial concentration of dye for all samples was 5 mM

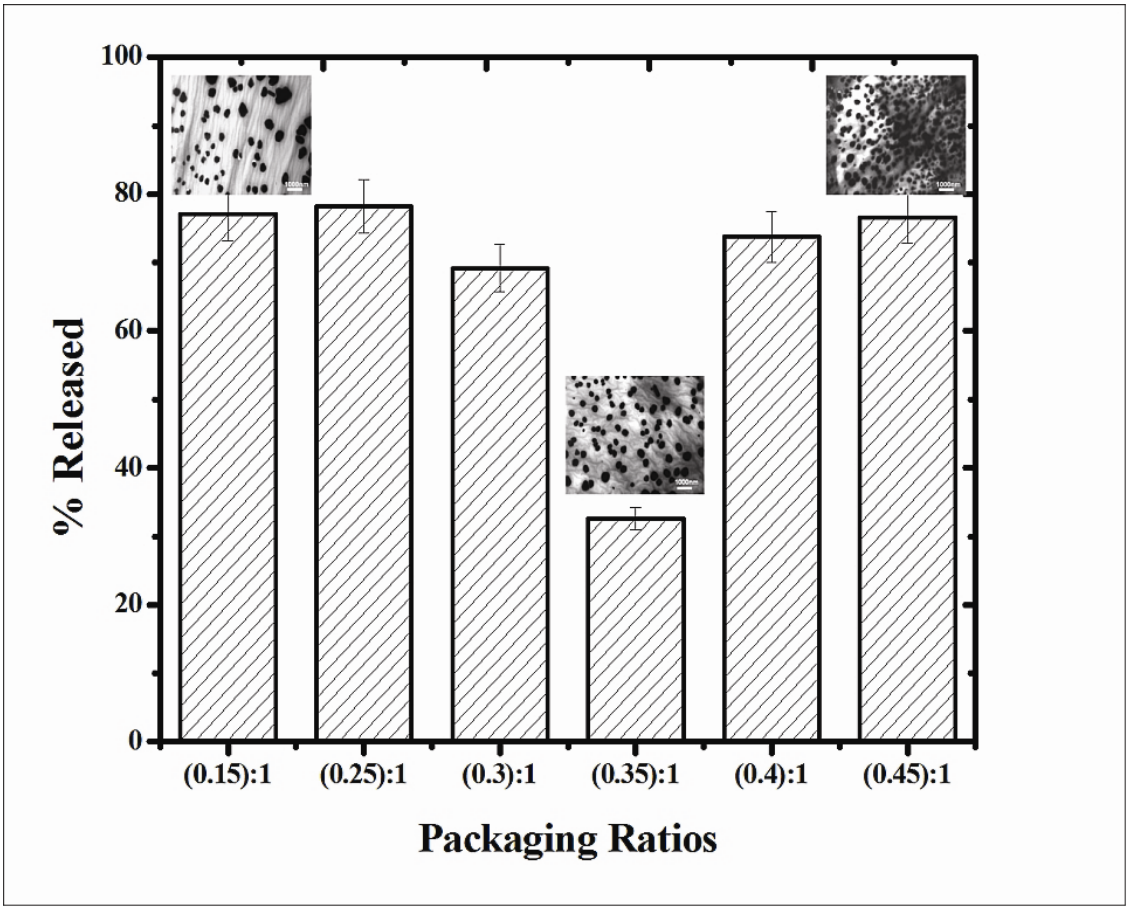


**Figure 3.7** The % release of the content of the niosomes embedded in the chitosan gel as a function of the packaging ratio. TEM images of the chitosan: niosomes ratios for low (0.15:1), medium (0.35:1) and high (0.45:1) packaging density are shown above of each column.

The second parameter of the chitosan structure that affects the release rate was the cross-link density of the chitosan gel. The manipulation of this parameter alters the mesh size of the chitosan gel. The corresponding TEM images are shown in figure 3.8. Addition of the cross-linker was seen to have an effect on the pH of the resultant solution. Table 3.3 shows the various ratios of the cross-linker β-glycerophosphate and chitosan and their corresponding pH. Since gelling of the system occurred only in the ratio range 3.5:1 to 4.5:1, only this range was investigated for release rates. Chitosan gel with a cross-link ratio 3.5:1 forms a loose network with a uniform mesh with an average mesh area of 0.124 $\mu m^2$ (Figure 3.8A). The mesh area for a cross-link ratio of 4:1 (Figure 3.8B) was 0.096 $\mu m^2$, and for a cross-link ratio of 4.5:1 (Figure 3.8C) was 0.0702 $\mu m^2$. Addition of the niosomes to the gelling solution resulted in a slight loosening of the compact structure of chitosan as seen in figure 3.8D.

The release rate with each cross-link ratio is shown in figure 3.9. The slowest release occurred at the cross-link ratio of 4:1. This behavior occurs due to the fact that at this ratio, the size of the mesh is entirely commensurate with the size of a niosome. Higher release rates are obtained when the mesh size and the niosome size are not similar. The mesh size is smaller than the niosome size for the ratio 4.5:1. Hence, it is postulated that the niosomes interfered with the formation of the gel resulting in higher number of imperfections. Furthermore, the smaller mesh size promoted the accumulation of niosomes in the outer surface of the chitosan gel which additionally augmented the release rates.

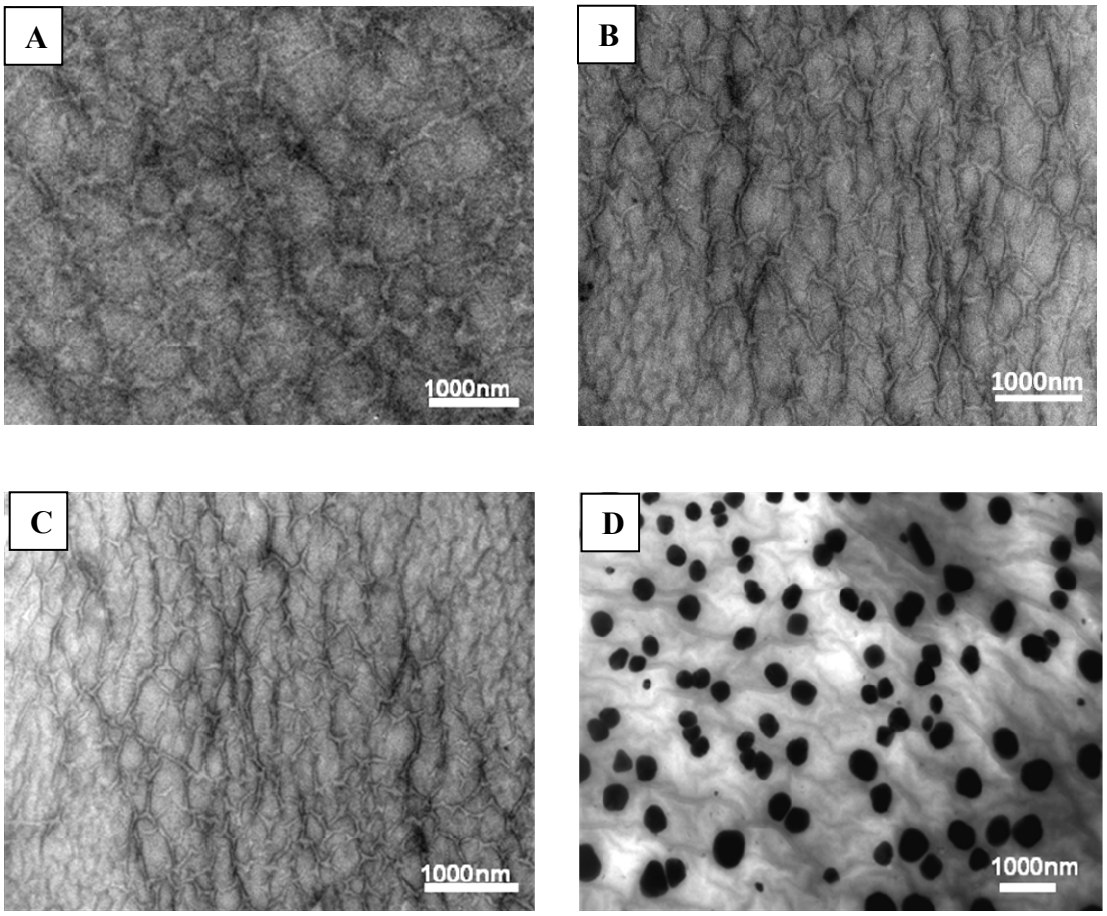


**Figure 3.8** TEM images showing chitosan formulations with: crosslink ratio 3.5:1 (loose network) (A); crosslink ratio 4:1 (B); crosslink ratio 4.5:1(tight network) (C); chitosan-(5mM) niosome formulation with a crosslink ratio 4:1 (D).

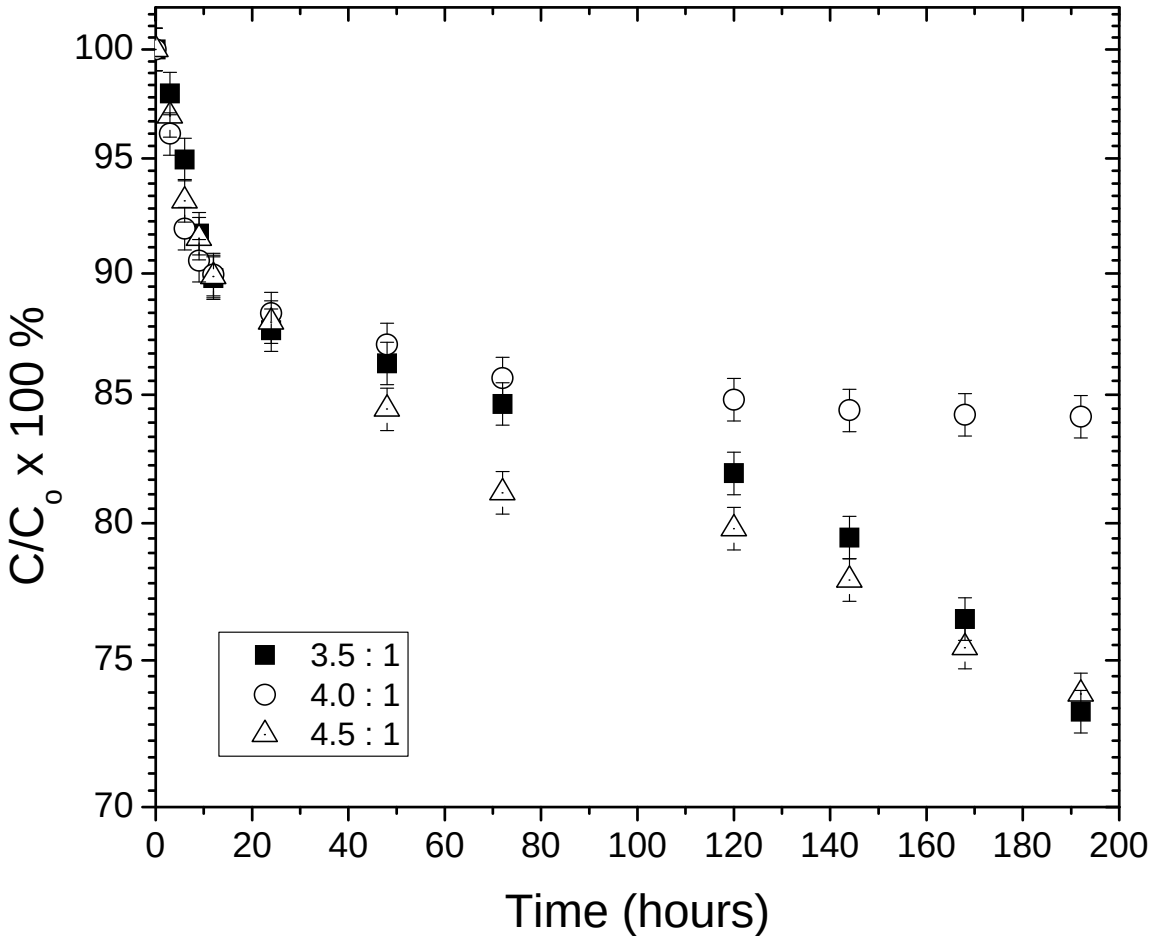


**Figure 3.9** Fraction ($C/C_o$) of 5,6-carboxyfluorescein dye retained in embedded Span-60 niosomes as a function of the cross-link ratio. The initial concentration of dye for all samples was 5 mM.

**Table 3.3** pH variation with the cross-link density

| **β-GP: Chitosan** | 3.0:1 | 3.25:1 | 3.5:1 | 4.0:1 | 4.5:1 | 4.75:1 | 5.0:1 |
|---|---|---|---|---|---|---|---|
| **pH** | 6.6 | 6.7 | 6.9 | 7.4 | 7.9 | 8.1 | 8.3 |

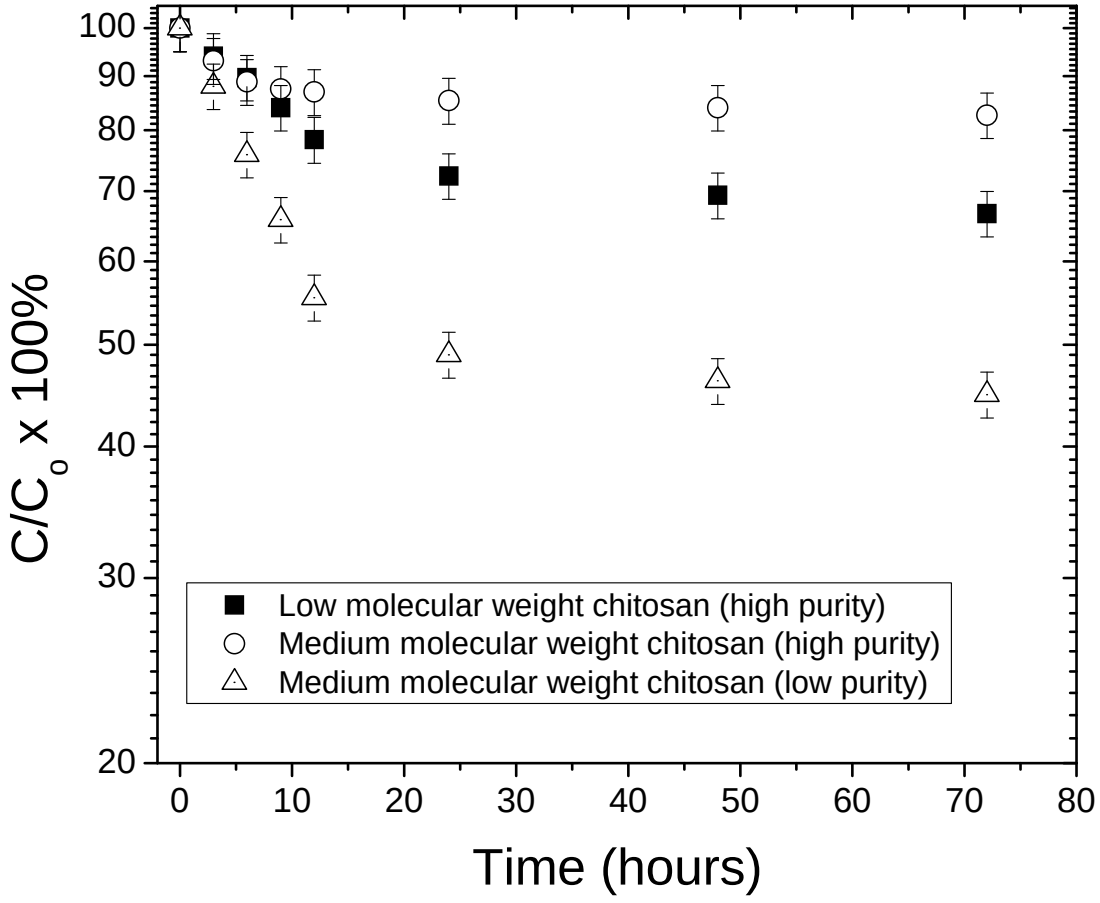


**Figure 3.10** Fraction ($C/C_o$) of 5,6-carboxyfluorescein dye retained in embedded Span-60 niosomes as a function of molecular weight and purity. The initial concentration of dye for all samples was 5 mM.

The precursor chitosan's molecular weight and purity also play an important role in the release rates of the encapsulated cargo. Here again, the release depends on the compactness or closely packed structure of the cross-linked mesh network of chitosan. For these experiments, chitosan with two different molecular weight ranges and two different purities were used. A constant cross-link density of 4:1 molar ratio of β-glycerophosphate to chitosan was maintained for all these samples. Corresponding release rates are plotted in figure 3.10. By comparing same purity and different molecular weights of precursor chitosan, a slower release rate is attained for pure grade medium molecular weight (MMW) chitosan (190,000-310,000 Da) as compared to pure grade low molecular weight (LMW) chitosan (50,000-190,000 Da). This behavior occurs due to the fact that at lower molecular weights, there are more chain ends in the mesh network which leads to the formation of less organized or looser mesh network since each chain end signifies a flaw in the final networked structure. With the increase in the molecular weight, there is a reduction in chain ends, augmentation of inter-chain bonding, and chain packing. The resulting chitosan gel forms a well-organized and compact mesh structure thereby reducing paths for cargo diffusion, hence promoting a slower release rate. For the same molecular weight and different purities, the precursor chitosan with a lower purity resulted in a higher release. This arises due to the presence of insolubles that obstruct the strong bonding and packing between the precursor chitosan and the cross-linker β-glycerophosphate resulting in a less organized mesh network. Hence these results confirm the dependence of release rates on the local structure of chitosan, with higher release obtained for less organized or looser mesh structures which promotes greater clearance

rates for dye diffusion and a slower controlled release obtained from a tightly packed mesh structure.

### 3.3 Conclusion

In this chapter the author highlights the importance of the sizes of the cross-link mesh network and niosome in the controlled release of the encapsulated cargo. The results demonstrate that control in the release rates could be attained by fine tuning either or both of these parameters. Contingent to external tonicity, the release of the encapsulated cargo can be regulated to culminate from 24 hours (1 day) to more than 1320 hours (55 days). Bare niosomes exposed to tumor-like conditions imparted absolute release in 144 hours (6 days). Controlled release is achievable by providing bare niosomes with a protective layer in the form of a cross-linked chitosan network, which can be used to regulate the release of encapsulated cargo till more than 55 days. Additionally, parameters of the precursor chitosan such as the cross-link density, packing density, molecular weight and purity can be manipulated as needed to obtain desired release rates of drugs. An optimum in the release rates are achieved with high purity medium molecular weight chitosan with a cross-link density of 4:1 (β-glycerophosphate: chitosan) and a packing ratio of 0.35:1 (niosome: chitosan). This “Smart Packaged Drug Delivery” design approach, due to its fine tuning ability, will have huge positive implications for application in localized intra-cavitary drug deliveries in ovarian cancer, brain tumors, and in the administration of labile drugs, and can be very effectively exploited by medical practitioners for these types of drug deliveries.

# CHAPTER 4 A COMPARATIVE STUDY OF THE BEHAVIOR OF NIOSOME EMBEDDED CROSS-LINKED CHITOSAN IN THE DELIVERY OF HYDROPHILIC AND HYDROPHOBIC MOLECULES

## 4.1 Introduction

The current treatment regimen for ovarian cancer includes administration of the chemotherapeutic drug paclitaxel [1, 39]. Recent studies have shown that a combination of Paclitaxel and a Platinum analogue Cisplatin/ Carboplatin [39] is more effective than the traditional one drug approach. Paclitaxel, being a hydrophobic drug is conventionally administered along with a formulation vehicle Cremophor EL [132, 148]. However, reports suggest numerous disadvantages associated with this formulation vehicle. Aggregation of erythrocytes, hyperlipidaemia, peripheral neuropathy [148] are some of the shortcomings of this vehicle. In addition it has also been shown to alter the toxicity profile of certain drugs [148]. In recent years localized drug delivery has gained prominence due to the various advantages it possesses over existing treatment techniques in systemic delivery [149]. A varied number of therapeutic loaded particles have been proposed and investigated in literature. All of these particles have been shown to provide a better alternative than the traditional drug administration technique. However, there are certain drawbacks associated with each of these particles. For instance, polymeric

nanoparticles provide greater clearance for drugs compared to nanoparticles formulated from lipids and surfactants [150]. Lipid nanoparticles are prone to degradation due to oxidation of the phospholipids [63, 64, 66, 79, 82], hence making storage and handling difficult. In addition, the synthesis of phospholipids is expensive as is the case with naturally occurring phospholipids [63, 64, 66, 68, 82]. Microspheres, on the other hand, are difficult to manufacture and each distinct application requires a customized fabrication process [47-52, 80]. This puts a large burden on its cost efficiency. All the more, nearly 25-50% of drugs can be lost during the encapsulation process [80]. Niosomes are a better alternative for therapeutic encapsulation since they are chemically and physically stable in solution [85], less expensive [79] and easier to manufacture and store [68] as compared to other categories of bilayer vesicles such as liposomes and drug delivery carriers such as microspheres. The utmost advantage of niosomes is that, since they are uncharged, there is no charge-charge interaction between the encapsulated drug and the niosome.

This chapter focuses on the benefit of using an improved and inventive version of our earlier one drug niosome. The new version, also called the 'cocktail niosomal formulation' has the ability to encapsulate multiple drugs in a single niosome. Drugs with different polarity can be packaged into the same niosomal vehicle. Ovarian cancer drugs paclitaxel and carboplatin are the drugs of interest which have been used in this study. Hydrophobic drug paclitaxel was encapsulated in the bilayer and carboplatin in the core of the niosome. Since the drugs are enclosed in different areas within the niosome they do not interact hence preserving the efficacy of the drugs. The "cocktail niosomal

formulation" eliminates the need of Cremophor EL for paclitaxel altogether. This further indicates elimination of the drawbacks associated with Cremophor EL. Additionally, the niosomal formulation, when embedded in cross-linked chitosan provides an added advantage of controlled delivery.

**4.2 Results and Discussion**

The figures below show the schematic representation of the 'cocktail niosomal formulation'. The following sections show the comparison between different niosomal formulations and the advantages of each system:

a) System 1: Single drug niosomal formulation where the hydrophobic drug was encapsulated in the hydrophobic bilayer of the niosome. The schematic representation of the formulation is shown in figure 4.2. TEM images are shown in figure 4.3 (A), and the size distribution as obtained from dynamic light scattering apparatus in table 4.2.

b) System 2: Single drug niosomal formulation where the hydrophilic drug carboplatin is encapsulated in the hydrophilic core of the niosome. The schematic representation of the formulation is shown in figure 4.2. The corresponding TEM image is shown in figure 4.3 (B) and the size distribution is shown in table 4.2.

c) System 3: **'**Cocktail niosomal formulation' where the hydrophobic drug paclitaxel is encapsulated in the hydrophobic bilayer and the hydrophilic drug carboplatin in the hydrophilic core of a single niosome. Figure 4.1 shows the schematic representation of the 'cocktail niosomal formulation'. TEM image is shown in figure 4.3 (C) and the size distribution in table 4.2.

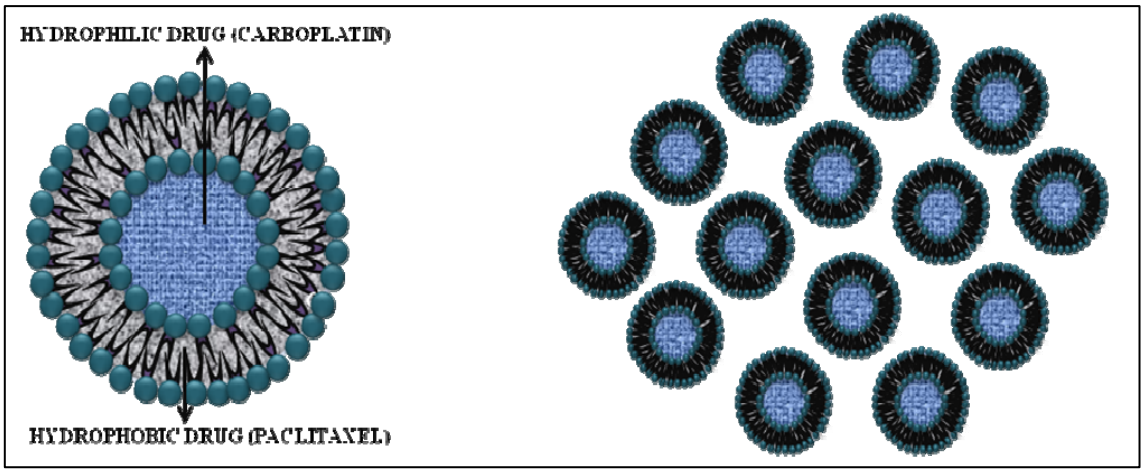


**Figure 4.1** Hydrophobic drug paclitaxel and hydrophilic drug carboplatin encapsulated in the same niosome, the 'cocktail niosomal formulation'.

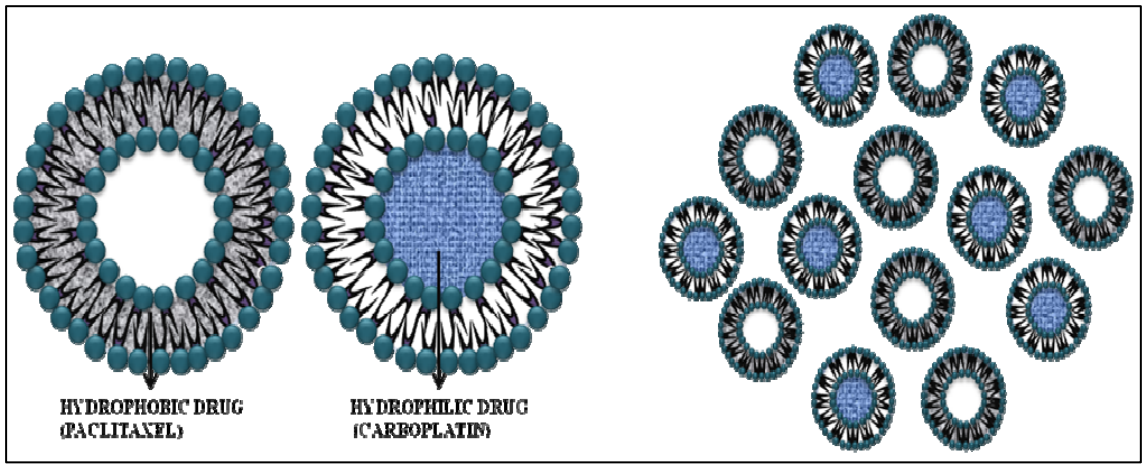


**Figure 4.2** Schematic representation of the niosomal system containing two types of niosomes: i) hydrophobic drug paclitaxel within the bilayer; ii) hydrophilic drug carboplatin in the hydrophilic core.

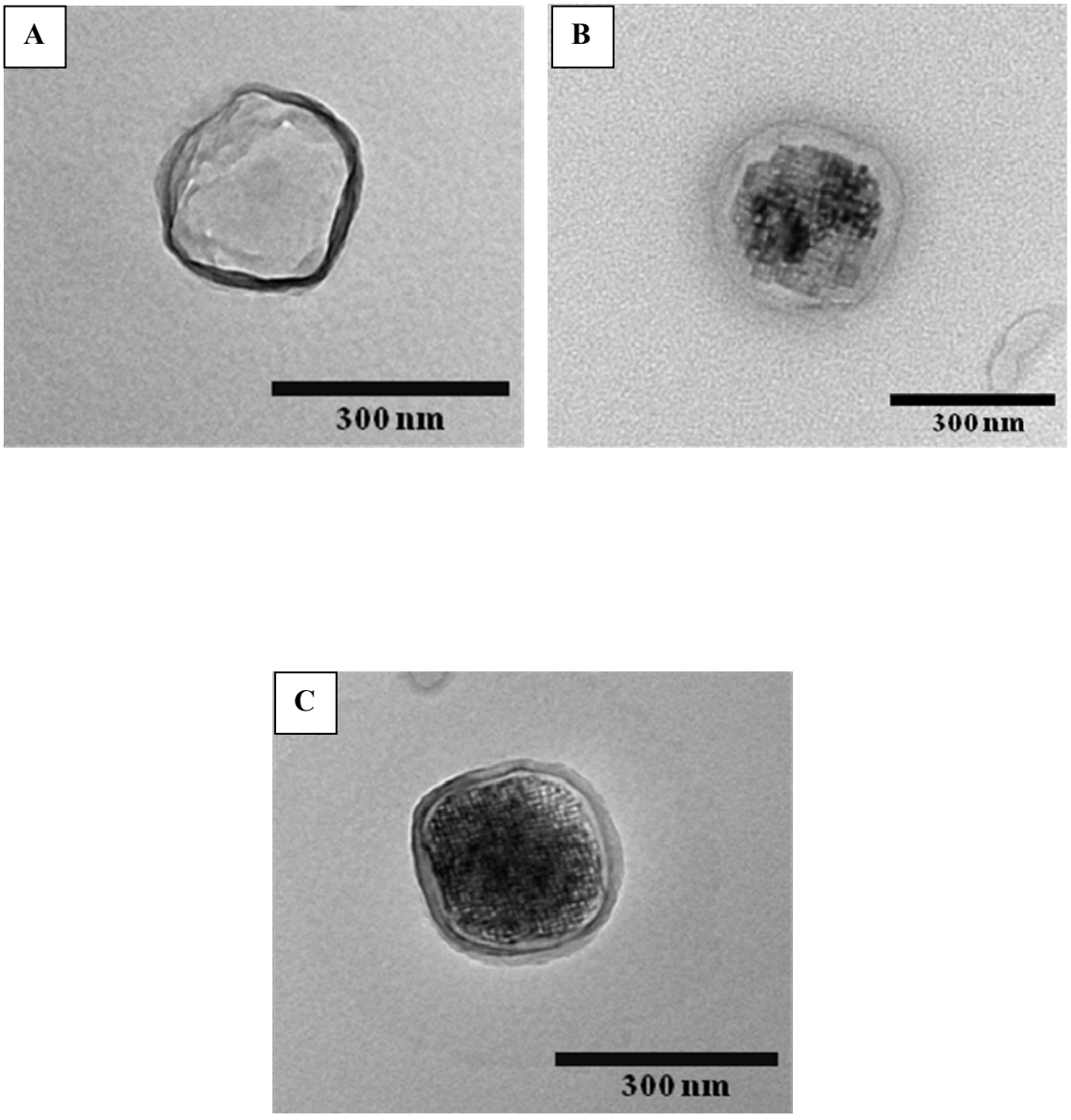


**Figure 4.3** TEM images showing various niosomal formulations. (A) niosome encapsulated with 5mM paclitaxel; (B) niosome encapsulated with 5mM carboplatin; (C) 'cocktail niosomal formulation' encapsulated with 5mM of paclitaxel and 5mM of carboplatin

Table 4.1 shows the entrapment efficiencies of encapsulated molecules in the niosomes. Niosomes encapsulated with paclitaxel only, show an entrapment efficiency of 85%. This is a huge improvement from the values reported in literature for paclitaxel encapsulated bilayer vesicles where the entrapment efficiency was 70% [151]. Even this entrapment was possible only after the addition of a non-ionic surfactant in the formulation of the liposomes. Lipids by themselves were seen to form very unstable vesicles with paclitaxel, with even lower entrapment efficiencies [78, 151].

Non-ionic surfactants have been reported in literature to have an increase in paclitaxel solubility and entrapment in vesicles [132]. This is where our system holds an enormous advantage over other liposomal systems. Since the niosomal bilayer is formulated with non-ionic surfactants, they provide a suitable environment for paclitaxel to reside as compared to liposomes. This is probably the reason for the higher encapsulation efficiency of the drug in niosomes.

It also needs to be noted that in lipid systems, there is a limit to which the surfactants can be added, since the large hydrocarbon tail of the surfactant was believed to penetrate the lipid bilayer leading to leakage [152]. Since the entrapment is directly related to the amount of surfactants, this also limits the entrapment efficiencies. Also, drug-to-lipid molar ratio higher than 3% led to the formation of precipitates of paclitaxel [153].

Niosomes do not face these problems since the bilayer is made of surfactants itself and these vesicles were found to encapsulate very high concentrations of paclitaxel upto

20mM with stabilities lasting over 3 months. Niosomes encapsulated with carboplatin showed an encapsulation efficiency of 68% consistent with those reported in literature [154]. The two drug niosome showed similar encapsulation efficiency for paclitaxel. However, for carboplatin, the efficiency showed a slight decrease which could be due to the rigidity of the paclitaxel containing bilayer.

**Table 4.1** Encapsulation efficiencies of niosomes with various entrapped molecules

| | Niosome with Paclitaxel | Niosomes with Carboplatin | Cocktail niosomal formulation | |
|---|---|---|---|---|
| | | | Paclitaxel | Carboplatin |
| Encapsulation efficiency (%) | 85.04 | 68.24 | 85.01 | 66.33 |

The size distributions of niosomes encapsulated with various molecules are shown in table 4.2. For niosomes encapsulated with paclitaxel only, the size was seen to increase with the drug concentration. Balasubramanian et al. [152] reported that a hydrophobic or low polarity environment leads to concentration dependent self-aggregation of paclitaxel by forming intermolecular hydrogen bonds. Since in our system, the paclitaxel is encapsulated in the hydrophobic bilayer of the niosome, the observation holds true in this case as well. This aggregation is certainly the reason for the increased niosome size with the paclitaxel concentration.

Niosomes encapsulated with both paclitaxel and carboplatin also showed a similar trend in the size distribution pattern with an increase with the paclitaxel concentration. Niosomes encapsulated with carboplatin on the other hand showed only slight increase in size with concentration.

**Table 4.2** Average size distribution for various niosomes

| Concentration (mM) | Size Distribution (nm) | | |
|---|---|---|---|
| | Niosome with Paclitaxel | Niosomes with Carboplatin | Cocktail niosomal formulation |
| 2 | 253 | 257 | 259 |
| 5 | 260 | 262 | 264 |
| 10 | 272 | 268 | 269 |
| 15 | 281 | 283 | 280 |
| 20 | 293 | 298 | 301 |

The plot shown in figure 4.4 compares the release rate of two hydrophilic encapsulated molecules, carboplatin and 5(6) carboxyfluorescein, as well as a hydrophobic molecule paclitaxel encapsulated in the bilayer of the niosome. The site of encapsulation was seen to have an influence over the release of the molecules. The hydrophilic molecules which were encapsulated in the hydrophilic core had a higher release rate as compared to the hydrophobic molecule. The addition of a hydrophobic molecule into the niosomal bilayer increases its hydrophobicity while decreasing the permeability [78]. This creates a barrier

for the release of the encapsulated molecule. When molecules are encapsulated into the hydrophilic core of the niosomes it does not affect the bilayer membrane. Since the stability and permeability of the membrane are not altered, the release would undoubtedly be higher in this case. It needs to be mentioned that the niosomes encapsulated with 5(6)-carboxyfluorescein showed higher release than those with carboplatin. As discussed earlier, the release from the chitosan-niosome system depends on the mesh size of the chitosan cross-link as well as the size of the niosome, with the slowest release observed when their sizes were commensurate. The size of carboplatin encapsulated niosome was much smaller (300nm) whereas those with 5(6)-carboxyfluorescein were around 800nm. The optimum cross-link ratio for the carboxyfluorescein niosome was found to be 4:1 (data shown in chapter 3). To accommodate for the smaller sized carboplatin niosomes the cross-link density was increased to a molar ratio of 4.5:1. The average mesh area for this ratio was found to be 0.07 $\mu m^2$ which commensurate with the cross-sectional area of a 0.3μm niosome. This resulted in a lower release from carboplatin niosome as compared to carboxyfluorescein at the same cross-link ratio.

Figure 4.5 shows the release rates of 'one drug niosome' encapsulated with various concentrations of paclitaxel. Predictably, the release was observed to decrease with concentration. As mentioned before, the presence of paclitaxel in the bilayer membrane increases the niosomal rigidity. Rigidity restricts the swelling of the niosome thereby decreasing its permeability. With decreased permeability the passages for the drug diffusion decreases, thereby hampering the release of encapsulated drug from its bilayer.

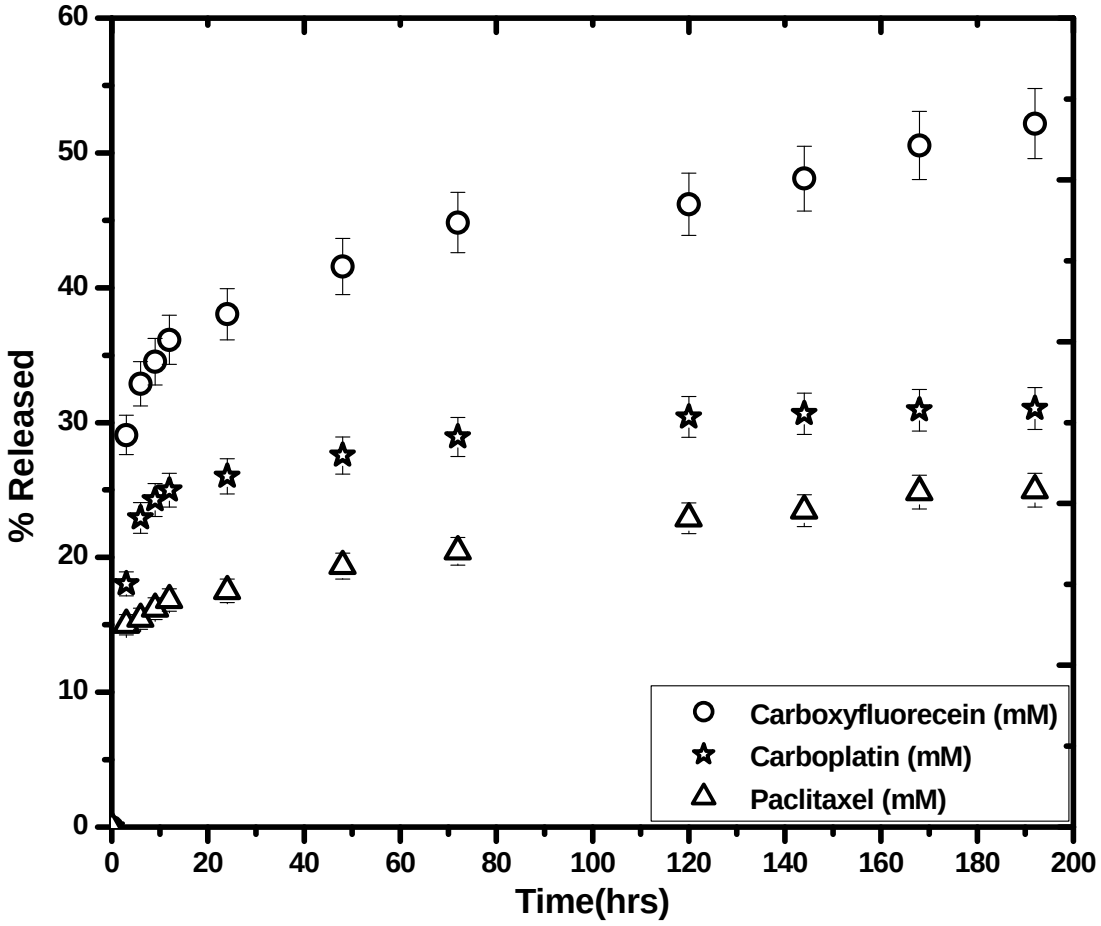


**Figure 4.4** Effect of encapsulation site on the release rates. Paclitaxel encapsulated into the bilayer of the niosome showed the slowest release since it interfered with the membrane stability and permeability. Hydrophilic molecules, carboplatin and 5(6)-carboxyfluorescein encapsulated into the core of the niosome had a higher release rate.

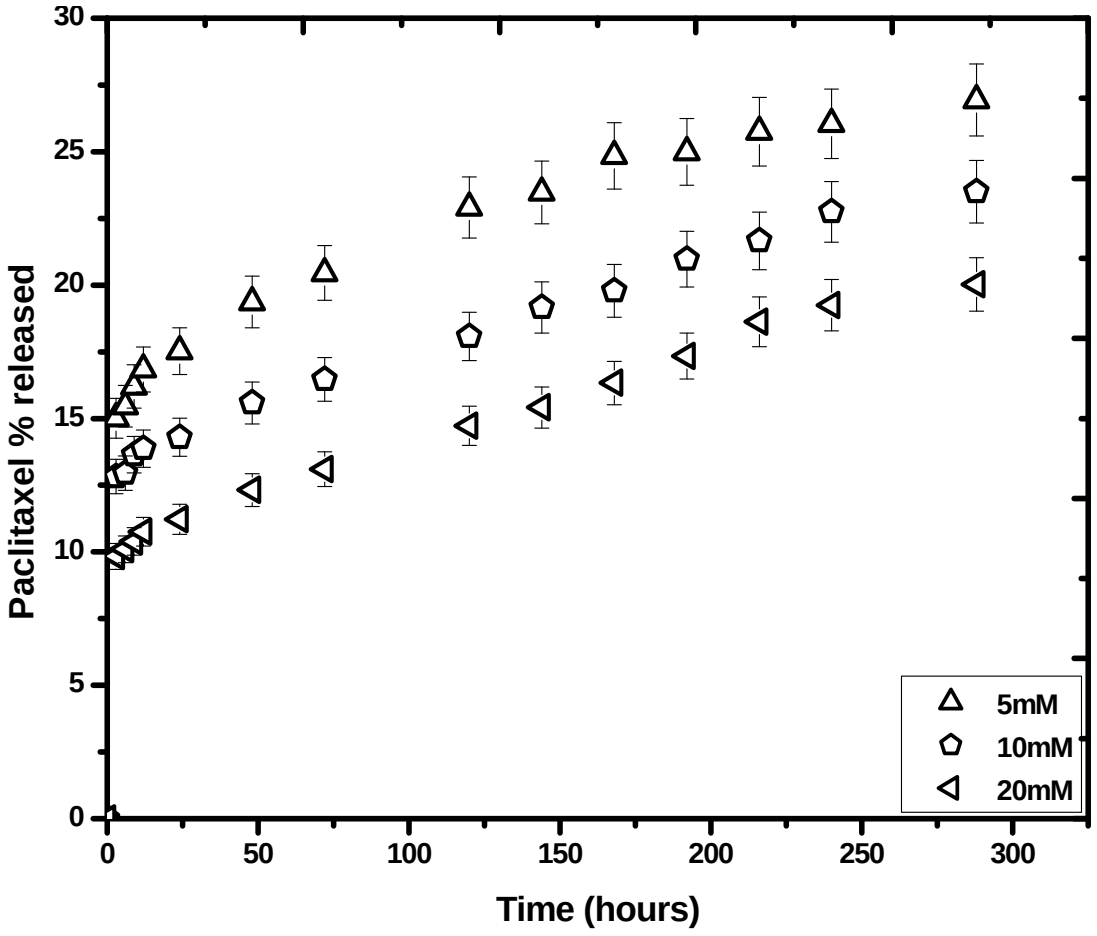


**Figure 4.5** Increasing the paclitaxel content in the bilayer of the niosome increases the stability while decreasing the permeability of the niosomal membrane. Hence as the concentration of paclitaxel increases the release rate decreases.

It needs to be mentioned that although the niosome size increased with concentration, the increase was not significant enough to be a limiting factor. The cross-link mesh dimensions were large enough to be able to accommodate the niosomes without significantly affecting the release. Hence, in this case the membrane permeability appears to be the limiting factor in the release of paclitaxel. Therefore as the concentration of paclitaxel increased in the bilayer, the release rate decreased.

Figure 4.6 shows the comparison of release rates of carboplatin from two niosomal systems: i) where the carboplatin was encapsulated in a single niosome; and ii) where carboplatin was encapsulated into the 'two drug niosome' where the amounts of paclitaxel content in the bilayer was varied. In all these experiments the concentration of carboplatin was kept constant at 5mM. Although the carboplatin concentration was identical in all the cases, their release rates were dissimilar. For 'two drug niosomes' an interesting phenomenon was observed. The release of carboplatin from the hydrophilic core was dependent on the amount of the hydrophobic paclitaxel content in its bilayer. The release decreased with increased paclitaxel content. This can be explained by the increased stability and decreased permeability of the bilayer restricting the release rates. It is interesting to note that varying the paclitaxel content not only affects the paclitaxel release but also it can be used to alter the release of the encapsulated carboplatin from the niosomal core. As expected, single drug carboplatin niosomes had a higher release rate as compared to the multi-drug niosomal formulation.

In order to study the release behavior of carboplatin from the hydrophilic core of the 'two drug niosome', the paclitaxel content in the bilayer was kept constant while changing the carboplatin concentration. A change in the release trend was noticed in such a case. Paclitaxel showed a comparable release irrespective of its encapsulation in either a single drug niosome or a multi-drug niosome (Figure 4.7A). This further goes to prove that the release from the hydrophobic bilayer is independent of the concentration of molecules encapsulated in the hydrophilic core. Since paclitaxel is encapsulated inside the bilayer, it has two pathways for diffusion. It could either diffuse into the exterior of the niosome or into the interior hydrophilic core. Since the niosome exterior consists of a salt free pH 6.0 medium, it is more hypotonic than the interior and would be the preferred pathway for paclitaxel diffusion. Hence addition of molecules into the core does not affect the release from the bilayer.

In this system, however, carboplatin showed an interesting trend. The release increased with concentration (Figure 4.7B). It needs to be mentioned that although the total percentage release was still lower than the single drug carboplatin niosome, the trend was similar, which is, an increase in the release with concentration. This result is consistent with our earlier results with carboxyfluorescein niosomes and is due to the osmotic difference across the membranes. Since the niosomes were exposed to a hypotonic salt free medium at pH 6.0, the tonicity difference between the niosome interior and exterior caused the swelling of the niosomes, thereby increasing the permeability. With permeability the release increases as well which is undoubtedly the reason for the increase of carboplatin release with concentration.

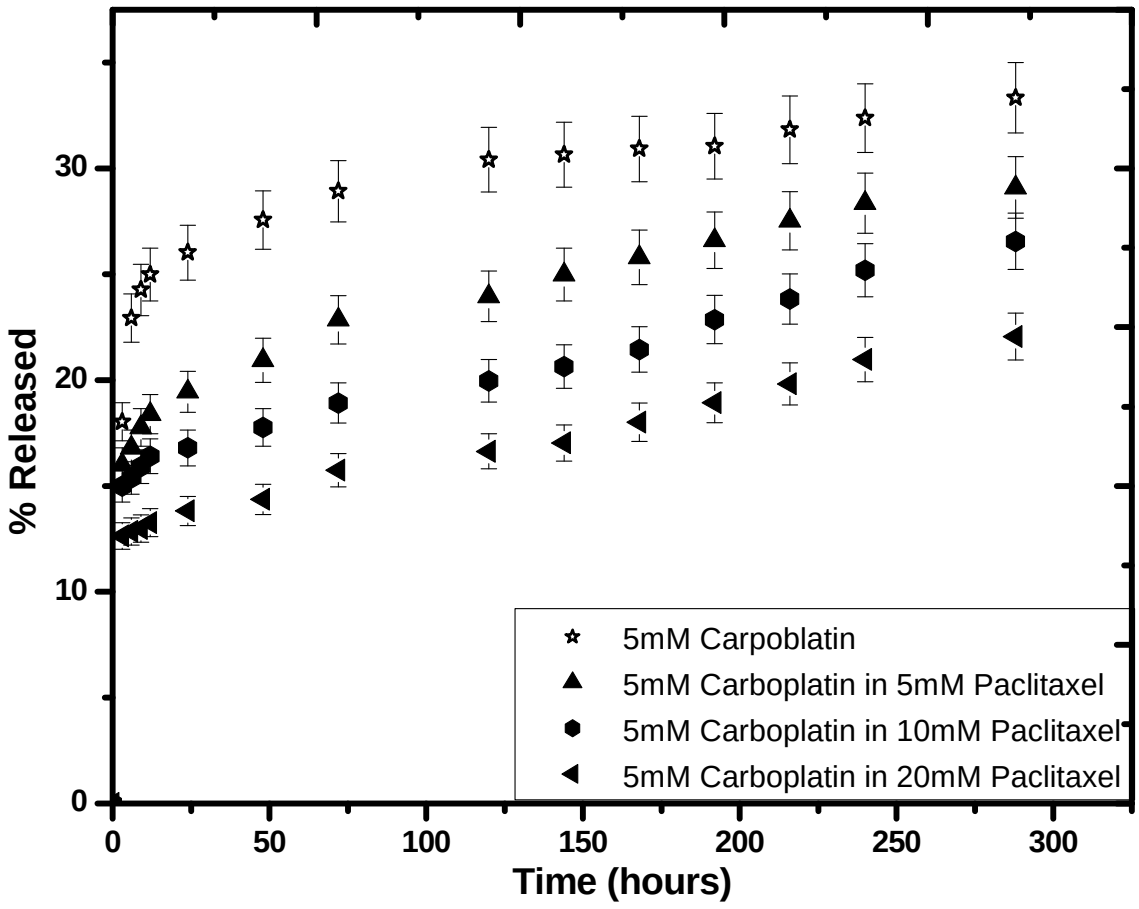


**Figure 4.6** Niosomes with **s**imilar carboplatin concentrations showed different release rates which were seen to be dependent on the paclitaxel concentration.

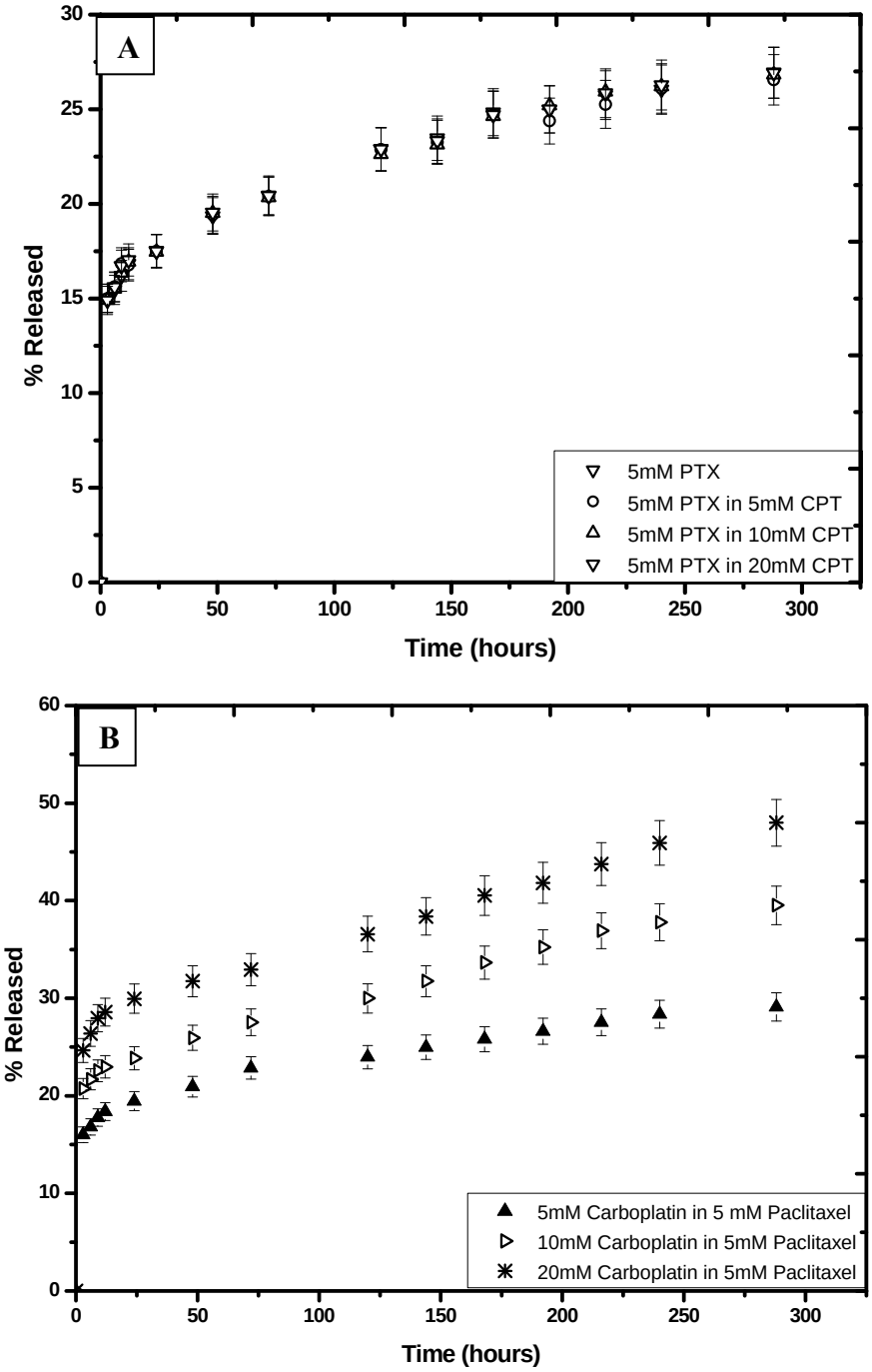


**Figure 4.7** Increasing the hydrophilic drug concentration was seen to have no effect on the hydrophobic drug release **(A)**. However, under the same conditions the hydrophilic drug release showed an increase **(B)**.

## 4.3 Conclusion

The results presented in this chapter illustrate that niosomes were able to encapsulate a higher percentage of paclitaxel as compared to traditional bilayer vesicles such as liposomes since: i) non-ionic surfactants aid in the solubility of paclitaxel and; ii) presence of long alkyl chain of Span-60 increases the hydrophobic environment or area in the bilayer. The permeability of the bilayer membrane decreases with the addition of paclitaxel. This in turn provides an additional control over the release rates of the encapsulated molecules from either its hydrophilic core or the hydrophobic bilayer. Increase in paclitaxel concentration decreases the rates of carboplatin release in addition to a decrease in its own release. However, addition of carboplatin in the core does not affect the bilayer and its release followed a trend similar to niosomes with 5(6) carboxyfluorescein as seen in chapter 3. These results demonstrate that fine control over the release of the encapsulated drugs from the bilayer or core can be achieved by altering the concentration of the drug in the bilayer. Hence, desired release rates can be attained by fine tuning of the bilayer characteristics of the niosomes in the 'Smart Packaged Drug Delivery System'.

# CHAPTER 5 SELECTIVE DRUG DELIVERY *IN VITRO* USING SMART PACKAGED DRUG DELIVERY SYSTEM

## 5.1 Introduction

Through the years localized and targeted delivery has proven to be more effective than conventional methods of drug delivery. Systemic delivery has varied shortcomings. Frequent drug dosage, fluctuations in circulating drug levels, little control over drug release kinetics are some of the drawbacks of systemic delivery [45, 155-158]. However, the greatest disadvantage of current chemotherapeutics is its inability to isolate cancer cells for its preferential treatment [45, 80, 155, 156, 158]. The inability of the drugs to distinguish between cancer and normal cells is the root cause of many of the side effects associated with the treatment. Recent studies have shown the benefits of attaching receptors to the drugs in the enhancement of the drug efficacy [159-160]. The receptors are molecules that have an enhanced/preferred affinity to cancer cells while showing lesser affinity to normal cells, thus sparing them from the harmful effects of the therapeutics [159-160].

This chapter explores the potential of the niosome-chitosan drug delivery system in preferential treatment in cell lines such as ovarian carcinoma and normal ovarian

epithelial cells. Each of the cell lines were studied for their drug uptake, drug efficacy, toxicity and their affinity to the chitosan-niosome system. This drug delivery system holds promise not only in the controlled and localized delivery of chemotherapeutics but it also shows potential in targeted delivery as well.

**5.2 Results and Discussion**

Paclitaxel conjugated with BODIPY 564⁄570 has been used in this study. BODIPY 564⁄570 is a red-orange fluorescent dye with an excitation of 564nm and emission of 570nm. Live cell imaging were obtained with a Leica TCS SP5 laser scanning confocal microscopy through a 63 ×/1.4NA or 100 ×/1.4 NA (Leica Microsystems, Germany). Confocal microscopy is a technique used for optical imaging. It works by illuminating the specimen point-by-point thus eliminating out of field light. This enables shallow depth of field imaging. Imaging of successive optical sections in thick samples is hence possible through this technique. The resulting images have high contrast and resolution. This technique is advantageous over conventional fluorescence microscopy where the whole sample has to be illuminated thus leading to blurred images due to the interference by the out of field light.

Confocal images of two cell lines: i) normal ovarian epithelial (Ilow) and, ii) epithelial ovarian carcinoma (OV2008) when in contact with the cross-linked hydrogel chitosan are shown in Figure 5.1 Within 10 minutes of contact, chitosan was seen to accumulate around OV2008 (ovarian cell line). This behavior was absent in Ilow (normal ovarian

epithelial cell line). This behavior is due to the fact that chitosan is known to be highly mucoadhesive, especially to the antigen MUC 1.

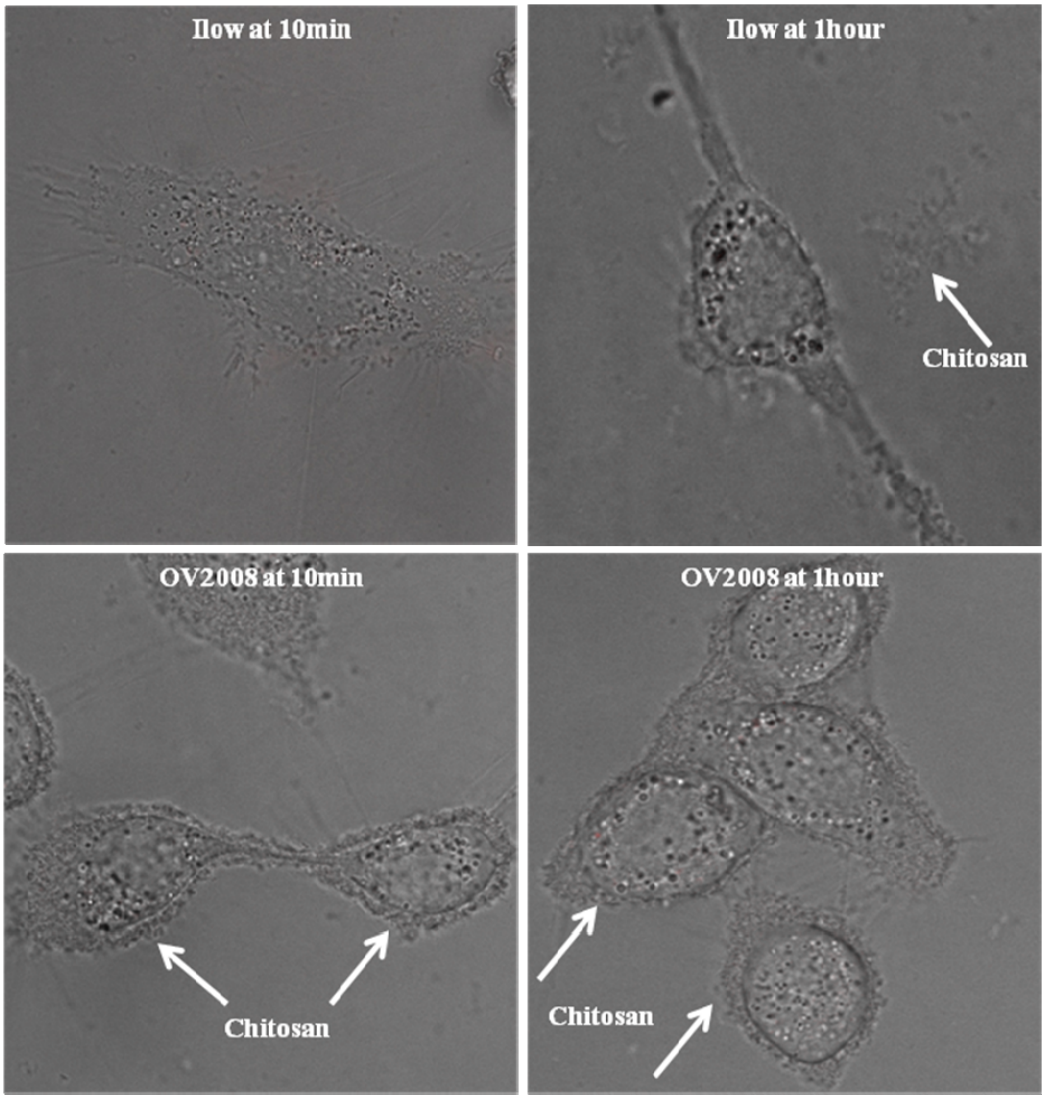


**Figure 5.1** Confocal images depicting chitosan accumulation in OV2008 (ovarian carcinoma) cells due to the affinity of chitosan to MUC1 antigen over-expressed in ovarian carcinomas. Such accumulation was not observed for Ilow (normal ovarian epithelial) cell line. The magnification of the images is 1890x

MUC 1 is a tumor associated antigen that is over expressed in certain carcinomas [149]. It is a highly O-glycosylated protein where carbohydrates constitute 50-90% of the molecular mass [163]. MUC1, a trans membrane glycoprotein, consists of a phosphorylated cytoplasmic tail [163] and a large extracellular domain (1000-2200 amino acids) [149] .

MUC1 is expressed at low levels in the ducts and glands of simple secretory epithelial tissues [149, 162] and is over expressed in carcinomas such as ovarian, breast and colon. Over-expression generally correlates with metastatic potential and poor survival [163]. The over-expression of MUC 1 however can be turned into our advantage since it provides a favorable condition for chitosan adhesion and can essentially be used in its selective treatment.

The confocal images show the affinity of chitosan to cells where the expression of MUC 1 was high enough for the adhesion effect. Although MUC 1 is expressed in normal cells as well, its expression is low so as not to warrant chitosan adhesion. The accumulation of chitosan to the cells could be observed within 10 minutes. By the end of an hour, chitosan buildup around the cells was seen to increase rapidly. In normal cells, although chitosan could be seen in the vicinity, it was not observed to accumulate around the cells.

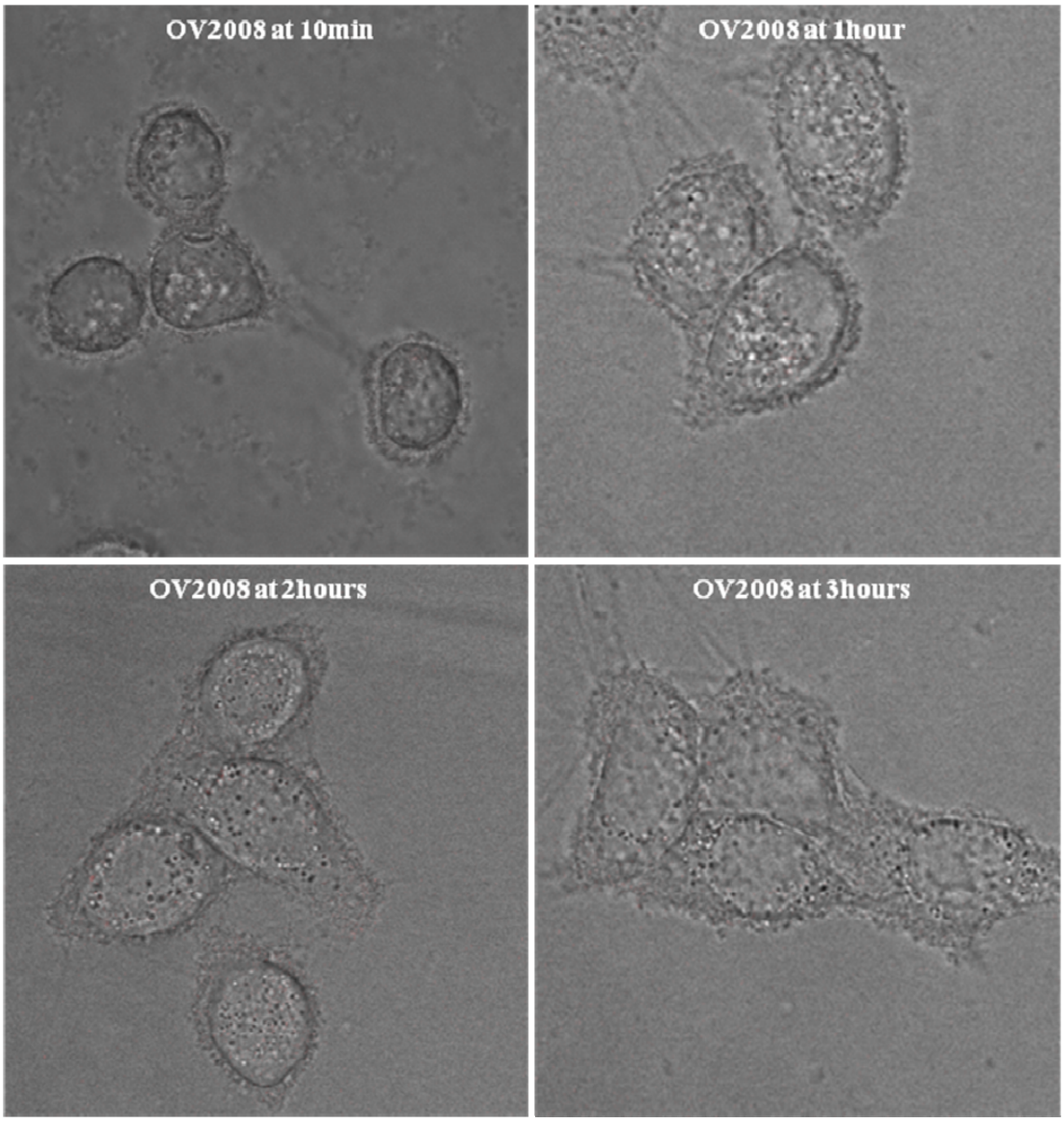


**Figure 5.2** OV2008 exposed to chitosan over time. The cells did not show a change in their morphology with time. The magnification of the images is 1890x

Chitosan by itself does not have any adverse effect on the cells. The morphology of the cells which were exposed to chitosan were not altered (Figure 5.2). And the cells seemed to survive and thrive beyond 24hours. Apart from the increase in the chitosan accumulation with time on the surface of OV2008, the cells did not seem to be critically affected by chitosan. This is expected since chitosan is a naturally occurring biopolymer and is biocompatible, biodegradable and not known to be toxic.

Chitosan is a safe haven for cells and it has been reported in literature that cells can actually grow on the surface of chitosan microspheres. Chitosan microspheres have been used in the delivery of chemotherapeutics in recent years. However, the problem associated with such systems is that they provide a greater clearance for the transport of drugs thus preventing its controlled delivery. This is where our drug delivery system holds advantage since the presence of niosomes in the chitosan gel prevents the premature release of drugs, and the presence of cross-link mesh in the chitosan network adds an additional control by immobilizing the niosomes.

To evaluate how the system compares with the traditional route of drug administration, the cells were exposed to the drugs alone as opposed to when they were packaged in the chitosan-niosome drug delivery system. Figure 5.3 shows the confocal images of the normal ovarian epithelial cell line Ilow. When the cells were exposed to the drug paclitaxel without the chitosan-niosome packaging, the effect on the cells was almost instantaneous. The cells were seen to be saturated with the drug within the first 10 minutes of treatment. Blebbing was seen on the surface of these cells instantaneously

which implies the initiation of apoptosis. Within 1 hour shrinkage of the cells were observed. By the end of 2 hours cell death was observed with shrinkage and absolute blebbing of the cells along with condensed morphology and nuclear fragmentation.

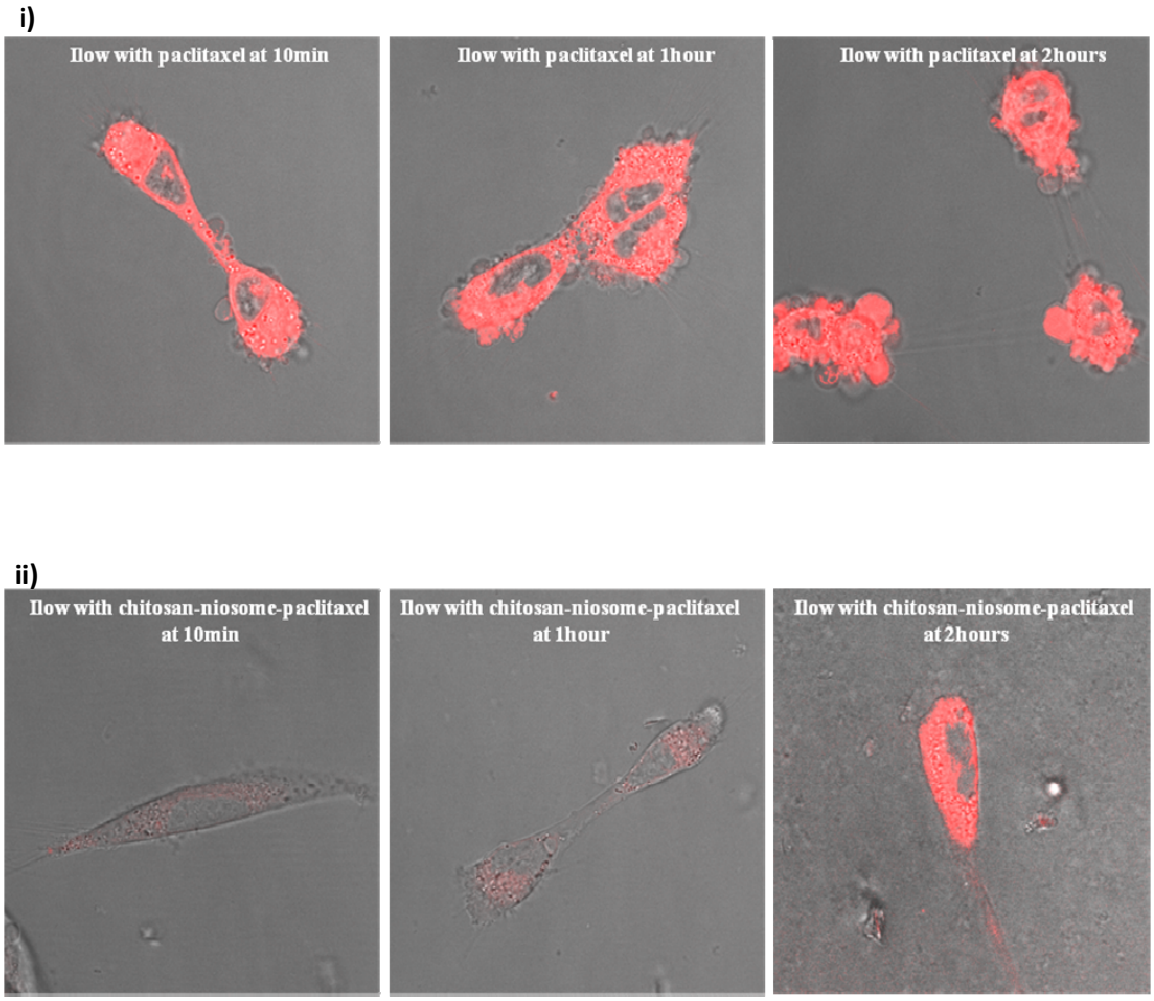


**Figure 5.3** Normal ovarian epithelial cells (Ilow) when exposed to: i) 0.4 µM paclitaxel alone and ii) chitosan-niosome-paclitaxel system containing 0.4 µM paclitaxel. The magnification of the images is 1890x

Ilow cells exposed to the chitosan-niosome packaged paclitaxel showed a controlled release of the drug from the delivery system. Slight staining of the cells with the drugs was observed within the first 10 minutes of treatment.

A quantitative analysis revealed that the intensity of paclitaxel in the cells almost doubled in an hour and a 4 fold increase was observed within 2 hours. However it needs to be mentioned that the intensity of paclitaxel in these cells at 2 hours were only one third of those exposed to paclitaxel alone at 10 min. Blebbing of the cells had not initiated by the end of the second hour although shrinking and condensed morphology had commenced.

Instantaneous cell death occurs when the cells are exposed directly to paclitaxel whereas a slow death occurs for cells exposed to the chitosan-niosome packaged paclitaxel. One of the reasons why the slow process is beneficial is that it would give the chitosan enough time to attach to the ovarian cells as opposed to normal cells and assist in its preferential treatment.

Figure 5.4 and 5.5 show the confocal images of OV2008 exposed to various concentrations of paclitaxel packaged in the chitosan-niosome system. Cell death can be extended to last from hours to days by decreasing the paclitaxel concentration. Three concentrations of the drug were used for these studies: 0.4μM, 0.04μM and 0.01μM.

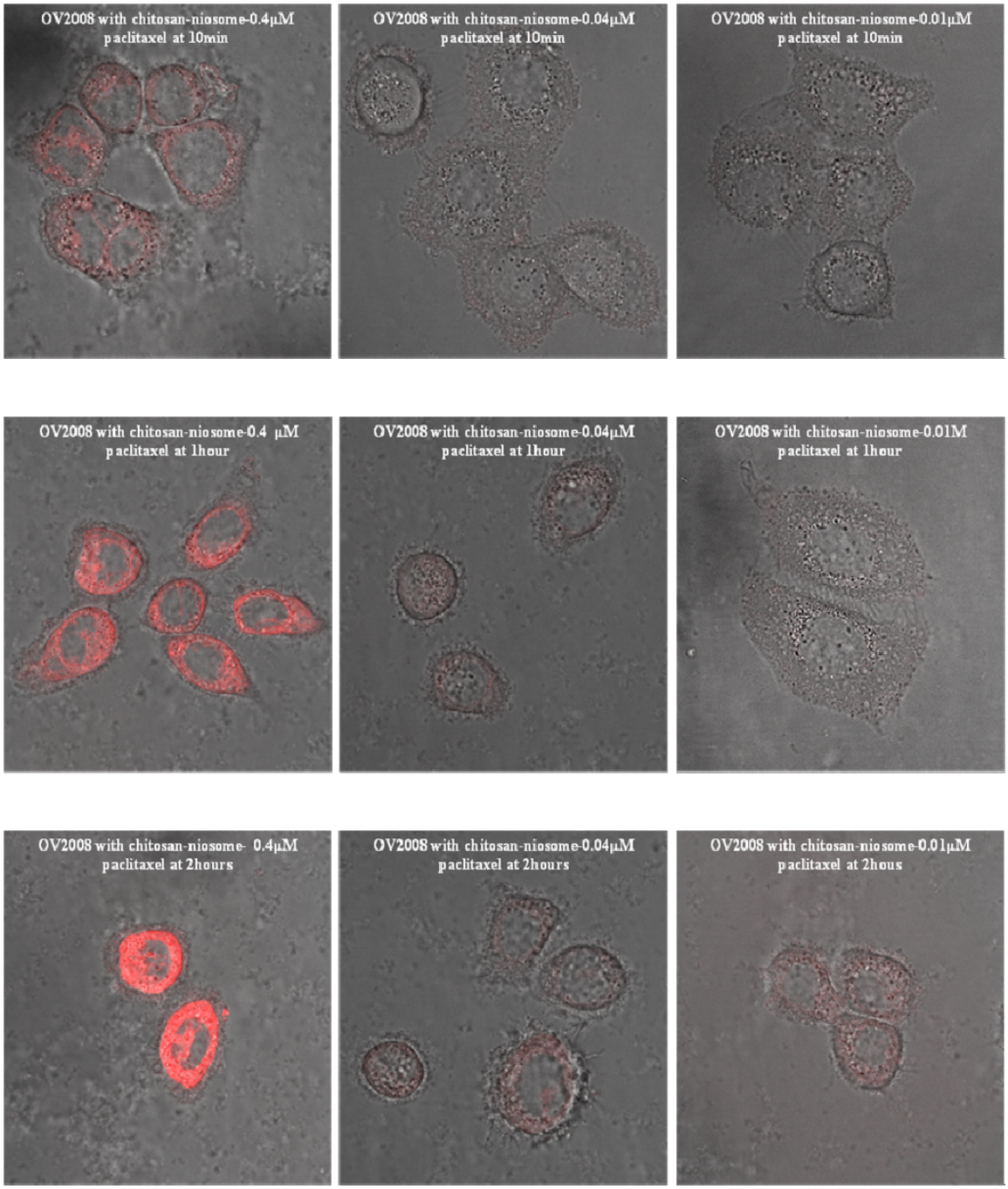


**Figure 5.4** Ovarian carcinoma cell line OV2008 exposed to chitosan-niosome-paclitaxel system with varying concentrations of paclitaxel. The magnification of the images is 1890x

With the highest concentration of 0.4μM, blebbing was seen within 3 hours. Paclitaxel was seen to accumulate in the cytoplasm of the cell and cell shrinkage occurred within an hour. With a tenfold decrease in the paclitaxel concentration, cell death was extended from 3 hours to 24 hours. At the point of cell death, the intensity of paclitaxel in the cells was almost 8 times higher in the first case (0.4μM) than in the second case (0.04 μM). It is interesting to note that cell death occurred in the second case without saturation of the cells with paclitaxel, suggesting that lower doses are just as effective in promoting cell death as higher doses and the potency of paclitaxel is intact at very low doses. A further decrease in the paclitaxel concentration to 0.01μM increased the time of cell death to 48 hours providing additional proof of the paclitaxel potency at very low concentrations.

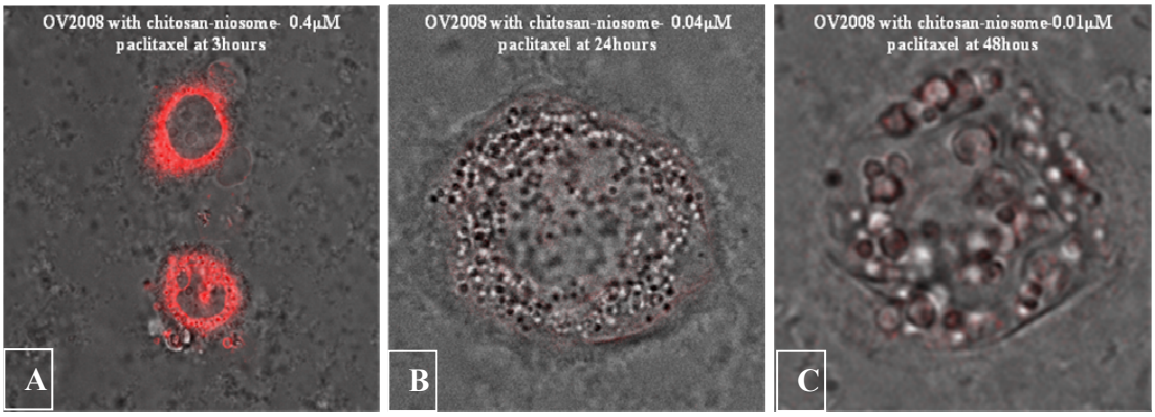


**Figure 5.5** Ovarian carcinoma cell line OV2008 showing cell death at different time points when exposed to chitosan-niosome-paclitaxel system with varying concentrations of paclitaxel. The magnification of the images are 1890x (A), 2000x (B,C)

To investigate chitosan affinity and interaction towards specific cell lines (OV2008) while showing no interaction to others (Ilow), Attenuated Total Reflectance- Fourier Transform Infra-Red (ATR-FTIR) spectroscopy was employed.

ATR-FTIR spectroscopy is a surface diagnostic technique which has been utilized since the past three decades. The infra-red beam is focused at an angle of 45$^{o}$C onto the beveled faces of the ATR crystal. The beam undergoes multiple internal reflections as it traverses through the sample. This creates an evanescent electric field, E(z) that permeates into the film on the crystal surface and interacts with IR-active species (e.g., C-Hx and N-Hx, COx or COC) in the film [164, 165]. Each reflection adds to the IR absorbance, which results in sub-monolayer detection sensitivity to surface adsorbates [164, 165].

Figure 5.6 A shows comparative spectra showing OV2008 cell lines, OV2008 exposed to the chitosan in the "Smart Packaged System" and, chitosan from "Smart Packaged System" alone. One of the main differences is that the chitosan strong vibration bands from C-O-C compounds disappeared after being in contact with OV2008 (centered at 1100 cm-1). We believe MUC1 is responsible for such dramatic change. The fingerprint for MUC1 is convoluted in the Amide I band (from 1600-1700 cm-1), so it cannot be appreciated in these spectra. However, one can appreciate that the Amide I band intensifies. Figure 5.6 B shows comparative spectra of two cell lines OV2008 and Ilow exposed to chitosan in the "Smart Packaged System" and chitosan from "Smart Packaged System". The spectra seem to suggest that interaction between chitosan and OV2008

could be through increases in the intensity and shifts in -OH peak from 3237cm$^{-1}$to 3357 cm$^{-1}$ and the Amide I peak from 1647cm$^{-1}$ to 1637cm$^{-1}$. Such changes were not observed for the normal cell line Ilow exposed to the "Smart Packaged System" depicting a lack of interaction with chitosan.

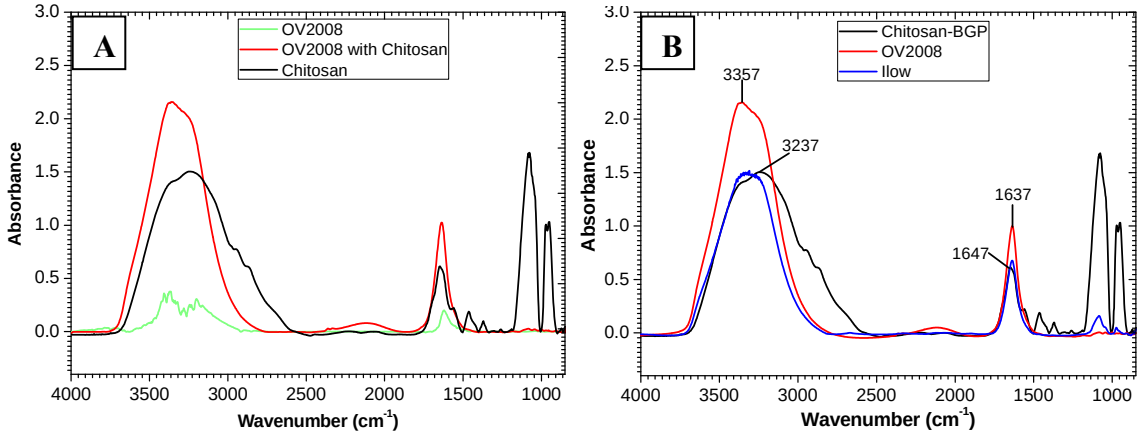


**Figure 5.6** Comparison between OV2008 cell lines and OV2008 cells exposed to the "Smart Packaged Drug Delivery System". (A); Comparison between OV2008 and Ilow cells exposed to the "Smart Packaged Drug Delivery System" (B)

In order to test the efficiency of the system in preferential treatment in ovarian cells, the following treatment regimen was proposed. The cell lines were each given a 15 minute treatment after which the chitosan-niosome-paclitaxel system was removed and the cells incubated for 5 days. Confocal images were taken for an hour on the first day and at time points 24, 48, 51 54, 72, 75, 78 and 120 hours which are shown in figures 5.7 A and B.

In the first 15minutes of the treatment, not much change in the cell structure and morphology were observed. Attachment of chitosan to the OV2008 cell surface could be

seen whereas such a behavior was not observed for the normal cell line MCC3. The intensity of paclitaxel was low in both the cell lines. In the first hour the morphology remained unaffected. In the next 24 hours, the morphology showed a slight change with the cells rounding up in both the cases. Cell death was observed for OV2008 in the following 54 hours. However the MCC3 did not show much change in its morphology in 54 hours and total cell death was achieved in 78hours. OV2008 showed complete destruction at a much faster rate than MCC3. A glance at figure 5.8 would assist in explaining this behavior. The plot shows the average intensity of the cell lines for different time points. The error bars represent the standard deviation (SD) at each time point with $p< 0.05$ and $n=15$. The intensity was observed to increase within the first 15 minutes of the treatment after which a gradual decrease was observed till the $5^{th}$ day.

Another significant observation is that the intensity of paclitaxel was much higher in OV2008 than MCC3 for all the time points. Since chitosan has an affinity for MUC1 over-expressed in ovarian carcinoma they accumulate on the surface of these cells. Hence after the 15 minute treatment more paclitaxel was available to OV2008 than MCC3 and this is the reason for the delayed cell death for MCC3. These results suggest that our drug delivery system has great potential for targeted delivery and would aid in the preferential treatment of ovarian carcinoma.

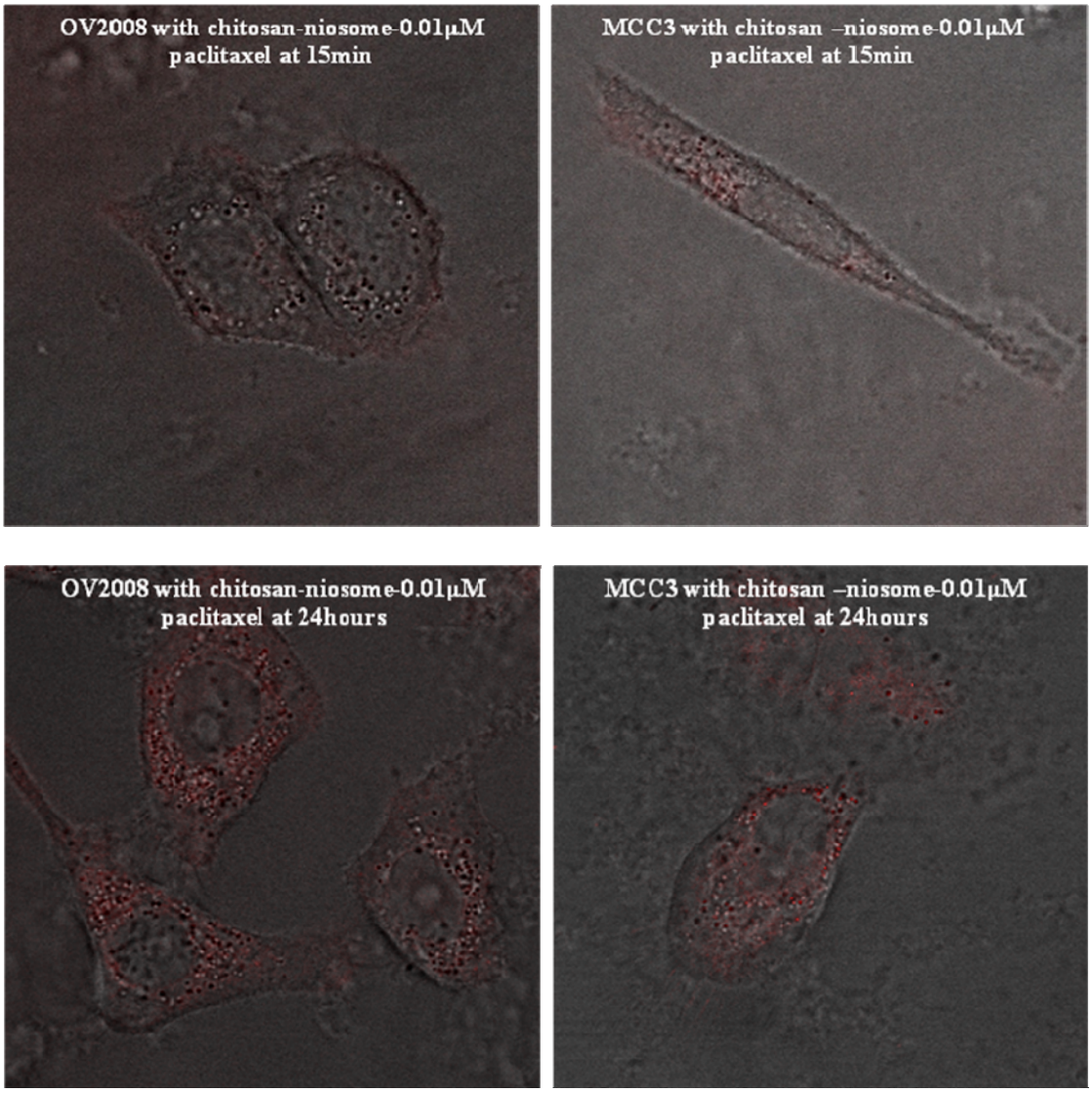


**Figure 5.7 A** Ovarian carcinoma OV2008 and normal ovarian epithelial MCC3 cell lines exposed to 15 minutes of treatment. Time points of 15minutes and 24 hours are shown

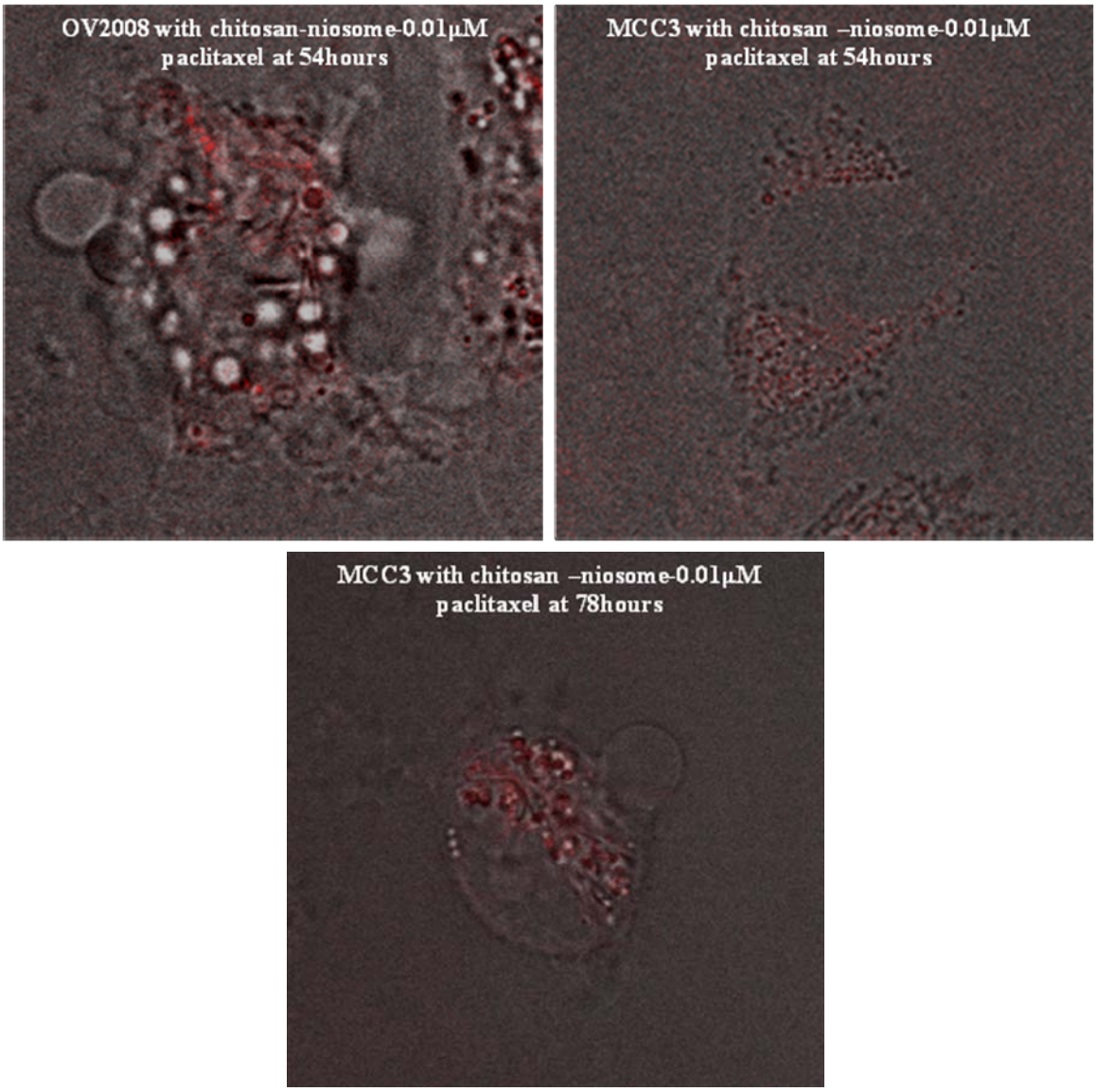


**Figure 5.7 B** Ovarian carcinoma OV2008 and normal ovarian epithelial MCC3 cell lines exposed to 15 minutes of treatment showing cell death at different time points. The magnification of the images is 2000x

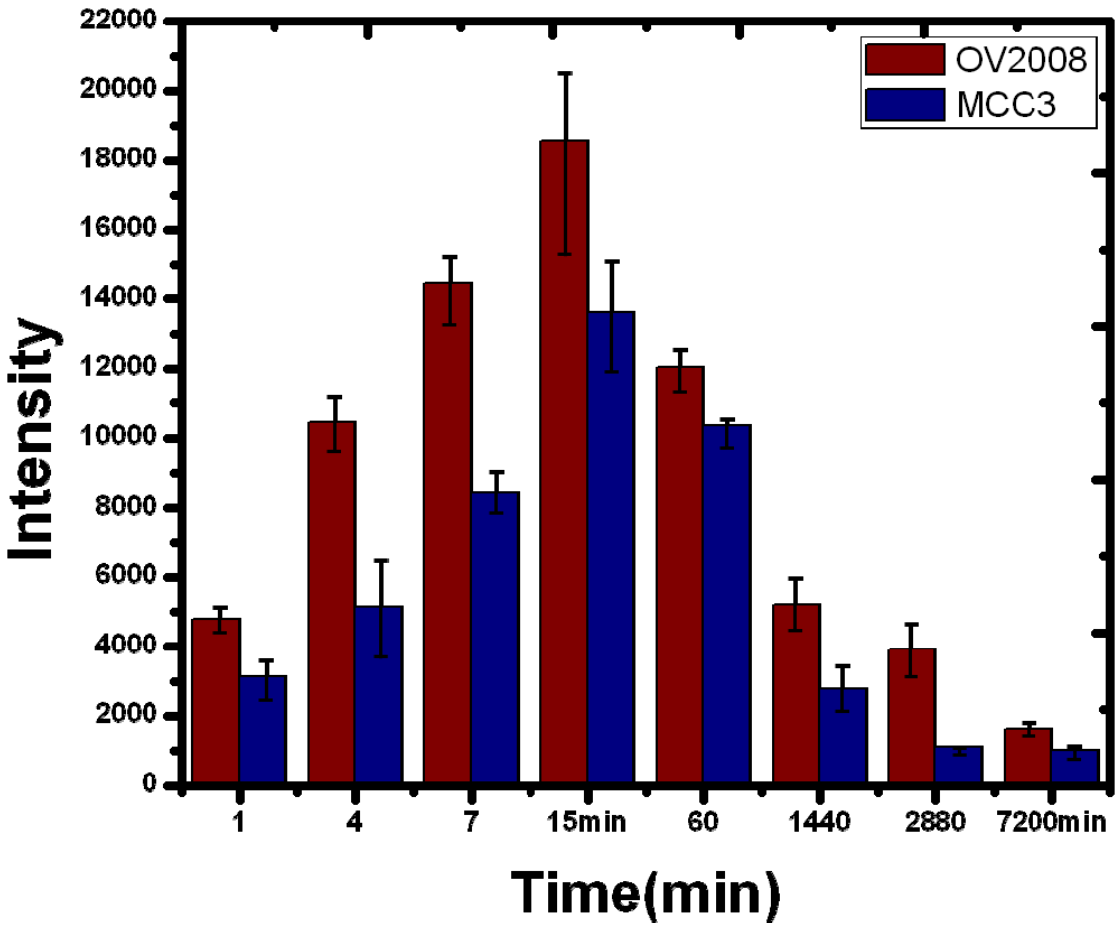


**Figure 5.8** Plot showing intensity of paclitaxel in the cell lines OV2008 and MCC3 after they were each given a 15 minute treatment with chitosan-niosome-paclitaxel system (0.1 μM paclitaxel with a fluorescence probe). The error bars represent the SD at each time point with $p < 0.05$ and $n=15$.

## 5.3 Conclusion

From the results described in the previous section it can be safely concluded that chitosan has high affinity towards ovarian carcinoma cell lines (OV2008) but not to normal cells (Ilow and MCC3). Confocal imaging showed that chitosan accumulated around OV2008 within 10 minutes of application of the 'Smart Packaged Drug Delivery System' and its buildup around the cells increased with time. Quantitative analysis of the fluorescence of paclitaxel conjugated with BODIPY® 564⁄570 on OV2008 and MCC3 cells after 15 minute treatment showed that the intensity of paclitaxel- BODIPY® 564⁄570 conjugate was significantly higher in OV2008 than MCC3 for all the time points. This proves that there is a preferential affinity of the 'Smart Packaged Drug Delivery System' to ovarian carcinoma cells (OV2008) than to normal epithelial cells (MCC3). Hence, this system can be exploited for preferential treatment to cancer cells.

# CHAPTER 6 TOXICITY AND RELEASE STUDIES OF THE 'SMART PACKAGED SYSTEM' *IN VIVO*

## 6.1 Introduction

The previous chapters have shown the efficiency of the drug delivery system in cell free system as well as in ovarian carcinoma and normal cell lines. The 'smart packaged system' was shown to be biocompatible and non-toxic to the cells. Further, results showed that the system could be manipulated to meet the dosage requirements. Cross-link mesh dimensions as well as the niosome packaging ratio contributed to the ability to fine tune the system for dosage requirements. What needed to be done next was to test the feasibility of the system *in vivo*. This chapter focuses on the rheological behavior of the 'smart packaged system' in solution, in addition to its toxicity and release rates *in vivo*. The gelling behavior as well as the release characteristics were examined in this chapter and were compared to the previous results.

## 6.2 Results and Discussion

The gelling behavior of the thermo-responsive chitosan-niosome drug delivery system becomes highly essential when considering the practicality of the system for use in live

animals. The gelling behavior would determine whether the drug delivery system would stay at the tumor site or be cleared away by the blood stream. To study the gelling behavior, rheological measurements were made. These measurements of chitosan are shown in figure 6.1. These studies were carried out on a TA Instruments rheometer (model number AR 2000). The variation in storage modulus was recorded as a function of time at 37$^{o}$C. The frequency was set at 1Hz and the acquisition rate was set at one point per 10 s.

The increase in the storage modulus, G', indicates higher resistance to flow because of the immediate phase transition of liquid chitosan- β glycerophosphate to solid gel. The first plot represents the behavior for up to 10 min at constant shear rate. We observe that initially the storage modulus (G') slowly increases, and after 1.8 minutes the system shows dynamic arrangements as we try to shear the hydrogel (reptation-like flow). This behavior is classic and predictable in polymer melts or gels. The second plot in figure 6.1 is a zoom-in of the first when the maximum G' value is about 200 Pa (red points in figure 6.1). It was noted that the increase in G' starts immediately after a shear stress is induced. The time scale in our formulation to reach a G'= 200 Pa corresponds to 84 seconds. This is a huge improvement over the data reported from previous works (Ruel-Gariepy et al [166]) which showed that it would take about 8-10 minutes for the chitosan formulation to start gelling and inducing a resistance to flow, and it takes about 60 min to reach a G' of 180 Pa. In addition, we also corroborate that with a steep increase in the slope, at about 18 s, the gelation process happens immediately.

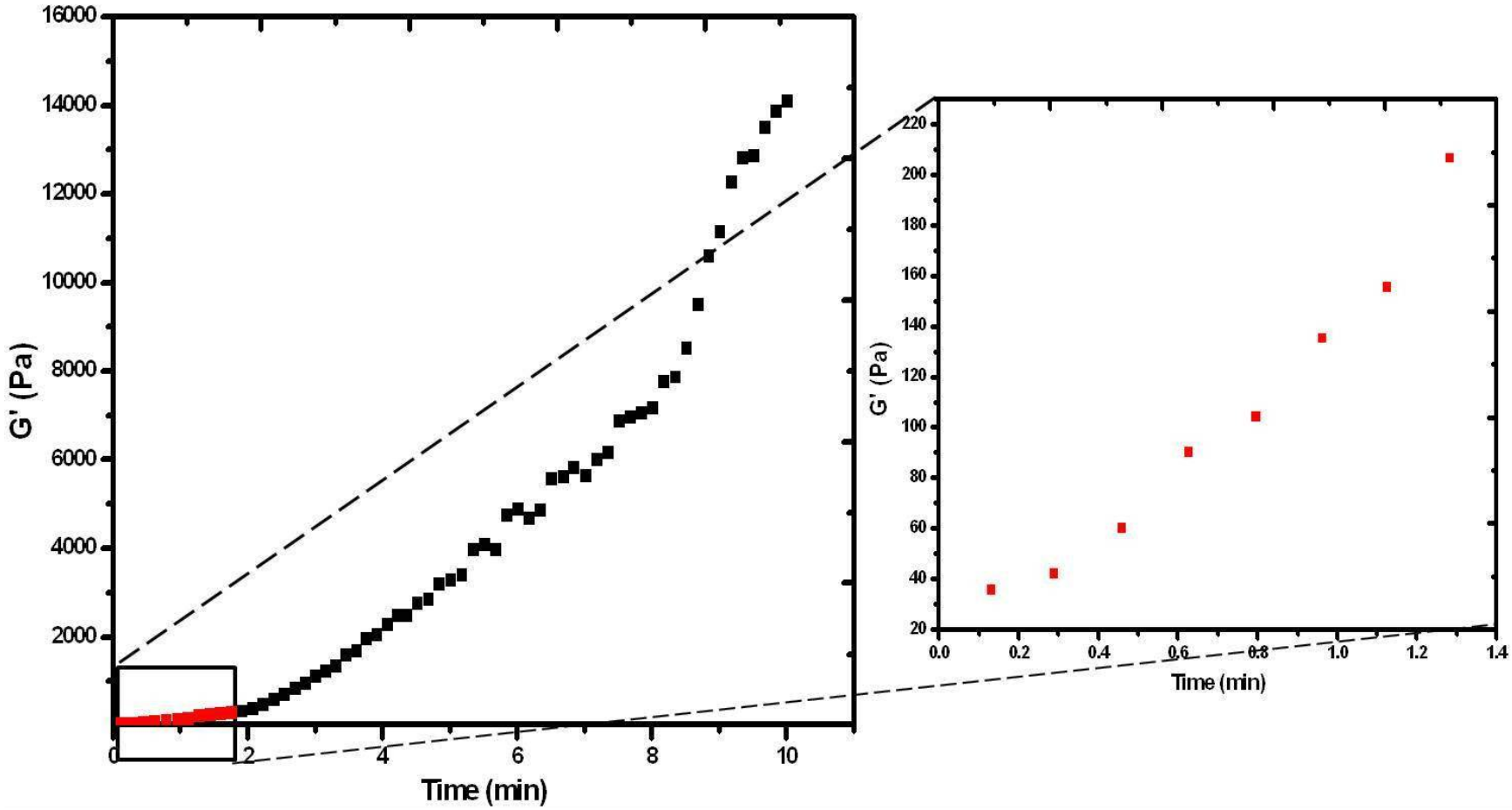


**Figure 6.1** Storage modulus as a function of time for chitosan formulation at 37$^{o}$C (body temperature)

The first plot in figure 6.2 shows that there are two different regions of flow for the niosomes-chitosan system. It was observed that within seconds of applying a constant shear rate at 37$^{o}$C, the system with niosomes embedded in chitosan showed a large storage modulus, G', which was much larger than that reported in literature by Ruel-Gariepy et al [100, 166]. One flow pattern has a rapid increase at very short times, less than 18 s, and then a low slope increase until about 8 min, followed by a rapid increase on the storage modulus that surpasses the chitosan alone system. The low slope increase confirms that the niosomes do not influence the gelation process. Rather, the presence of niosomes adds an additional traction to mobility indicating an instant locking of the niosomes in the chitosan gel. The inset shows how within 18 s of shearing, a storage modulus of 570 Pa was attained which was much higher than 160 Pa, which is the maximum value achieved by Ruel-Garipy et al [166]system after 60 min.

Rheological measurements were also made with our chitosan system and liposomes prepared according to the procedure in Ruel-Gariepy [166]. Figure 6.3 shows the storage moduli values as a function of time for the chitosan-niosome and chitosan-liposome systems, and for chitosan alone at 37°C and constant frequency (1 Hz). Conversely to the behavior found in the chitosan-niosome system, the chitosan-liposome system does not show the expected abrupt change in the slope. Instead, it follows similar general trends as presented in Ruel-Gariepy [166]. The values of G', when liposomes are present are lower than the values of G' when niosomes are embedded in chitosan (figure 6.3). This is an indication of certain intermolecular interactions interfering with the chitosan crosslinking process induced by liposomes, which results in a fluid-like behavior and

prevents the formation of the mesh network. The reason for this behavior is that liposomes are made of ionic surfactants and the charges would prevent the formation of the links within the chitosan mesh.

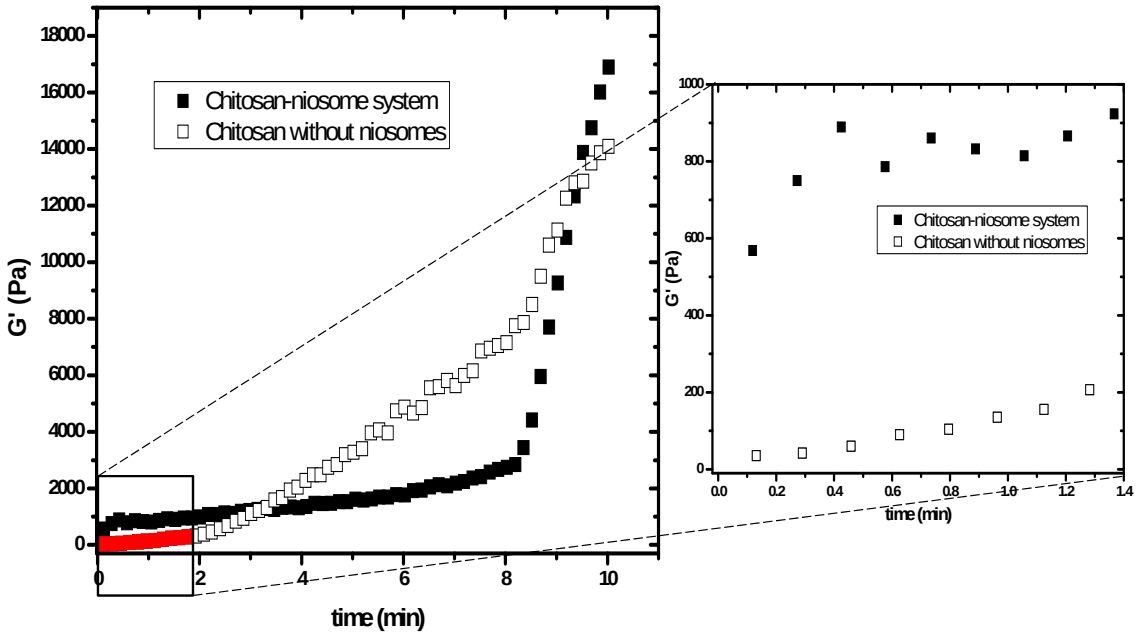


**Figure 6.2** Rheology measurements showing the comparison between a chitosan-niosome system vs. chitosan gel alone. The niosome concentration is 5mM and the packaging density is 0.15:1

Our chitosan system is designed to act much faster and it is more stable than the chitosan system presented by Ruel-Gariepy et al. [166]. The values of storage modulus are relatively higher than that of the chitosan-liposome system in the reference. However, the chitosan does not completely gel even after 30 min of shearing at constant T (37$^{o}$C) and shearing velocity (1 Hz) (Figure 6.4). This is a direct indication that the liposomes

interfere with the chitosan network, whereas the niosomes do not show such interaction. The results above suggest that the gelling of the chitosan-niosome system is very rapid and occurs within a few seconds and the presence of niosomes increases the storage modulus in the initial time periods resulting in rapid gelling. These results show a huge potential for the 'Smart Packaged Drug Delivery System' to be feasible *in vivo*. These finding are discussed in the next section.

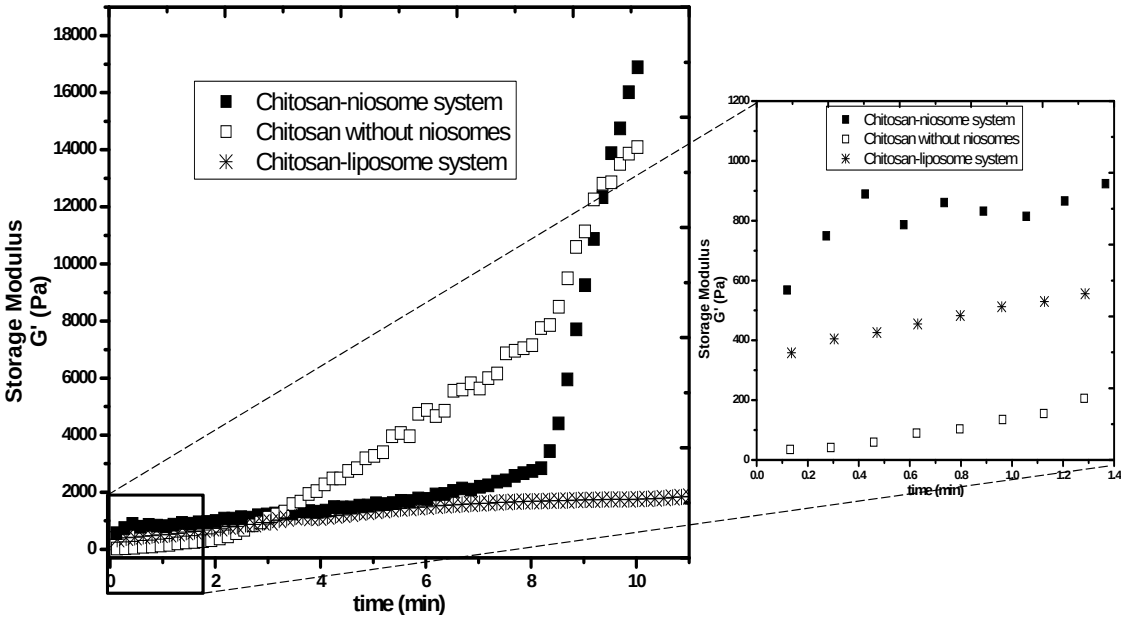


**Figure 6.3** Storage modulus vs. shearing time for chitosan-niosome system (■), chitosan-liposome system (∗), and chitosan alone (□) at 37°C and 1Hz. Insert shows the storage modulus for 1.4 min at 37°C and 1Hz

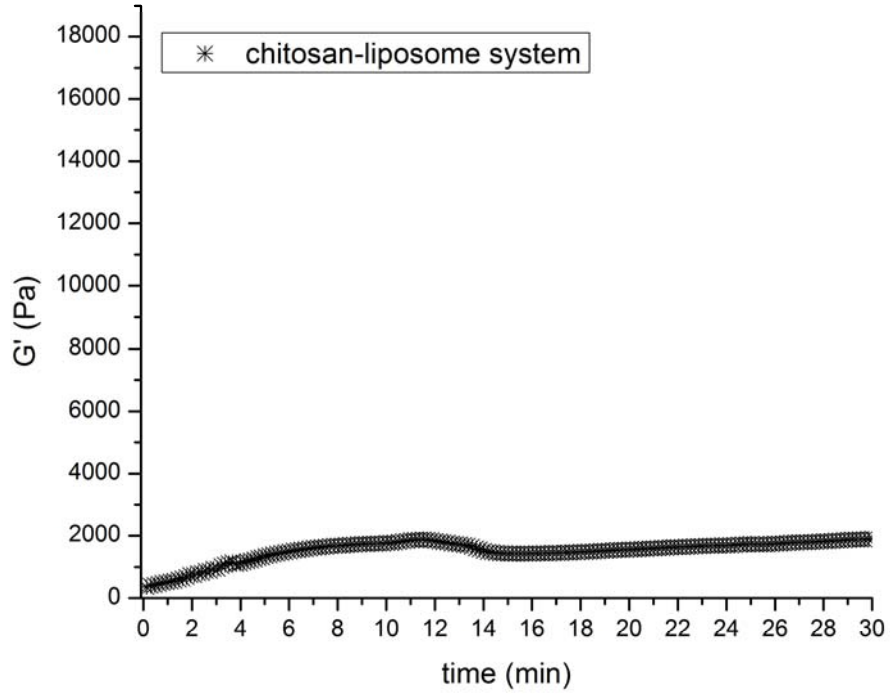


**Figure 6.4** Storage modulus vs. shearing for 30 min at 37°C and 1Hz

Toxicity and release kinetics *in vivo*: For the *in vivo* studies, 8 week old female mice (Strain: FVB/NJ) were chosen because of their short life span and fecundity. They have higher than average activity, anxiety, basal body temperature and low stress-induced hyperthermia. Although FVB/NJ typically does not develop spontaneous tumors, they are highly susceptible to chemically induced squamous cell carcinomas with a high rate of malignant conversion from papilloma to carcinoma. The average weight of the mice was 20grams. The hair was removed from the abdomen area of the mice so as to facilitate its imaging using Xenogen.

Xenogen is a high-sensitivity, low noise, non-invasive light imaging technique that is capable of imaging bioluminescence and fluorescence in living animals. It consists of a light imaging chamber coupled to a highly sensitive CCD camera system which is cooled to -95$^{o}$C. The CCD camera is sensitive enough to be able to quantify single-photon signals emanating within the tissue of the living animal. It is useful in the visualization and tracking of cellular and genetic activity within a living organism. Xenogen is connected to an integrated isoflurane gas manifold that provides temporary anesthesia to the mice during the imaging process. It has the capability of imaging five mice simultaneously.

The 'Smart Packaged Drug Delivery System' was injected subcutaneously into the right flank of the mice after they were anesthetized in the isoflurane chamber. The system was inspected for gelling. Gelling of the system occurred within twenty seconds of the injection and could be seen as a bulge on the flank. This result is comparable with the previous results where the gelling time was 18 s.

The 'Smart Packaged Drug Delivery System' was observed to be non-toxic and the mice survived for months after subcutaneous injection of the drug delivery system. *In vivo* images obtained through Xenogen are shown in figure 6.5. Imaging was done for 14 days with images collected every 10 minutes for the first 100 minutes after which they were collected every hour for the next 9 hours and subsequently every 24 hours for 14 days.

The image shows the release of the fluorescent dye from the injected chitosan-niosome system which appears as a bolus in the abdomen area. From time points 1 to 100 minutes the dye had spread from an area of 1.02cm$^2$ to 1.44cm$^2$ and a subsequent decrease in the intensity of the bolus was noticed.

A quantitative analysis of the intensity was performed using the Living image 3.1 program. Intensity decreased with time showing the release of the dye from the chitosan-niosome bolus. With time the bolus decreased in size indicating the degradation of the chitosan gel. Table 6.1 shows the decrease in size with time. By 312 hours (13 days) the size was not measurable and is an indication of complete chitosan degradation.

**Table 6.1** Change in the size of the chitosan-niosome bolus with time

| Time(hours) | 0 | 6 | 24 | 48 | 72 | 96 | 192 | 312 |
|---|---|---|---|---|---|---|---|---|
| Size (cm) | 2.01 | 1.97 | 1.51 | 1.02 | 0.74 | 0.38 | 0.05 | - |

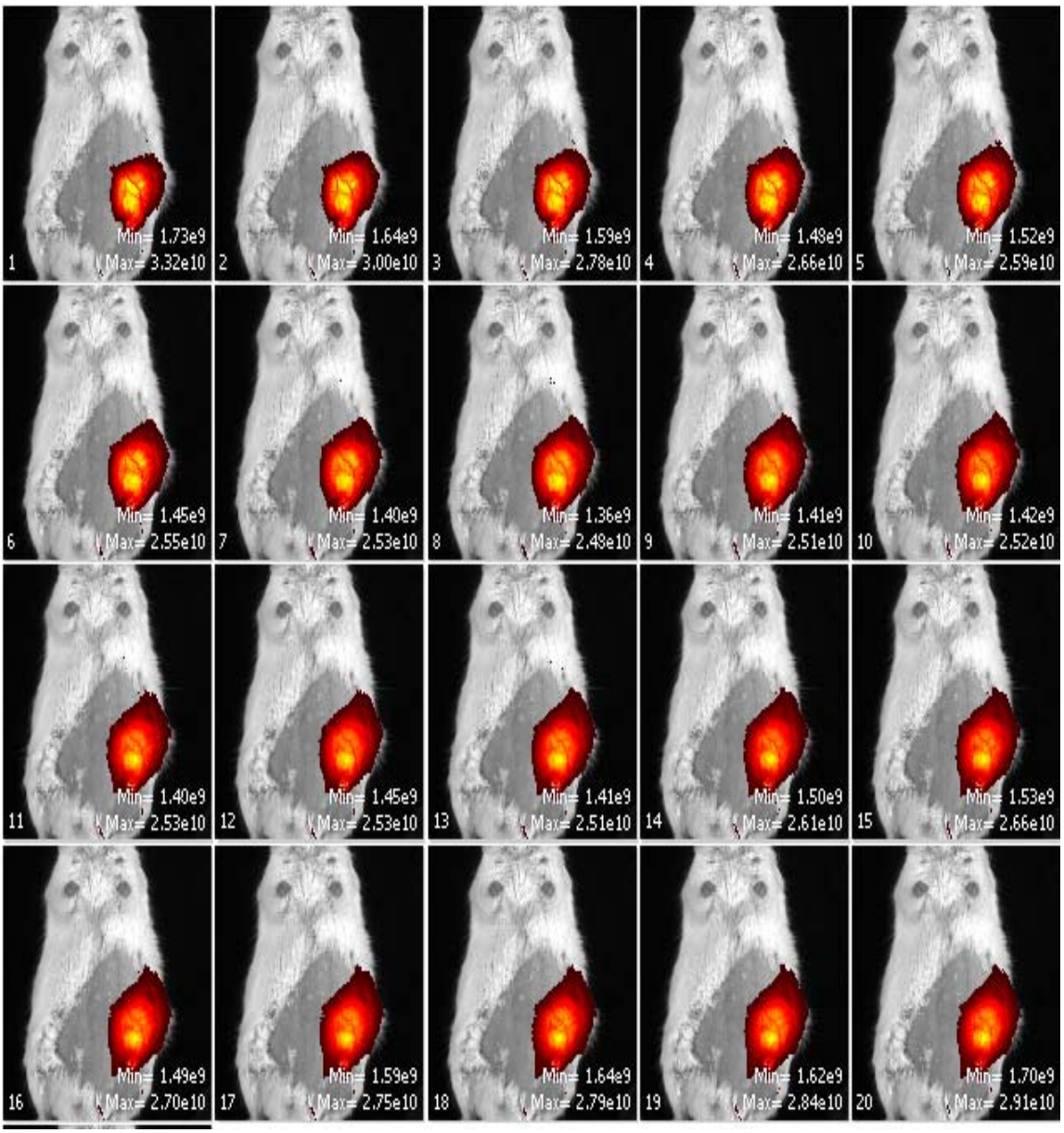


**Figure 6.5** *In vivo* images obtained through xenogen showing the dye release. The first scan is at 1 min. Release rate was captured by measuring the fluorescence intensity with flow of time (5 minute interval)

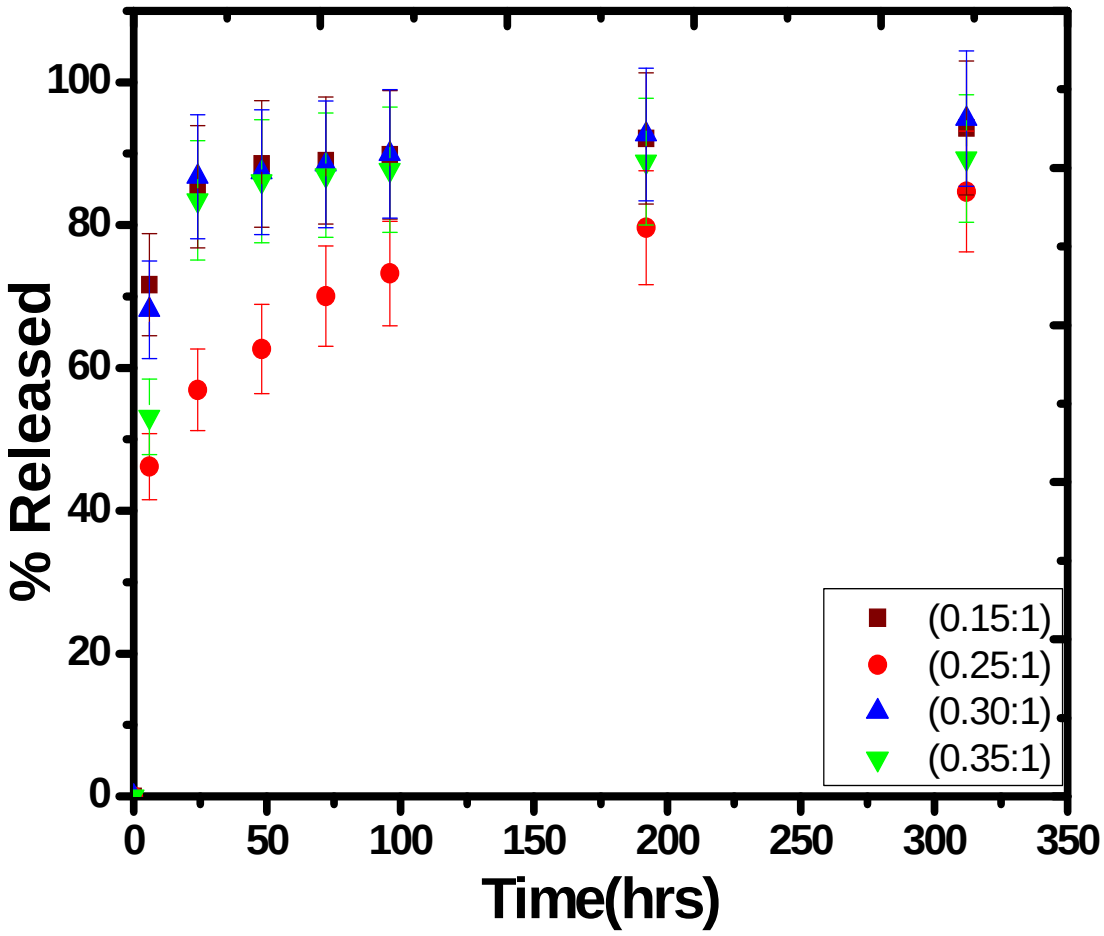


**Figure 6.6** Release rate dependence of drug on the packaging density of the chitosan-niosome system in mice. Each point represents the mean ± standard deviation with n= 3

Two parameters of the chitosan- niosome system were varied for *in vivo* studies: the packaging density and the cross-link density. Figure 6.6 shows the release rate of the dye obtained by varying the packaging density. Packing densities from 0.15:1 to 0.35:1 molar ratios were used for this study. The release trend was similar to the in-vitro studies with higher percentage release observed for greater niosome: chitosan ratios. Optimum value was obtained at 0.25:1 (finest controlled release), which shows a slight deviation from *in vitro* studies. The release in this case is a result of both diffusion through the niosomes

and also niosomal bursting due to osmotic difference (when the niosomes are exposed to body fluids as a result of chitosan degradation). This could be the reason for the deviation of the optimum from the *in vitro* results. Depending on the packaging density, 40 - 80% of release occurred within 24 hours, after which, the dye was released steadily. By the 13th day, 95% of dye was released. This is a huge improvement over the release rates reported in literature where 90% of the drug was released within the first 24hours (T. Yang et al. 2007).

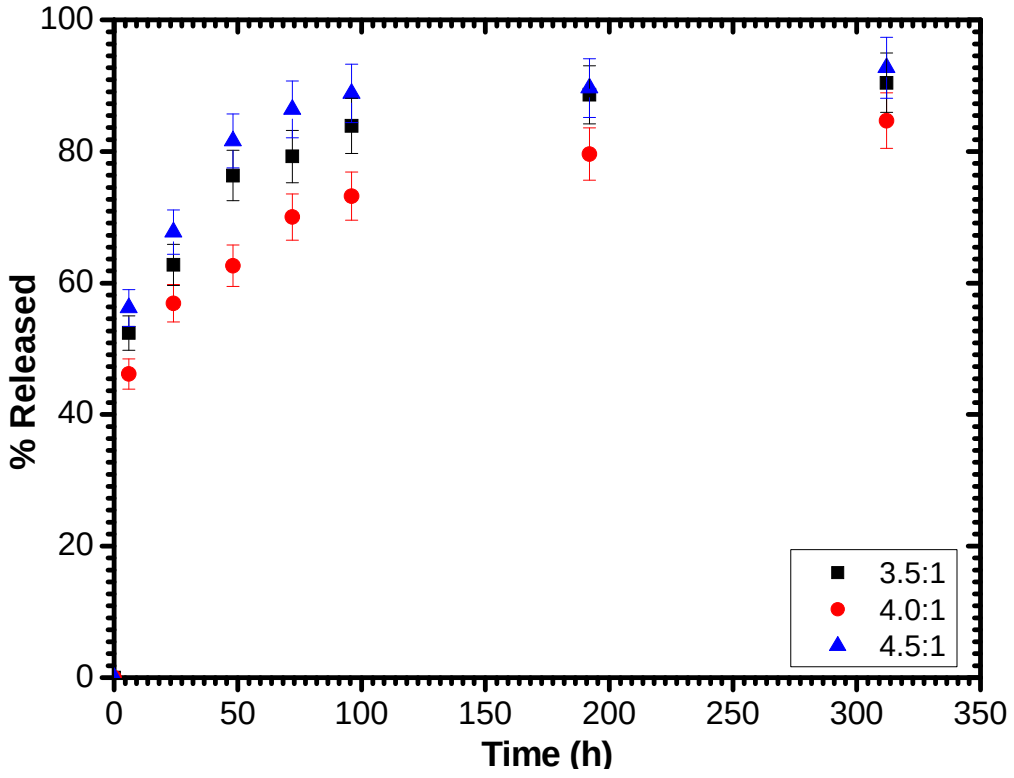


**Figure 6.7** Release rate dependence of drug on the cross-link density of the chitosan-niosome system in mice. Each point represents the mean ± standard deviation with n= 3 Cross-link density of the chitosan formulation was altered to evaluate its effect on the release.

Figure 6.7 shows the percentage released from the chitosan-niosome drug delivery system. The results indicate a trend similar to that observed in the *in vitro* studies with the cross-link molar ratio of 4:1 showing the slowest controlled release. As discussed earlier the size of the niosomes and the chitosan cross-link mesh was commensurate at this ratio. The local structure or compactness of the chitosan gel affects the release from the system with 'looser' mesh structure leading to greater clearance of the drugs and hence a higher release. An optimum is obtained when the sizes of the niosomes and the chitosan mesh are similar and each niosome is embedded into a single mesh. Although the release rates *in vitro* could be observed well after 55 days, the release *in vivo* was much faster with complete release occurring in two weeks. However, this release is still a huge improvement over the reported release times with similar systems where majority of the drugs were released within the first 24 hours.

## 6.3 Conclusion

Mice studies proved that the system is feasible in *in vivo* and has a great potential for controlled drug delivery. Gelling of the chitosan-niosome system is very rapid which would prevent the premature release of the encapsulated molecule. Release rate can be controlled to last from 24 hours to 14 days by fine tuning the chitosan or niosome parameters.

# CHAPTER 7 SUMMARY AND CONCLUSIONS

The results presented in this work illustrate that the 'Smart Packaged Drug Delivery System' has great potential to provide control over the drug release rates by fine tuning either of its components i.e. chitosan/ niosome or a combination of both. Release rates can be controlled to last from 24 hours (1 day) to more than 1320 hours (55 days) depending on the conditions to which niosomes are exposed. Exposing naked niosomes themselves to solutions of low tonicity resulted in an absolute release within 144 hours (6 days) whereas the addition of chitosan to the system resulted in a controlled release for more than 55 days. Dye concentration and size, chitosan molecular weight, cross-link density, packaging density are some of the characteristics that can be altered so as to obtain release rates as desired. The finest controlled release was obtained with medium molecular weight chitosan with a cross-link ratio of 4:1 (β-glycerophosphate: chitosan) and a packaging ratio of 0.35:1 (niosome: chitosan). Further it has been shown that niosomes were able to encapsulate a higher percentage of paclitaxel as compared to the traditional liposomes since non-ionic surfactants aid in the solubility of paclitaxel. The permeability of the bilayer membrane decreased with the addition of paclitaxel. This in turn affected the release rates of the encapsulated molecules either in its hydrophilic core or the hydrophobic bilayer. Increase in the paclitaxel concentration decreased the rates of carboplatin release in addition to a decrease in its own release. *In vitro* studies showed

that chitosan has affinity towards ovarian carcinoma cell lines (OV2008), but not to normal cells (Ilow and MCC3). Confocal imaging showed that chitosan accumulated around OV2008 within 10 minutes of application of the 'Smart Packaged Drug Delivery System' and its buildup around the cells increased with time. Quantitative analysis of the fluorescence of paclitaxel conjugated with BODIPY® 564⁄570 on OV2008 and MCC3 cells after 15 minute treatment showed that the intensity of paclitaxel- BODIPY® 564⁄570 conjugate was much higher in OV2008 than MCC3 for all the time points. This proves that there is a preferential affinity of the 'Smart Packaged Drug Delivery System' to ovarian carcinoma cells (OV2008) than to normal epithelial cells (MCC3). Hence, this system can be exploited for preferential treatment to cancer cells. Toxicity studies proved that the system is feasible in *in-vivo* and has a great potential for controlled drug delivery. Gelling of the chitosan- niosome system is very rapid (18 s) which would prevent the premature release of the encapsulated molecule. Further, release rates could be controlled to last from 24 hours to 14 days by fine tuning the chitosan or niosome parameters.

Hence, this design strategy, due to its ability to be tailored according to the need at hand, can be extended to include a wide variety of applications from administration of labile drugs to localized drug delivery for ovarian cancer and brain tumors.

# CHAPTER 8 FUTURE DIRECTIONS

The ‘cocktail niosomal formulation’ can be employed to include a wide variety of hydrophobic and hydrophilic drugs. Another combination that will be significant in future studies is to encapsulate triciribine and carboplatin. Prolonged chemotherapy regime leads to resistance of cells to drugs resulting in ineffective treatment. Latest studies indicate that triciribine prevents this behavior by disrupting a specific signaling pathway associated with chemo-resistance and cancer cell survival in ovarian cancer [51]. Hence using these drugs in combination in the niosomal formulation would ensure prolonged administration of the cancer drug carboplatin with reduced chances of developing cell resistance. The present research examined the effect of ‘Smart Packaged Drug Delivery System’ on cell lines using one drug niosome. An extension of this work would be to study the effect of the system on cell lines containing ‘cocktail niosomes’. This technology can further be examined in various carcinoma cell lines. Another possible area for future investigation involves characterization of the ‘Smart Packaged Drug Delivery System’ *in vivo* in mice tumor models. ‘Smart Packaged Drug Delivery System’ containing either ‘cocktail niosomes’ or one drug niosome can be utilized here employing either subcutaneous or intraperitoneal tumors.

## REFERENCES


1. Gore, M., A. du Bois, and I. Vergote, *Intraperitoneal chemotherapy in ovarian cancer remains experimental.* Journal of Clinical Oncology, 2006. **24**(28): p. 4528-4530.

2. *Cancer Facts and Figures 2009*. 2011 [cited 2660 January 18]; Available from: http://www.cancer.org/downloads/STT/CAFF_finalPWSecured.pdf.

3. Bjerrum, J.T., et al., *Technology insight: metabonomics in gastroenterology-basic principles and potential clinical applications.* Nat Clin Pract Gastroenterol Hepatol, 2008. **5**(6): p. 332-43.

4. Astin, M., et al., *The diagnostic value of symptoms for colorectal cancer in primary care: a systematic review.* Br J Gen Pract, 2011. **61**(586): p. e231-43.

5. Watson, A.J. and P.D. Collins, *Colon cancer: a civilization disorder.* Dig Dis, 2011. **29**(2): p. 222-8.

6. Kuper H, A.H., Boffetta P *Tobacco use, cancer causation and public health impact.* Journal of internal medicine, 2002. **251** (6): p. 455–466.

7. Kuper H, B.P., Adami HO, *Tobacco use and cancer causation: association by tumour type.* Journal of internal medicine, 2002. **252** (3 ): p. 206–224.

8. Thun, M.J., *How much of the decrease in cancer death rates in the United States is attributable to reductions in tobacco smoking?* Tobacco Control, 2006. **15** (5): p. 345–347.

9. Pagano JS, B.M., Buendia MA, *Infectious agents and cancer: criteria for a causal relation.* Cancer Biol, 2004. **14** ((6)): p. 453–471.

10. Samaras, V.R., Petros I.; Mourtzoukou, Eleni G.; Peppas, George; Falagas, Matthew E, *Chronic bacterial and parasitic infections and cancer: a review.* The Journal of Infection in Developing Countries, 2010. **4**( (5)): p. 267–281.

11. Berrington de González A, M.M., Kim KP, et al, *Projected cancer risks from computed tomographic scans performed in the United States in 2007.* Arch. Intern. Med, 2009. **169(**22):2071–7.

12. Brenner DJ, H.E., *Computed tomography--an increasing source of radiation exposure.* N. Engl. J. Med, 2007. **357** (22): 2277–84.

13. Cappellani, A.D.V., M, Zanghi, A, Cavallaro, A, Piccolo, G, Veroux, M, Berretta, M, Malaguarnera, M, Canzonieri, V, Lo Menzo, E *Diet, obesity and breast cancer: an update.* Frontiers in bioscience (Scholar edition), 2012 **4**: p. 90–108.

14. Key, T., *Fruit and vegetables and cancer risk.* British journal of cancer, 2011 **104** (1): 6–11.

15. Maltoni, C.F.M., and James F Holland *Chapter 16: Physical Carcinogens*. Holland-Frei Cancer Medicine (5th ed.). 2000: Hamilton, Ontario: B.C. Decker.

16. John R, R.H. (2010) *The Global Economic Cost of Cancer*. http://www.cancer.org/AboutUs/GlobalHealth/global-economic-cost-of-cancer-report

17. WHO. *The World Health Report working together for health*. 2006 [cited; Available from: www.who.int/whr/2006/en.

18. Greenlee RT, H.-H.M., Murray T, Thun M (2005) *Cancer Statistics*. Cancer J Clin **8**(2);p 15-36

19. Jemal, A., A. Thomas, T. Murray, and M. Thun (2002) *Cancer Statistics*. CA: A Cancer Journal for Clinicians **13**(2);p 23-47

20. Schwartz, P.E. and K.J. Taylor, *Is early detection of ovarian cancer possible?* Ann Med, 1995. **27**(5): p. 519-28.

21. Carney, M.E., et al., *A Population-Based Study of Patterns of Care for OvarianCancer: Who Is Seen by a Gynecologic Oncologist and Who Is Not?* Gynecologic Oncology, 2002. **84**(1): p. 36-42.

22. King, M.C., J.H. Marks, and J.B. Mandell, *Breast and Ovarian Cancer Risks Due to Inherited Mutations in BRCA1 and BRCA2.* Science Magazine, 2003. **302**(5645): p. 643-646.

23. Claus, E.B., et al., *The genetic attributable risk of breast and ovarian cancer.* Cancer, 1996. **77**(11): p. 2318-24.

24. Bailey, C.L., et al., *The malignant potential of small cystic ovarian tumors in women over 50 years of age.* Gynecol Oncol, 1998. **69**(1): p. 3-7.

25. Lefkowitz, E.S. and C.F. Garland, *Sunlight, vitamin D, and ovarian cancer mortality rates in US women.* Int J Epidemiol, 1994. **23**(6): p. 1133-6.

26. Le, T., et al., *Does Debulking Surgery Improve Survival in Biologically Aggressive Ovarian Carcinoma?* Gynecologic Oncology, 1997. **67**(2): p. 208-214.

27. Christian, J. and H. Thomas, *Ovarian cancer chemotherapy.* Cancer Treat Rev, 2001. **27**(2): p. 99-109.

28. Hannun, Y.A., *Apoptosis and the dilemma of cancer chemotherapy.* Blood, 1997. **89**(6): p. 1845-53.

29. Kyrgiou, M., et al., *Survival benefits with diverse chemotherapy regimens for ovarian cancer: meta-analysis of multiple treatments.* J Natl Cancer Inst, 2006. **98**(22): p. 1655-63.

30. McGuire, W.P., 3rd and M. Markman, *Primary ovarian cancer chemotherapy: current standards of care.* Br J Cancer, 2003. **89** Suppl 3: p. S3-8.

31. Armstrong, D.K., et al., *Intraperitoneal cisplatin and paclitaxel in ovarian cancer.* New England Journal of Medicine, 2006. **354**(1): p. 34-43.

32. Markman, M., et al., *Combination Intraperitoneal Chemotherapy with Cisplatin, Cytarabine, and Doxorubicin for Refractory Ovarian-Carcinoma and Other Malignancies Principally Confined to the Peritoneal-Cavity.* Journal of Clinical Oncology, 1984. **2**(12): p. 1321-1326.

33. Alberts, D.S., et al., *Intraperitoneal cisplatin plus intravenous cyclophosphamide versus intravenous cisplatin plus intravenous cyclophosphamide for stage III ovarian cancer.* N Engl J Med, 1996. **335**(26): p. 1950-5.

34. Kaye, S.B., *Intravenous chemotherapy for ovarian cancer - the state of the art?* Int J Gynecol Cancer, 2000. **10**(S1): p. 19-25.

35. Priestman, T.J., *Results in fifty cases of advanced squamous cell carcinoma of the head and neck treated by intravenous chemotherapy.* Br J Cancer, 1973. **27**(5): p. 400-5.

36. Geomini, P.M., P.L. Dellemijn, and G.L. Bremer, *Paraneoplastic cerebellar degeneration: neurological symptoms pointing to occult ovarian cancer.* Gynecol Obstet Invest, 2001. **52**(2): p. 145-6.

37. Hawkins, T.R., Jr., *Symptoms of ovarian cancer.* Obstet Gynecol, 2001. **98**(6): p. 1150-1.

38. Olson, S.H., et al., *Symptoms of ovarian cancer.* Obstet Gynecol, 2001. **98**(2): p. 212-7.

39. Armstrong, D.K., et al., *Intraperitoneal cisplatin and paclitaxel in ovarian cancer.* N Engl J Med, 2006. **354**(1): p. 34-43.

40. Jones, R.B., et al., *High volume intraperitoneal chemotherapy ("belly bath") for ovarian cancer. Pharmacologic basis and early results.* Cancer Chemother Pharmacol, 1978. **1**(3): p. 161-6.

41. Kirmani, S., et al., *A comparison of intravenous versus intraperitoneal chemotherapy for the initial treatment of ovarian cancer.* Gynecol Oncol, 1994. **54**(3): p. 338-44.

42. Markman, M. and J.L. Walker, *Intraperitoneal chemotherapy of ovarian cancer: a review, with a focus on practical aspects of treatment.* J Clin Oncol, 2006. **24**(6): p. 988-94.

43. McClay, E.F., et al., *A phase I trial of intraperitoneal carboplatin and etoposide with granulocyte macrophage colony stimulating factor support in patients with intraabdominal malignancies.* Cancer, 1994. **74**(2): p. 664-9.

44. Plaxe, S., et al., *Phase I trial of cisplatin in combination with glutathione.* Gynecol Oncol, 1994. **55**(1): p. 82-6.

45. Hamilton, C.A. and J.S. Berek, *Intraperitoneal chemotherapy for ovarian cancer.* Current Opinion in Oncology, 2006. **18**(5): p. 507-515.

46. Walker, J.L., et al., *Intraperitoneal catheter outcomes in a phase III trial of intravenous versus intraperitonealchemotherapy in optimal stage III ovarian and primary peritoneal cancer: A Gynecologic Oncology Group Study.* Gynecologic Oncology, 2006. **100**(1): p. 27-32.

47. Herrero-Vanrell, R. and M.F. Refojo, *Biodegradable microspheres for vitreoretinal drug delivery.* Advanced Drug Delivery Reviews, 2001. **52**(1): p. 5-16.

48. Lorenzo-Lamosa, M.L., et al., *Design of microencapsulated chitosan microspheres for colonic drug delivery.* Journal of Controlled Release, 1998. **52**(1-2): p. 109-118.

49. Cohen, S., et al., *Controlled delivery systems for proteins based on poly(lactic/glycolic acid) microspheres.* Pharm Res, 1991. **8**(6): p. 713-20.

50. Mathiowitz, E., et al., *Biologically erodable microspheres as potential oral drug delivery systems.* Nature, 1997. **386**(6623): p. 410-4.

51. Okada, H. and H. Toguchi, *Biodegradable microspheres in drug delivery.* Crit Rev Ther Drug Carrier Syst, 1995. **12**(1): p. 1-99.

52. Shive, M.S. and J.M. Anderson, *Biodegradation and biocompatibility of PLA and PLGA microspheres.* Adv Drug Deliv Rev, 1997. **28**(1): p. 5-24.

53. Soppimath, K.S., et al., *Biodegradable polymeric nanoparticles as drug delivery devices.* Journal of Controlled Release, 2001. **70**(1-2): p. 1-20.

54. Hans, M.L. and A.M. Lowman, *Biodegradable nanoparticles for drug delivery and targeting.* Current Opinion in Solid State & Materials Science, 2002. **6**(4): p. 319-327.

55. Hans, M.L. and A.M. Lowman, *Biodegradable nanoparticles for drugdelivery and targeting.* Current Opinion in Biotechnology, 2002. **6**(4): p. 319-327.

56. Cho, K., et al., *Therapeutic nanoparticles for drug delivery in cancer.* Clin Cancer Res, 2008. **14**(5): p. 1310-6.

57. McBain, S.C., H.H. Yiu, and J. Dobson, *Magnetic nanoparticles for gene and drug delivery.* Int J Nanomedicine, 2008. **3**(2): p. 169-80.

58. Kataoka, K., A. Harada, and Y. Nagasaki, *Block copolymer micelles for drug delivery: design, characterization and biological significance.* Advanced Drug Delivery Reviews, 2001. **47**(1): p. 113-131.

59. Liu, M.J., K. Kono, and J.M.J. Frechet, *Water-soluble dendritic unimolecular micelles: Their potential as drug delivery agents.* Journal of Controlled Release, 2000. **65**(1-2): p. 121-131.

60. Lasic, D.D., *Mixed micelles in drug delivery.* Nature, 1992. **355**(6357): p. 279-80.

61. Kazunori, K., et al., *Block copolymer micelles as vehicles for drugdelivery.* Journal of Controlled Release, 1993. **24**(1-3): p. 119-132.

62. Chonn, A. and P.R. Cullis, *Recent Advances in Liposomal Drug-Delivery Systems.* Current Opinion in Biotechnology, 1995. **6**(6): p. 698-708.

63. Gregoriadis, G., *Liposomes as Drug Carriers.* Pharmacy International, 1983. **4**(2): p. 33-37.

64. Gregoriadis, G., *Engineering liposomes for drug delivery: progress and problems.* Trends Biotechnol, 1995. **13**(12): p. 527-37.

65. Mezei, M. and V. Gulasekharam, *Liposomes--a selective drug delivery system for the topical route of administration. Lotion dosage form.* Life Sci, 1980. **26**(18): p. 1473-7.

66. Sharma, A. and U.S. Sharma, *Liposomes in drugdelivery: Progress and limitations.* International Journal of Pharmaceutics, 1997. **154**(2): p. 123-140.

67. Lasic, D.D., *Liposomes in Drug Delivery*. Vesicles, ed. M. Rosoff. Vol. 62. 1996, California: Marcel Dekker, Inc.

68. Uchegbu, I.F. and A.T. Florence, *Nonionic Surfactant Vesicles (Niosomes) - Physical and Pharmaceutical Chemistry.* Advances in Colloid and Interface Science, 1995. **58**(1): p. 1-55.

69. Uchegbu, I.F. and S.P. Vyas, *Non-ionic surfactant based vesicles (niosomes) in drug delivery.* International Journal of Pharmaceutics, 1998. **172**(1-2): p. 33-70.

70. Jeong, B., et al., *New biodegradable polymers for injectable drug delivery systems.* Journal of Controlled Release, 1999. **62**(1-2): p. 109-114.

71. Chasin, M. and R. Langer, *Biodegradable Polymers as Drug Delivery Systems.* Technology, 1991. **26**(5): p. 572- 581.

72. Gombotz, W.R. and D.K. Pettit, *Biodegradable polymers for protein and peptide drug delivery.* Bioconjug Chem, 1995. **6**(4): p. 332-51.

73. Heller, J., *Biodegradable polymers in controlled drug delivery.* Crit Rev Ther Drug Carrier Syst, 1984. **1**(1): p. 39-90.

74. Panyam, J. and V. Labhasetwar, *Biodegradable nanoparticles for drug and gene delivery to cells and tissue.* Adv Drug Deliv Rev, 2003. **55**(3): p. 329-47.

75. Pillai, O. and R. Panchagnula, *Polymers in drug delivery.* Curr Opin Chem Biol, 2001. **5**(4): p. 447-51.

76. Allen, T.M. and P.R. Cullis, *Drug delivery systems: entering the mainstream.* Science, 2004. **303**(5665): p. 1818-22.

77. Park, H. and K. Park, *Biocompatibility issues of implantable drug delivery systems.* Pharm Res, 1996. **13**(12): p. 1770-6.

78. Mohammed, A.R., et al., *Liposome formulation of poorly water soluble drugs: optimisation of drug loading and ESEM analysis of stability.* International Journal of Pharmaceutics, 2004. **285**(1-2): p. 23-34.

79. Uchegbu, I.F. and S.P. Vyas, *Non-ionic surfactant based vesicles (niosomes) in drug delivery (vol 172, pg 33, 1998).* International Journal of Pharmaceutics, 1998. **176**(1): p. 139-139.

80. Judy Senior, M.R., *Sustained-Release Injectable Products*. 2000: CRC Press.

81. Baillie, A.J., et al., *Non-ionic surfactant vesicles, niosomes, as a delivery system for the anti-leishmanial drug, sodium stibogluconate.* J Pharm Pharmacol, 1986. **38**(7): p. 502-5.

82. Choi, M.J. and H.I. Maibach, *Liposomes and niosomes as topical drug delivery systems.* Skin Pharmacol Physiol, 2005. **18**(5): p. 209-19.

83. Manconi, M., et al., *Niosomes as carriers for tretinoin. I. Preparation and properties.* Int J Pharm, 2002. **234**(1-2): p. 237-48.

84. Vyas, S.P., et al., *Non-ionic surfactant based vesicles (niosomes) for non-invasive topical genetic immunization against hepatitis B.* Int J Pharm, 2005. **296**(1-2): p. 80-6.

85. Manosroi, A., et al., *Characterization of vesicles prepared with various non-ionic surfactants mixed with cholesterol.* Colloids and Surfaces B-Biointerfaces, 2003. **30**(1-2): p. 129-138.

86. Teijon, J.M., et al., *Cytarabine trapping in poly(2-hydroxyethyl methacrylate) hydrogels: drug delivery studies.* Biomaterials, 1997. **18**(5): p. 383-8.

87. Casadei, M.A., et al., *Biodegradable and pH-sensitive hydrogels for potential colon-specific drug delivery: Characterization and in vitro release studies.* Biomacromolecules, 2008. **9**(1): p. 43-49.

88. Chang, Y.H. and L. Xiao, *Preparation and Characterization of a Novel Drug Delivery System: Biodegradable Nanoparticles in Thermosensitive Chitosan/Gelatin Blend Hydrogels.* Journal of Macromolecular Science Part a-Pure and Applied Chemistry, 2010. **47**(6): p. 608-615.

89. Hoare, T.R. and D.S. Kohane, *Hydrogels in drug delivery: Progress and challenges.* Polymer, 2008. **49**(8): p. 1993-2007.

90. Kamath, K.R. and K. Park, *Biodegradable Hydrogels in Drug-Delivery.* Advanced Drug Delivery Reviews, 1993. **11**(1-2): p. 59-84.

91. Mandracchia, D., et al., *New Biodegradable Hydrogels Based on Inulin and alpha,beta-Polyaspartylhydrazide Designed for Colonic Drug Delivery: In Vitro Release of Glutathione and Oxytocin.* Journal of Biomaterials Science-Polymer Edition, 2011. **22**(1-3): p. 313-328.

92. Peppas, N.A., *Hydrogels and drug delivery.* Current Opinion in Colloid & Interface Science, 1997. **2**(5): p. 531-537.

93. Peppas, N.A. and N.K. Mongia, *Ultrapure poly(vinyl alcohol) hydrogels with mucoadhesive drug delivery characteristics.* European Journal of Pharmaceutics and Biopharmaceutics, 1997. **43**(1): p. 51-58.

94. Schwarte, L.M. and N.A. Peppas, *Preparation and characterization of peg-containing, pH-sensitive, cationic hydrogels for drug delivery applications.* Abstracts of Papers of the American Chemical Society, 1997. **214**: p. 292-POLY.

95. Molinaro, G., et al., *Biocompatibility of thermosensitive chitosan-based hydrogels: an in vivo experimental approach to injectable biomaterials.* Biomaterials, 2002. **23**(13): p. 2717-2722.

96. Chen, G. and A.S. Hoffman, *Synthesis of carboxylated poly(NIPAAm) oligomers and their application to form thermo-reversible polymer-enzyme conjugates.* J Biomater Sci Polym Ed, 1994. **5**(4): p. 371-82.

97. Chilkoti, A., et al., *Site-specific conjugation of a temperature-sensitive polymer to a genetically-engineered protein.* Bioconjug Chem, 1994. **5**(6): p. 504-7.

98. Ding, Z., G. Chen, and A.S. Hoffman, *Unusual properties of thermally sensitive oligomer-enzyme conjugates of poly(N-isopropylacrylamide)-trypsin.* J Biomed Mater Res, 1998. **39**(3): p. 498-505.

99. Qiu, Y. and K. Park, *Environment-sensitive hydrogels for drug delivery.* Adv Drug Deliv Rev, 2001. **53**(3): p. 321-39.

100. Ruel-Gariepy, E., et al., *Characterization of thermosensitive chitosan gels for the sustained delivery of drugs.* International Journal of Pharmaceutics, 2000. **203**(1-2): p. 89-98.

101. Greenwald, R.B., et al., *Effective drug delivery by PEGylated drug conjugates.* Adv Drug Deliv Rev, 2003. **55**(2): p. 217-50.

102. Kwon, G.S., *Polymeric micelles for delivery of poorly water-soluble compounds.* Crit Rev Ther Drug Carrier Syst, 2003. **20**(5): p. 357-403.

103. Patri, A.K., I.J. Majoros, and J.R. Baker, *Dendritic polymer macromolecular carriers for drug delivery.* Curr Opin Chem Biol, 2002. **6**(4): p. 466-71.

104. Veronese, F.M. and G. Pasut, *PEGylation, successful approach to drug delivery.* Drug Discov Today, 2005. **10**(21): p. 1451-8.

105. Cheng, J., et al., *Formulation of functionalized PLGA-PEG nanoparticles for in vivo targeted drug delivery.* Biomaterials, 2007. **28**(5): p. 869-76.

106. Gao, X., et al., *Lectin-conjugated PEG-PLA nanoparticles: preparation and brain delivery after intranasal administration.* Biomaterials, 2006. **27**(18): p. 3482-90.

107. Ruan, G. and S.S. Feng, *Preparation and characterization of poly(lactic acid)-poly(ethylene glycol)-poly(lactic acid) (PLA-PEG-PLA) microspheres for controlled release of paclitaxel.* Biomaterials, 2003. **24**(27): p. 5037-44.

108. Riley, T., et al., *Core−Shell Structure of PLA−PEG Nanoparticles Used for Drug Delivery.* Langmuir, 2003. **19**(20): p. 8428-8435.

109. Hagan, S.A., et al., *Polylactide−Poly(ethylene glycol) Copolymers as Drug Delivery Systems. 1. Characterization of Water Dispersible Micelle-Forming Systems.* Langmuir, 1996. **12**(9): p. 2153-2161.

110. Riley, T., et al., *Physicochemical Evaluation of Nanoparticles Assembled from Poly(lactic acid)−Poly(ethylene glycol) (PLA−PEG) Block Copolymers as Drug Delivery Vehicles.* Langmuir, 2001. **17**(11): p. 3168-3174.

111. Jeong, B., et al., *Biodegradable block copolymers as injectable drug-delivery systems.* Nature, 1997. **388**(6645): p. 860-862.

112. Cho, J.Y., et al., *Physical gelation of chitosan in the presence of beta-glycerophosphate: The effect of temperature.* Biomacromolecules, 2005. **6**(6): p. 3267-3275.

113. Felt, O., P. Buri, and R. Gurny, *Chitosan: a unique polysaccharide for drug delivery.* Drug Dev Ind Pharm, 1998. **24**(11): p. 979-93.

114. Ko, J.A., et al., *Preparation and characterization of chitosan microparticles intended for controlled drug delivery.* Int J Pharm, 2002. **249**(1-2): p. 165-74.

115. Lorenzo-Lamosa, M.L., et al., *Design of microencapsulated chitosan microspheres for colonic drug delivery.* J Control Release, 1998. **52**(1-2): p. 109-18.

116. Shu, X.Z. and K.J. Zhu, *A novel approach to prepare tripolyphosphate/chitosan complex beads for controlled release drug delivery.* Int J Pharm, 2000. **201**(1): p. 51-8.

117. Tozaki, H., et al., *Chitosan capsules for colon-specific drug delivery: improvement of insulin absorption from the rat colon.* J Pharm Sci, 1997. **86**(9): p. 1016-21.

118. Cho, J. and M.C. Heuzey, *Dynamic scaling for gelation of a thermosensitive chitosan-beta-glycerophosphate hydrogel.* Colloid and Polymer Science, 2008. **286**(4): p. 427-434.

119. De Campos, A.M., A. Sanchez, and M.J. Alonso, *Chitosan nanoparticles: a new vehicle for the improvement of the delivery of drugs to the ocular surface. Application to cyclosporin A.* International Journal of Pharmaceutics, 2001. **224**(1-2): p. 159-168.

120. Chenite, A., et al., *Rheological characterization of thermogelling chitosa/glycerophosphate solutions.* Carbohydrate Polymers, 2001. **46** p. 39 - 47.

121. Israelachvili, J.N., *Intermolecular and Surface Forces: With Applications to Colloidal and Biological Systems*. 1985: Orlando: Academic Press.

122. Nasseri, B., *Effect of cholesterol and temperature on the elastic properties of niosomal membranes.* International Journal of Pharmaceutics, 2005. **300**(1-2): p. 95-101.

123. Baillie, A.J., et al., *The preparation and properties of niosomes--non-ionic surfactant vesicles.* J Pharm Pharmacol, 1985. **37**(12): p. 863-8.

124. Israelachvili, J.N., S. Marcelja, and R.G. Horn, *Physical principles of membrane organization.* Q Rev Biophys, 1980. **13**(2): p. 121-200.

125. Israelachvili, J.N., D.J. Mitchell, and B.W. Ninham, *Theory of self-assembly of lipid bilayers and vesicles.* Biochim Biophys Acta, 1977. **470**(2): p. 185-201.

126. Chenite, A., et al., *Novel injectable neutral solutions of chitosan form biodegradable gels in situ.* Biomaterials, 2000. **21**(21): p. 2155-2161.

127. J. Cho, J., et al., *Physical Gelation of Chitosan in the Presence of ß-Glycerophosphate: The Effect of Temperature.* Biomacromolecules, 2005. **6**: p. 3267-3275.

128. Leroux, J.C., et al., *Thermosensitive chitosan-based hydrogel containing liposomes for the delivery of hydrophilic molecules.* Journal of Controlled Release, 2002. **82**(2-3): p. 373-383.

129. Ta, H.T., C.R. Dass, and D.E. Dunstan, *Injectable chitosan hydrogels for localised cancer therapy.* Journal of Controlled Release, 2008. **126**(3): p. 205-216.

130. Biotium, I. *5-(and-6)-Carboxyfluorescein (5-(and-6)-FAM, mixed isomer)*.[cited; Available from: http://www.biotium.com/product/product_types/Fluo_Cl/price_and_info.asp?item=51013&layer1=02;&layer2=02B;.

131. Dumitriu, I.E., et al., *5,6-carboxyfluorescein diacetate succinimidyl ester-labeled apoptotic and necrotic as well as detergent-treated cells can be traced in composite cell samples.* Anal Biochem, 2001. **299**(2): p. 247-52.

132. Singla, A.K., A. Garg, and D. Aggarwal, *Paclitaxel and its formulations.* International Journal of Pharmaceutics, 2002. **235**(1-2): p. 179-192.

133. Invitrogen. *Paclitaxel, BODIPY® 564/570 Conjugate (BODIPY® 564/570 Taxol)*. [cited; Available from: http://products.invitrogen.com/ivgn/product/P7501?ICID=search-product.

134. Gilligan, T., W.K. Oh, and P.W. Kantoff, *Carboplatin for stage I seminoma.* J Clin Oncol, 2006. **24**(18): p. 2971-2; author reply e32-3.

135. Canetta, R., M. Rozencweig, and S.K. Carter, *Carboplatin: the clinical spectrum to date.* Cancer Treat Rev, 1985. **12** Suppl A: p. 125-36.

136. Overbeck, T.L., J.M. Knight, and D.J. Beck, *A comparison of the genotoxic effects of carboplatin and cisplatin in Escherichia coli.* Mutat Res, 1996. **362**(3): p. 249-59.

137. Travis, L.B., et al., *Risk of leukemia after platinum-based chemotherapy for ovarian cancer.* N Engl J Med, 1999. **340**(5): p. 351-7.

138. Yang, H., et al., *MicroRNA expression profiling in human ovarian cancer: miR-214 induces cell survival and cisplatin resistance by targeting PTEN.* Cancer Res, 2008. **68**(2): p. 425-33.

139. Wheate, N.J., et al., *The status of platinum anticancer drugs in the clinic and in clinical trials.* Dalton Trans. **39**(35): p. 8113-27.

140. Yang, X.L. and A.H. Wang, *Structural studies of atom-specific anticancer drugs acting on DNA.* Pharmacol Ther, 1999. **83**(3): p. 181-215.

141. Cho, Y.I. and J.P. Hartnett, *The falling ball viscometer- a new instrument for viscoelastic fluids.* Letters in Heat and Mass Transfer, 1979. **6**(4): p. 335-342.

142. Bewlay, S.L., et al., *Conductivity improvements to spray-produced LiFePO4 by addition of a carbon source.* Materials Letters, 2004. **58**(11): p. 1788-1791.

143. Berne, B.J. and R. Pecora, *Dynamic Light Scattering: With Applications to Chemistry, Biology, and Physics*. 1976 ed. 2000: Courier Dover Publications.

144. Schmitz, K.S., *An introduction to dynamic light scattering of macromolecules*. 1990, San Diego, CA: Academic Press Inc. 472

145. Williams, D.B. and C.B. Carter, *Transmission Electron Microscopy. A Textbook for Materials Science*. 2009: Springer US.

146. Reimer, L. and C. Braun, *Transmission Electron Microscopy, Physics of Image Formation and Microanalysis*. 1989: Springer.

147. Gillies, R.J., Z. Liu, and Z. Bhujwalla, *P-31-Mrs Measurements of Extracellular Ph of Tumors Using 3-Aminopropylphosphonate.* American Journal of Physiology, 1994. **267**(1): p. C195-C203.

148. Gelderblom, H., et al., *Cremophor EL: the drawbacks and advantages of vehicle selection for drug formulation.* Eur J Cancer, 2001. **37**(13): p. 1590-8.

149. Jauhari, S. and A.K. Dash, *A mucoadhesive in situ gel delivery system for paclitaxel.* AAPS PharmSciTech, 2006. **7**(2): p. E53.

150. Ruel-Gariepy, E. and J.C. Leroux, *In situ-forming hydrogels - review of temperature-sensitive systems.* European Journal of Pharmaceutics and Biopharmaceutics, 2004. **58**(2): p. 409-426.

151. Yang, T., et al., *Enhanced solubility and stability of PEGylated liposomal paclitaxel: In vitro and in vivo evaluation.* International Journal of Pharmaceutics, 2007. **338**(1-2): p. 317-326.

152. Balasubramanian, S.V. and R.M. Straubinger, *Taxol-lipid interactions: taxol-dependent effects on the physical properties of model membranes.* Biochemistry, 1994. **33**(30): p. 8941-7.

153. Kan, P., et al., *A liposomal formulation able to incorporate a high content of Paclitaxel and exert promising anticancer effect.* J Drug Deliv. **2011**: p. 629234.

154. Bayindir, Z.S, N.Y., *Characterization of Niosomes Prepared With Various Nonionic Surfactants for Paclitaxel Oral Delivery.* Pharmaceutical Technology, 2009. **99**(4): p. 2049-2059.

155. Markman, M., *Intraperitoneal drug delivery of antineoplastics.* Drugs, 2001. **61**(8): p. 1057-65.

156. Markman, M., *Intraperitoneal antineoplastic drug delivery: rationale and results.* Lancet Oncol, 2003. **4**(5): p. 277-83.

157. Sudimack, J. and R.J. Lee, *Targeted drug delivery via the folate receptor.* Adv Drug Deliv Rev, 2000. **41**(2): p. 147-62.

158. Vassileva, V., et al., *Novel biocompatible intraperitoneal drug delivery system increases tolerability and therapeutic efficacy of paclitaxel in a human ovarian cancer xenograft model.* Cancer Chemother Pharmacol, 2007. **60**(6): p. 907-14.

159. Choi, H., et al., *Iron oxide nanoparticles as magnetic resonance contrast agent for tumor imaging via folate receptor-targeted delivery.* Acad Radiol, 2004. **11**(9): p. 996-1004.

160. Konda, S.D., et al., *Specific targeting of folate-dendrimer MRI contrast agents to the high affinity folate receptor expressed in ovarian tumor xenografts.* MAGMA, 2001. **12**(2-3): p. 104-13.

161. Williams, E.C, et al, *Controlled Release Niosome Embedded Chitosan System: Effect of Cross-Link Mesh Dimension on Drug Release.* J Biomed Mat Res Part A. DOI: 10.1002/jbm.a.34275

162. Sinha, R., et al., *Nanotechnology in cancer therapeutics: bioconjugated nanoparticles for drug delivery.* Mol Cancer Ther, 2006. **5**(8): p. 1909-17.

163. Gendler, S.J., *MUC1, the renaissance molecule.* J Mammary Gland Biol Neoplasia, 2001. **6**(3): p. 339-53.

164. Smith, B.C., *Fundamentals of Fourier Transform Infrared Spectroscopy* 2009, CRC Press.

165. Stuart, B.H., *Infrared Spectroscopy: Fundamentals and Applications*. 2004: J. Wiley.

166. Ruel-Gariepy, E., et al., *A thermosensitive chitosan-based hydrogel for the local delivery of paclitaxel.* European Journal of Pharmaceutics and Biopharmaceutics, 2004. **57**(1): p. 53-63.

# APPENDIX A PERMISSIONS



**JOHN WILEY AND SONS LICENSE TERMS AND CONDITIONS**

Jun 28, 2012

This is a License Agreement between Eva Christabel Williams ("You") and John Wiley and Sons ("John Wiley and Sons") provided by Copyright Clearance Center ("CCC"). The license consists of your order details, the terms and conditions provided by John Wiley and Sons, and the payment terms and conditions.

**All payments must be made in full to CCC. For payment instructions, please see information listed at the bottom of this form.**

| | |
|---|---|
| License Number | 2937921280652 |
| License date | Jun 28, 2012 |
| Licensed content publisher | John Wiley and Sons |
| Licensed content publication | Journal of Biomedical Materials Research |
| Licensed content title | Controlled release niosome embedded chitosan system: Effect of crosslink mesh dimensions on drug release |
| Licensed content author | Eva Christabel Williams,Ryan Toomey,Norma Alcantar |
| Licensed content date | Jun 26, 2012 |
| Start page | n/a |
| End page | n/a |
| Type of use | Dissertation/Thesis |
| Requestor type | Author of this Wiley article |
| Format | Electronic |
| Portion | Full article |
| Will you be translating? | No |
| Order reference number | |
| Total | 0.00 USD |
| Terms and Conditions | |

**TERMS AND CONDITIONS**

This copyrighted material is owned by or exclusively licensed to John Wiley & Sons, Inc. or one of its group companies (each a "Wiley Company") or a society for whom a Wiley Company has exclusive publishing rights in relation to a particular journal (collectively WILEY"). By clicking "accept" in connection with completing this licensing transaction, you agree that the following terms and conditions apply to this transaction (along with the billing and payment terms and conditions established by the Copyright Clearance Center Inc., ("CCC's Billing and Payment terms and conditions"), at the time that you opened your Rightslink account (these are available at any time at http://myaccount.copyright.com)

Terms and Conditions

1. The materials you have requested permission to reproduce (the "Materials") are protected by copyright.

# APPENDIX A (CONTINUED)



2. You are hereby granted a personal, non-exclusive, non-sublicensable, non-transferable, worldwide, limited license to reproduce the Materials for the purpose specified in the licensing process. This license is for a one-time use only with a maximum distribution equal to the number that you identified in the licensing process. Any form of republication granted by this licence must be completed within two years of the date of the grant of this licence (although copies prepared before may be distributed thereafter). The Materials shall not be used in any other manner or for any other purpose. Permission is granted subject to an appropriate acknowledgement given to the author, title of the material/book/journal and the publisher. You shall also duplicate the copyright notice that appears in the Wiley publication in your use of the Material. Permission is also granted on the understanding that nowhere in the text is a previously published source acknowledged for all or part of this Material. Any third party material is expressly excluded from this permission.

3. With respect to the Materials, all rights are reserved. Except as expressly granted by the terms of the license, no part of the Materials may be copied, modified, adapted (except for minor reformatting required by the new Publication), translated, reproduced, transferred or distributed, in any form or by any means, and no derivative works may be made based on the Materials without the prior permission of the respective copyright owner. You may not alter, remove or suppress in any manner any copyright, trademark or other notices displayed by the Materials. You may not license, rent, sell, loan, lease, pledge, offer as security, transfer or assign the Materials, or any of the rights granted to you hereunder to any other person.

4. The Materials and all of the intellectual property rights therein shall at all times remain the exclusive property of John Wiley & Sons Inc or one of its related companies (WILEY) or their respective licensors, and your interest therein is only that of having possession of and the right to reproduce the Materials pursuant to Section 2 herein during the continuance of this Agreement. You agree that you own no right, title or interest in or to the Materials or any of the intellectual property rights therein. You shall have no rights hereunder other than the license as provided for above in Section 2. No right, license or interest to any trademark, trade name, service mark or other branding ("Marks") of WILEY or its licensors is granted hereunder, and you agree that you shall not assert any such right, license or interest with respect thereto.

5. NEITHER WILEY NOR ITS LICENSORS MAKES ANY WARRANTY OR REPRESENTATION OF ANY KIND TO YOU OR ANY THIRD PARTY, EXPRESS, IMPLIED OR STATUTORY, WITH RESPECT TO THE MATERIALS OR THE ACCURACY OF ANY INFORMATION CONTAINED IN THE MATERIALS, INCLUDING, WITHOUT LIMITATION, ANY IMPLIED WARRANTY OF MERCHANTABILITY, ACCURACY, SATISFACTORY QUALITY, FITNESS FOR A PARTICULAR PURPOSE, USABILITY, INTEGRATION OR NON-INFRINGEMENT AND ALL SUCH WARRANTIES ARE HEREBY EXCLUDED BY WILEY AND ITS LICENSORS AND WAIVED BY YOU.

6. WILEY shall have the right to terminate this Agreement immediately upon breach of this Agreement by you.

7. You shall indemnify, defend and hold harmless WILEY, its Licensors and their respective directors, officers, agents and employees, from and against any actual or threatened claims, demands, causes of action or proceedings arising from any breach of this Agreement by you.

8. IN NO EVENT SHALL WILEY OR ITS LICENSORS BE LIABLE TO YOU OR ANY OTHER PARTY OR ANY OTHER PERSON OR ENTITY FOR ANY SPECIAL, CONSEQUENTIAL, INCIDENTAL, INDIRECT, EXEMPLARY OR PUNITIVE DAMAGES, HOWEVER CAUSED, ARISING OUT OF OR IN CONNECTION WITH THE DOWNLOADING, PROVISIONING, VIEWING OR USE OF THE MATERIALS REGARDLESS OF THE FORM OF ACTION, WHETHER FOR BREACH OF CONTRACT, BREACH OF WARRANTY, TORT, NEGLIGENCE, INFRINGEMENT OR OTHERWISE (INCLUDING, WITHOUT LIMITATION, DAMAGES BASED ON LOSS OF PROFITS, DATA, FILES, USE, BUSINESS OPPORTUNITY OR CLAIMS OF THIRD PARTIES), AND WHETHER OR NOT THE PARTY HAS BEEN ADVISED OF THE POSSIBILITY OF SUCH DAMAGES. THIS LIMITATION SHALL APPLY NOTWITHSTANDING ANY FAILURE OF ESSENTIAL PURPOSE OF ANY LIMITED REMEDY PROVIDED HEREIN.

9. Should any provision of this Agreement be held by a court of competent jurisdiction to be illegal, invalid, or unenforceable, that provision shall be deemed amended to achieve as nearly as possible the same economic effect as the original provision, and the legality, validity and enforceability of the remaining provisions of this Agreement shall not be affected or impaired thereby.

# APPENDIX A (CONTINUED)



10. The failure of either party to enforce any term or condition of this Agreement shall not constitute a waiver of either party's right to enforce each and every term and condition of this Agreement. No breach under this agreement shall be deemed waived or excused by either party unless such waiver or consent is in writing signed by the party granting such waiver or consent. The waiver by or consent of a party to a breach of any provision of this Agreement shall not operate or be construed as a waiver of or consent to any other or subsequent breach by such other party.

11. This Agreement may not be assigned (including by operation of law or otherwise) by you without WILEY's prior written consent.

12. Any fee required for this permission shall be non-refundable after thirty (30) days from receipt.

13. These terms and conditions together with CCC's Billing and Payment terms and conditions (which are incorporated herein) form the entire agreement between you and WILEY concerning this licensing transaction and (in the absence of fraud) supersedes all prior agreements and representations of the parties, oral or written. This Agreement may not be amended except in writing signed by both parties. This Agreement shall be binding upon and inure to the benefit of the parties' successors, legal representatives, and authorized assigns.

14. In the event of any conflict between your obligations established by these terms and conditions and those established by CCC's Billing and Payment terms and conditions, these terms and conditions shall prevail.

15. WILEY expressly reserves all rights not specifically granted in the combination of (i) the license details provided by you and accepted in the course of this licensing transaction, (ii) these terms and conditions and (iii) CCC's Billing and Payment terms and conditions.

16. This Agreement will be void if the Type of Use, Format, Circulation, or Requestor Type was misrepresented during the licensing process.

17. This Agreement shall be governed by and construed in accordance with the laws of the State of New York, USA, without regards to such state's conflict of law rules. Any legal action, suit or proceeding arising out of or relating to these Terms and Conditions or the breach thereof shall be instituted in a court of competent jurisdiction in New York County in the State of New York in the United States of America and each party hereby consents and submits to the personal jurisdiction of such court, waives any objection to venue in such court and consents to service of process by registered or certified mail, return receipt requested, at the last known address of such party.

**Wiley Open Access Terms and Conditions**

All research articles published in Wiley Open Access journals are fully open access: immediately freely available to read, download and share. Articles are published under the terms of the Creative Commons Attribution Non Commercial License, which permits use, distribution and reproduction in any medium, provided the original work is properly cited and is not used for commercial purposes. The license is subject to the Wiley Open Access terms and conditions:
Wiley Open Access articles are protected by copyright and are posted to repositories and websites in accordance with the terms of the Creative Commons Attribution Non Commercial License. At the time of deposit, Wiley Open Access articles include all changes made during peer review, copyediting, and publishing. Repositories and websites that host the article are responsible for incorporating any publisher-supplied amendments or retractions issued subsequently.
Wiley Open Access articles are also available without charge on Wiley's publishing platform, **Wiley Online Library** or any successor sites.

**Use by non-commercial users**

For non-commercial and non-promotional purposes individual users may access, download, copy, display and redistribute to colleagues Wiley Open Access articles, as well as adapt, translate, text- and data-mine the content subject to the following conditions:

# APPENDIX A (CONTINUED)



- The authors' moral rights are not compromised. These rights include the right of "paternity" (also known as "attribution" - the right for the author to be identified as such) and "integrity" (the right for the author not to have the work altered in such a way that the author's reputation or integrity may be impugned).
- Where content in the article is identified as belonging to a third party, it is the obligation of the user to ensure that any reuse complies with the copyright policies of the owner of that content.
- If article content is copied, downloaded or otherwise reused for non-commercial research and education purposes, a link to the appropriate bibliographic citation (authors, journal, article title, volume, issue, page numbers, DOI and the link to the definitive published version on Wiley Online Library) should be maintained. Copyright notices and disclaimers must not be deleted.
- Any translations, for which a prior translation agreement with Wiley has not been agreed, must prominently display the statement: "This is an unofficial translation of an article that appeared in a Wiley publication. The publisher has not endorsed this translation."

**Use by commercial "for-profit" organisations**

Use of Wiley Open Access articles for commercial, promotional, or marketing purposes requires further explicit permission from Wiley and will be subject to a fee. Commercial purposes include:

- Copying or downloading of articles, or linking to such articles for further redistribution, sale or licensing;
- Copying, downloading or posting by a site or service that incorporates advertising with such content;
- The inclusion or incorporation of article content in other works or services (other than normal quotations with an appropriate citation) that is then available for sale or licensing, for a fee (for example, a compilation produced for marketing purposes, inclusion in a sales pack)
- Use of article content (other than normal quotations with appropriate citation) by for-profit organisations for promotional purposes
- Linking to article content in e-mails redistributed for promotional, marketing or educational purposes;
- Use for the purposes of monetary reward by means of sale, resale, licence, loan, transfer or other form of commercial exploitation such as marketing products
- Print reprints of Wiley Open Access articles can be purchased from: corporatesales@wiley.com

Other Terms and Conditions:

BY CLICKING ON THE "I AGREE..." BOX, YOU ACKNOWLEDGE THAT YOU HAVE READ AND FULLY UNDERSTAND EACH OF THE SECTIONS OF AND PROVISIONS SET FORTH IN THIS AGREEMENT AND THAT YOU ARE IN AGREEMENT WITH AND ARE WILLING TO ACCEPT ALL OF YOUR OBLIGATIONS AS SET FORTH IN THIS AGREEMENT.

v1.7

**If you would like to pay for this license now, please remit this license along with your payment made payable to "COPYRIGHT CLEARANCE CENTER" otherwise you will be**

# APPENDIX A (CONTINUED)



**invoiced within 48 hours of the license date. Payment should be in the form of a check or money order referencing your account number and this invoice number RLNK500808883. Once you receive your invoice for this order, you may pay your invoice by credit card. Please follow instructions provided at that time.**

**Make Payment To:**
**Copyright Clearance Center**
**Dept 001**
**P.O. Box 843006**
**Boston, MA 02284-3006**

**For suggestions or comments regarding this order, contact RightsLink Customer Support: customercare@copyright.com or +1-877-622-5543 (toll free in the US) or +1-978-646-2777.**

**Gratis licenses (referencing $0 in the Total field) are free. Please retain this printable license for your reference. No payment is required.**